



HAL
open science

West African lateritic pediments: Landform-regolith evolution processes and mineral exploration pitfalls

Dominique Chardon, Jean-Louis Grimaud, Anicet Beauvais, Ousmane Bamba

► To cite this version:

Dominique Chardon, Jean-Louis Grimaud, Anicet Beauvais, Ousmane Bamba. West African lateritic pediments: Landform-regolith evolution processes and mineral exploration pitfalls. *Earth-Science Reviews*, 2018, 179, pp.124-146. 10.1016/j.earscirev.2018.02.009 . hal-01744579

HAL Id: hal-01744579

<https://amu.hal.science/hal-01744579>

Submitted on 27 Mar 2018

HAL is a multi-disciplinary open access archive for the deposit and dissemination of scientific research documents, whether they are published or not. The documents may come from teaching and research institutions in France or abroad, or from public or private research centers.

L'archive ouverte pluridisciplinaire **HAL**, est destinée au dépôt et à la diffusion de documents scientifiques de niveau recherche, publiés ou non, émanant des établissements d'enseignement et de recherche français ou étrangers, des laboratoires publics ou privés.

1
2
3
4 1 **West African lateritic pediments: Landform-regolith**
5
6 2 **evolution processes and mineral exploration pitfalls**
7
8
9 3

10 4
11 5
12 6 **Dominique Chardon^{a,b,c*}, Jean-Louis Grimaud^{c,d}, Anicet Beauvais^e, Ousmane Bamba^b**
13
14
15 7

16 8
17 9
18 10 ^a IRD, 01 BP 182 Ouagadougou 01, Burkina Faso

19 11
20 12 ^b Département des Sciences de la Terre, Université Ouaga I Professeur Joseph Ki-Zerbo,
21 13
22 14 BP 7021, Ouagadougou, Burkina Faso

23 15
24 16 ^c GET, Université de Toulouse, CNRS, IRD, UPS, France.

25 17
26 18 ^d MINES ParisTech, PSL Research University, Centre de Géosciences,
27 19
28 20 35 rue St Honoré, 77305 Fontainebleau Cedex, France

29 21
30 22 ^e Aix-Marseille Univ, CNRS, IRD, Coll France, CEREGE BP 80,
31 23
32 24 13545 Aix-en-Provence, Cedex 4, France
33 25
34 26
35 27
36 28
37 29
38 30
39 31
40 32
41 33
42 34
43 35
44 36
45 37
46 38
47 39
48 40
49 41
50 42
51 43
52 44
53 45
54 46
55 47
56 48
57 49
58 50
59 51
60 52

53 43 Submitted to ***Earth-Science Reviews***, 14 September 2017

54 44 Revised 28 January 2018

55 45 Accepted 09 February 2018

56 46 doi:10.1016/j.earscirev.2018.02.009
57 47
58 48
59 49
60 50

51 51 * **Corresponding author**

52 52 E-mail address: dominique.chardon@ird.fr
53 53
54 54
55 55
56 56
57 57
58 58
59 59
60 60

61
62
63 **26 HIGHLIGHTS**
64

- 65 27 - Review of the geomorphology, regolith and age of the West African pediment systems
66
67 28 - Duricrusted and loose transported sediments are dominant on pediments
68
69 29 - Specific geomorphological exploration guides are required for lateritic pediment terrains
70
71
72 30 - Pediments typify slow (<10 m/Ma) denudation regimes and their stepping patterns are not
73
74 31 gauges of regional uplift
75

76 32

77
78 **33 Abstract**
79

80 34 This paper is a contribution to the understanding of surface dynamics of tropical shields over
81
82 35 geological timescales. Emphasis is put on the fundamental and applied implications of
83
84 36 regolith production and dispersion processes through the formation, dissection and
85
86 37 preservation of landforms. It is based on the case study of sub Saharan West Africa, which
87
88 38 recorded Neogene stepwise dissection of its topography through the emplacement of three
89
90 39 lateritic pediment systems, which still occupy most of its surface. Pediments are erosional /
91
92 40 transportation slopes having been weathered and duricrusted. Pediment-regolith
93
94 41 associations therefore depend on the parent rock, transport dynamics and preservation of
95
96 42 the material having transited on their surface as well as on the intensity of their weathering /
97
98 43 duricrusting. Iron oxy-hydroxide-cemented clastic sediments (detrital ferricretes) and
99
100 44 unconsolidated clastic sediments are the dominant outcropping material, and as such
101
102 45 represent a challenge for mineral exploration that relies on surface geochemical sampling to
103
104 46 detect metal concentration in the bedrock. Landform-regolith mapping beyond the scale of
105
106 47 modern interfluves combined with paleolandscape reconstitution are relevant to provide
107
108 48 exploration guides for (i) interpreting geochemical anomalies on pediments, (ii) tracing their
109
110 49 potential source when they have been “transported” on pediments and (iii) targeting
111
112 50 suspected ore bodies concealed beneath pediment(s). Past and present latitudinal climatic
113
114
115
116
117
118
119
120

121
122
123 51 zonation of pedimentation and weathering patterns suggests a gradation of pedimentation
124
125 52 process across the intertropical zone and explains why pediments may have been
126
127 53 overlooked in equatorial environments, with implications for mineral exploration.
128
129 54 Successive pediment systems adapted to uneven, knickzone bearing river networks,
130
131 55 producing a spatially consistent and reduced (<80 m) stepping pattern of pediments
132
133 56 independent from elevation or position in the drainage. Pediments / pediplains are therefore
134
135 57 not proxies of uplift and their preservation over geological timescales typifies regions
136
137 58 submitted to less than 10 m/My erosion rates. The identification and study of lateritic
138
139 59 pediments bear important implications on shield sediment routing systems and a better
140
141 60 access to the bedrock and its resources, which may still be underestimated in the tropics.
142
143
144
145
146
147
148
149
150
151
152

153 62 **keywords:** Pediment; Regolith; Landform evolution processes; Mineral exploration; Mega-
154
155 63 geomorphology
156
157
158
159
160
161
162
163
164
165
166
167
168
169
170
171
172
173
174
175
176
177
178
179
180

65 **1. Introduction**

66 Tropical shields of Africa, South America, India and Australia are mantled over large
67 areas by regolith derived from rock weathering. Regolith is a weathered, unconsolidated or
68 secondarily indurated cover that overlies fresh coherent bedrock (Scott and Pain, 2008). If
69 preserved on its parental bedrock, regolith constitutes a weathering profile (Fig. 1), which
70 acts as a filter for the chemical composition of the geological substrate. In this case,
71 weathering concentrates some metals (Fe, Al, Ni, Cu, Au, Mn) in the regolith compared to the
72 bedrock, which can result lateritic ore deposits (Nahon et al., 1992; Valetton, 1994; Freyssinet
73 et al., 2005). Once transported by slope or alluvial processes, regolith may act as a mask for
74 the underlying bedrock. As displaced regolith may undergo weathering after transport (Ollier
75 and Pain, 1996), deciphering regolith production / dispersion scenarios through landscapes

181
182
183 76 is key for mineral exploration, which mostly relies on soil geochemical surveys (Butt et al.,
184
185 77 2000; Porto, 2016). Throughout the Cenozoic, shield surfaces outside the influence of
186
187 78 glaciers have primarily evolved by landscape dissection, the process by which
188
189 79 paleolandscapes become isolated as relics overlooking younger active landforms as a result
190
191 80 of slow and unevenly distributed erosion. Thereby, the relief of shields increases through
192
193 81 geological time (Thomas, 1989; Twidale, 1991), while landscape dissection is instrumental in
194
195 82 exhuming regolith available to re-weathering and transportation. Therefore, the study of
196
197 83 regolith distribution patterns over shield landscapes should not only provide exploration
198
199 84 guides to better access bedrock geology and resources, but also constrain landform
200
201 85 evolution processes and sediment delivery of very large cratonic river systems (Beauvais and
202
203 86 Chardon, 2013; Grimaud et al., 2015, 2018).

206
207 87 Pediments are common landforms that typically form during, and contribute to, the
208
209 88 process of landscape dissection, especially over vast non-orogenic regions of the world (e.g.,
210
211 89 Dohrenwend and Parsons, 2009). In the broadest sense of the term, pediments may be
212
213 90 considered as gently inclined slopes of transportation and/or erosion that truncate bedrock
214
215 91 and/or regolith and connect eroding slopes or scarps to areas of sediment deposition or
216
217 92 alluvial transportation at lower levels (definition adapted from Oberlander, 1997).

219 93 Pedimentation involves the physic-chemical processes that concur to form pediments. As
220
221 94 transportation slopes feeding rivers with clastic sediments, pediments are a regulating
222
223 95 element of the sediment routing system. As transit landsurfaces, pediments also carry
224
225 96 transported regolith that masks the geological substrate. They are therefore an obstacle to
226
227 97 mineral exploration (Payne, 1969; Pease, 2015) but have not been recognized as such in
228
229 98 lateritic environments by exploration geologists and geochemists. Through the work of King
230
231 99 (1948, 1967), the pediment concept also contributed to landscape evolution theories
232
233 100 (Summerfield, 1991, pp. 457-467). However, no general agreement exists on the recognition
234
235
236
237
238
239
240

241
242
243 101 criteria, regional correlation and the geomorphic meaning of paleo-pediments. Remaining
244
245 102 questions are (i) whether and how pediplains (i.e., regional surfaces of coalescent
246
247 103 pediments) can form and be preserved over geological time-scales (10^6 - 10^7 yr) and (ii)
248
249 104 whether they may be gauges of continental deformation or whether they have another
250
251 105 geological signification (e.g., Tricart *in* Twidale, 1983; Summerfield, 1985, 1996; Thomas and
252
253 106 Summerfield, 1987; Twidale and Bourne, 2013; Dauteuil et al., 2015; Guillocheau et al., 2015,
254
255 107 2017).

258 108 Relationships amongst pediment development and preservation and regolith
259
260 109 production and remobilization are exceptionally exemplified over sub Saharan West Africa.
261
262 110 Pediment systems formed by stepwise dissection of the region West of 10°E and South of
263
264 111 20°N (Fig. 2) since the earliest Miocene (ca. 24 Ma) and still occupy an overwhelming part of
265
266 112 its surface. They exclusively expose lateritic regolith and are commonly capped by ferricrete
267
268 113 (a generic term used here for iron duricrust). The region hosts the southern West African
269
270 114 craton, which is an important metallogenic province (Milési et al., 1992; Markwitz et al., 2016)
271
272 115 and more specifically the largest Paleoproterozoic gold-producing region (Goldfarb et al.,
273
274 116 2017). The ubiquitous lateritic pediments of the region therefore pose an amazing
275
276 117 exploration challenge (e.g., Bamba, 2009). Building on decades of geomorphological
277
278 118 investigations throughout the sub region, recent progress made at dating, mapping and
279
280 119 regionally correlating lateritic pediments and earlier paleolandscape elements left by relief
281
282 120 dissection (Beauvais and Chardon, 2013) offered a new perspective for deciphering
283
284 121 denudation chronologies and landscape evolution processes on a sub-continental scale.
285
286 122

288 122 The present contribution is a review of the West African lateritic pediment systems
289
290 123 from the landscape to the sub continental scale. It addresses pediment landform-regolith
291
292 124 evolution processes to (i) evaluate the factors controlling the production and preservation of
293
294 125 pediments over geological timescales and their geological meaning, (ii) call attention to
295
296
297
298
299
300

301
302
303 126 geochemical exploration pitfalls in lateritic pediment dominated environments and provide
304
305 127 adapted geomorphological exploration guides or strategies. The ubiquity of pediment-
306
307 128 dominated terrains in West Africa suggests that pediments occupy vast regions of the
308
309 129 tropical belt and calls for geomorphic reassessment of shield surfaces from both a
310
311
312 130 fundamental and applied perspective.

313
314 131

315
316 132 **2. West African landscape-regolith evolution models for mineral exploration and the**
317
318 133 **recognition/study of pediments**

319
320 134 The “landscape geochemistry” approach to tropical geomorphology has prevailed
321
322 135 for decades in the exploration and surface geochemistry communities (Butt, 2016).
323
324 136 Following Zeegers and Leprun (1979), such an approach led to pedogenetic geochemical
325
326 137 dispersion models elaborated for West African base metal deposits and various bedrock
327
328 138 lithologies that consider ferricretes as forming the upper residuum of weathering profiles
329
330 139 preserved on their parental bedrock (Butt and Zeegers, 1989; Zeegers and Lecomte, 1992;
331
332 140 Lecomte and Zeegers, 1992; Freyssinet, 1993; Bowell et al., 1996; Tardy, 1997; Fig 1).
333
334 141 Accordingly, ferricretes are inferred to display various degrees of geochemical dependency
335
336 142 on the underlying bedrock via the successive horizons of the weathering profile i.e., from
337
338 143 bottom to top: saprolite, mottled clays and carapace (Fig. 1). Within such a paradigm,
339
340 144 variations in concentration and mode of occurrence of base metals or other elements from
341
342 145 the bedrock to the ferricrete result from solute loss, vertical mass transfers and compaction
343
344 146 of the residuum as a sole consequence of lateritic weathering, leading to the formation of
345
346 147 geochemical dispersion halos (Roquin et al., 1990; Colin and Vieillard, 1991; Freyssinet, 1993;
347
348 148 Freyssinet et al., 2005; Fig. 3). West African exploration models consider cases where
349
350 149 weathering profiles were truncated by erosion and weathering horizons deeper than the
351
352 150 ferricrete are exposed or cases where such truncated profiles are overlain by unconsolidated
353
354
355
356
357
358
359
360

361
362
363 151 colluviums (e.g., *Bowell et al., 1996*). But ferricretes are considered as formed from in-situ
364
365 152 regolith. A consequence of such popular landscape evolution models is that both the role of
366
367 153 pedimentation-driven relief dissection in redistributing regolith in the landscapes and
368
369 154 potential detrital origin of ferricretes have been overlooked for decades of mineral
370
371 155 exploration and geochemical investigations. However, among exploration geologists,
372
373 156 *Bolster (1999)* suggested that some West African ferricretes were detrital. More recently,
374
375 157 former advocates of the in-situ paradigm such as *Butt and Bristow (2013)* claimed that
376
377 158 ferricretes were “Fe oxydes-cemented sediments” and that “relief inversion [was] a very
378
379 159 widespread and important phenomenon” in West Africa (relief inversion being a case of relief
380
381 160 dissection that leads the lower part of an ancient landscape to become the highest part of
382
383 161 the new landscape; see *Summerfield, 1991*). Those findings were actually made 60 years ago
384
385 162 and documentation on those topics has accumulated since then from investigations by
386
387 163 geologists, soil scientists and geomorphologists.

390
391 164 Early geomorphological studies have shown that ferricretes occupying large surfaces
392
393 165 of the sub region contained gravels and cobbles of Al-Fe crusts, quartz and bedrock that had
394
395 166 no genetic relationships with their underlying saprolite or bedrock (*Dresch, 1952a; Lamotte*
396
397 167 *and Rougerie, 1953, 1962; Pélissier and Rougerie, 1953; Daveau et al., 1962*). In the meantime,
398
399 168 following reconnaissance by *Pélissier and Rougerie (1953), Brammer (1955, 1956), Tricart et*
400
401 169 *al. (1957), Michel (1959) and Vogt (1959a)* showed that these detrital ferricretes capped
402
403 170 generations of glacis - a French term for pediment(s). In his comprehensive geomorphic
404
405 171 investigation of the Senegambia drainage basin, *Michel (1959, 1973, 1974)* deciphered and
406
407 172 mapped the sequence of lateritic pediments over Central and Northern Guinea,
408
409 173 Southwestern Mali and Senegal, (*Fig. 2*). More recently, glacis of Eastern Senegal and their
410
411 174 regolith were investigated through combined petrological and near-surface geophysical
412
413 175 investigations (electrical resistivity tomography and ground penetrating radar: *Beauvais et*
414
415
416
417
418
419
420

421
422
423 176 al., 1999, 2004). The lateritic glacis of Senegal extend in southern and central Mauritania, but
424
425 177 they tend to be less iron-rich northward (Michel, 1977) and could even expose **even**
426
427
428 178 pedogenic calcretes (Nahon et al., 1977).

429
430 179 After Brückner (1955) and especially Hilton (1963) in Ghana (former Gold Coast), De
431
432 180 Swardt (1964) led the way for detailed investigations of the extensive lateritic pediment
433
434 181 systems of Nigeria that are correlated with the glacis sequence established in Guinea and
435
436 182 Senegal (Fölster, 1969a, 1969b; Rohdenburg, 1969; Burke and Durotoye, 1971; Fölster et al.,
437
438 183 1971; Fig. 2). Geomorphic description, petrological characterization and mapping of glacis
439
440 184 generations were undertaken over Burkina Faso (former Haute-Volta; Fig. 2) by Boulet (1970),
441
442 185 Eschenbrenner and Grandin (1970), Grandin (1976), Bamba (1996), Bamba et al. (2002) and
443
444 186 Grandin and Joly (2008). Works on glacis were also extended to the neighboring area of the
445
446 187 Republic of Niger by Mensching (1966) and Gavaud (1977). More recently, the mapping of the
447
448 188 glacis systems in Southwestern Burkina Faso by combinations of field surveys, airborne
449
450 189 geophysics and remote sensing was undertaken by Grimaud et al. (2015) and Metelka et al.
451
452
453 190 (2018).

454
455 191 In Côte d'Ivoire, intensive work was undertaken on glacis geomorphology and
456
457 192 weathering in the 1970s (e.g., Bonvallet and Boulangé, 1970; Eschenbrenner and Grandin,
458
459 193 1970; Boulangé et al., 1973; Grandin, 1976; Pèltre, 1977; see also Teeuw, 2002), whereas the
460
461 194 same glacis systems were reported in Sierra Leone (Fig. 2) by Grandin and Hayward (1975)
462
463 195 and studied by Thomas (1980, 1994), Thomas and Thorp (1985), Bowden (1987, 1997) and
464
465 196 Teeuw (1987), although the two later authors did not explicitly refer to pediments, but to
466
467 197 "footslope laterites (duricrust)" (e.g., Bowden, 1987). Reconnaissance by Dresch (1952b)
468
469 198 indicates that the ferricrete-capped pediments of Niger and Burkina Faso extend over Benin
470
471
472 199 (as confirmed by our field observations) as well as in Togo (Fig. 2), where they have been
473
474 200 described as such and studied by soil scientists (e.g., Le Cocq, 1986; Meyer, 1992).

481
482
483 201 Regional typologies and systematics of glacis were defined in the seminal
484
485 202 monographs of Michel (1973) and Grandin (1976). Three successive glacis systems have been
486
487 203 recognized, namely the High, Middle and Low glacis, stepwise landscape dissection being
488
489 204 documented as the key process having allowed the preservation of relict bauxitic,
490
491 205 Intermediate and pediment landforms of each generation (e.g., Grandin and Joly, 2008; see
492
493 206 also Beaudet and Coque, 1994; Gunnell, 2003). Weathering patterns of the glacis sequence
494
495 207 have been treated in the reviews of Tardy (1997) and Tardy and Roquin (1998). The pediment
496
497 208 sequence was incorporated by Burke and Gunnell (2008) into their model of the African
498
499 209 Surface, which encompasses the entire relief of the continent and would have been
500
501 210 generated by deformation and correlative erosion of a initially flat and low lying continent-
502
503 211 wide surface since the Cretaceous. Remnants of each West African glacis system have been
504
505 212 correlated and mapped regionally by combining regional field surveys, photointerpretation
506
507 213 and the available literature (e.g., Beauvais and Chardon, 2013; Grimaud et al., 2014, 2018).
508
509 214 The present work stems from the experience gained in the course of those regional
510
511 215 correlations and compilations as well as our own field experience in Benin, Burkina Faso,
512
513 216 Guinea, Côte d'Ivoire, Mali, Niger and Senegal (Fig. 2). By considering pediments and glacis in
514
515 217 the broadest sense of the definition given above, the two terms are used here
516
517 218 interchangeably.

519
520
521 219

522 220 **3. Pediments in the West African morphoclimatic sequence**

523
524
525 221 The West African landscape is the end product of the stepwise dissection of an old,
526
527 222 low relief topography called the African Surface (e.g., King, 1948; Boulangé and Millot, 1988;
528
529 223 Chardon et al., 2016). This old landscape is mantled by bauxitic duricrusts resulting from a
530
531 224 long period of intense weathering that culminated and ended in the Early and Middle Eocene
532
533 225 (Millot, 1970; Valeton, 1991; Colin et al., 2005; Chardon et al., 2006; Beauvais et al., 2008;
534
535
536
537
538
539
540

541
542
543 226 Beauvais and Chardon, 2013). The African surface is now preserved mostly as bauxite-
544
545 227 capped mesas dominating the current landscape. The High, Middle and Low glacis mark the
546
547 228 last main dissection stages of the African Surface. Remnants of a massive, nodular or
548
549 229 pisolitic ferricrete-capped landscape found below bauxite relics and above the glacis have
550
551 230 been used to define an Intermediate Surface (Michel, 1959, 1973; Vogt, 1959a). Bauxitic
552
553 231 duricrusts of the African Surface and the ferricretes of the Intermediate Surface top thick (>
554
555 232 80 m) weathering profiles that are preserved on their parental bedrock (Grandin, 1976;
556
557 233 Boulangé, 1984, 1986; Boulangé and Millot, 1988; Valeton, 1991).

560 234 Each glacis system in the West African sequence shows, in most cases, evidence for
561
562 235 duricrusting (or induration), and lateritic weathering, after its formation. Pediments/glacis
563
564 236 are the most conspicuous and common active landforms of dry or sub-humid regions of the
565
566 237 world (e.g., Dohrenwend and Parsons, 2009). The successive shifts from pedimentation to
567
568 238 lateritic weathering/duricrusting of the three glacis systems are indicative of repeated
569
570 239 transitions from semi-arid to seasonally contrasted wet tropical climate over West Africa
571
572 240 (Tricart et al., 1957; Michel, 1973; Grandin, 1976). Duricrusting took place during climate
573
574 241 shifts toward dryer conditions at the ends of humid weathering periods, before
575
576 242 abandonment and dissection of one glacis system and formation of a new one (Beauvais and
577
578 243 Chardon, 2013). Systematic Ar-Ar geochronology of K-Mn oxides (cryptomelane) from the
579
580 244 Mn-rich duricrust and weathering profile of each member of the West African landform-
581
582 245 regolith sequence allowed constraining their weathering and abandonment ages (Beauvais
583
584 246 et al., 2008; Beauvais and Chardon, 2013; Fig. 4). The African and Intermediate regolith-
585
586 247 landform associations yielded 59-45 and 29-24 Ma age groups, respectively. The High, Middle
587
588 248 and Low glacis weathered before abandonment at 18-11, 7-6 and around 3 Ma, respectively
589
590 249 (Fig. 4). Those age groups would therefore restrain the main pedimentation periods to 24-18,
591
592 250 11-7 and 6-3 Ma for the High, Middle and Low glacis, respectively (Fig. 4). Ages obtained on
593
594
595
596
597
598
599
600

601
602
603 251 alunite and jarosite (Vasconcelos et al., 1994), although indicative of lesser weathering
604
605 252 intensities than cryptomelane, are compatible with the period of bauxite formation,
606
607 253 weathering of the Intermediate landscape until the latest Oligocene (24 Ma) and the 18-11
608
609 254 Ma period of High glacis weathering (Fig. 4).
610

611
612 255

613 256 **4. Glacis landforms and landscape chronologies**

614 257 *4.1. Type-landforms and their spatial arrangements*

615
616 258 The three generations of West African glacis remnants are best distinguished on the
617
618
619 259 piedmonts of topographic massifs, which form up to hundreds of meters' high residual
620
621 260 reliefs that had not been leveled by pedimentation (Figs. 5 and 6a). Those massifs are
622
623 261 typically made of greenstone belt material (andesite, basalt, gabbro, volcano sedimentary
624
625 262 rocks) or early Mesozoic dolerite sills hosted by tabular sandstones and preserved from
626
627 263 erosion thanks to their capping bauxites and/or Intermediate duricrusts. Glacis are graded
628
629 264 upward-concave surfaces sloping away from the massifs (e.g., Grandin, 1976). The stepping
630
631 265 of successive glacis relics attests to the polycyclic nature of the landscapes due to renewed
632
633 266 periods of pedimentation (Fig. 6a). The uppermost portion of an early glacis (e.g., the High
634
635 267 glacis) is commonly eroded in such a way that a peripheral hollow separates the glacis
636
637 268 remnant from its upslope relict landscape (Fig. 6a and 7a; e.g., Beauvais et al., 1999). A later
638
639 269 glacis (e.g., the Middle glacis) may shape the inner slopes of the peripheral hollow so that it
640
641 270 can reach a higher elevation than the relics of the earlier glacis (Fig. 6a). Relative elevation
642
643 271 alone is therefore not a reliable criterion to decipher glacis generations given their slopes
644
645 272 and their dissection patterns. Careful investigation of the relative geomorphic position,
646
647 273 lateral extension and age of landscape elements should therefore be preferred to establish a
648
649 274 glacis landscape chronology.
650
651
652
653
654
655
656
657
658
659
660

661
662
663 275 Massifs to which piedmont glacis are connected may be eroded by headward river
664
665 276 erosion so that only an inselberg (i.e., a rocky topographic massif stripped from its regolith)
666
667 277 remains as a relic of the former bauxitic / Intermediate topography. Such an inselberg may
668
669 278 have a lower elevation than the piedmont glacis relicts (Fig. 7) and in many instances erosion
670
671 279 may even totally erase the massif to which glacis were connected. Likewise, glacis relict
672
673 280 surfaces carrying cobbles or boulders of bauxites are commonly preserved in areas where no
674
675 281 bauxite massifs remain (Bamba, 1996; Fig 7). River valleys connected upstream to peripheral
676
677 282 hollows generally have a lower slope gradient than the early (High) glacis (Fig. 7b). Later
678
679 283 (Middle or Low) glacis settle on their valley sides (Fig. 7b) that dip at a high angle to the
680
681 284 earlier glacis slope direction. This implies that slope direction – and therefore surface
682
683 285 material transport direction on the pediment – not only varies spatially for a given glacis
684
685 286 generation (for instance for the High glacis radiating around a residual topographic massif) -
686
687 287 it varies also from one glacis generation to the next.

690 288 Over vast granitoid or tabular sandstone / siltstone terrains, the landsurface is a
691
692 289 multi-convexo-concave plain that is occupied by undulating glacis encompassing the entire
693
694 290 relief i.e., from the top of smooth convex interfluves to the lower part of their concave slopes
695
696 291 (Fig. 6b). Following Rohdenburg (1969) in his review of Southern Nigerian pediment systems,
697
698 292 the term of rolling pediplain is used here to describe such glacis landscape regions (see also
699
700 293 Fölster, 1969a). They have 2 to 20 km wavelength and modest (< 30 m) amplitude and may
701
702 294 preserve a relict - and often dismantled - ferricrete inherited from a former glacis surface on
703
704 295 their interfluves (called, in this case, residual hills) (Fig. 6b). Rolling pediplains are by far the
705
706 296 most common regional landform associations in today's West Africa and are locally studded
707
708 297 with relict glacis plateaus of limited extent that were not reduced to residual hills. They are
709
710 298 mostly inherited from past glacis landscape stages. Middle glacis pediplains (Fig. 6b) are the
711
712 299 best preserved in today's landforms although the downslope portions of such
713
714
715
716
717
718
719
720

721
722
723 300 paleolandscapes are generally re-cut by the Low glacis (e.g., Fig. 6b). Regional correlations of
724
725 301 glacis systems chronology may be deciphered along 10-100 km long transects going from
726
727 302 piedmont contexts - where the pediment stepping pattern is well defined - to rolling
728
729 303 pediplain contexts. Field investigations restricted to the scale of an interfluvium or a few
730
731
732 304 interfluviums are indeed not sufficient to elaborate a landscape chronology given the lateral
733
734 305 variability of the paleolandforms preservation patterns (see section 6.2).
735

736 306

737 738 307 *4. 2. Relief dissection patterns*

739
740 308 Repeated relief dissection favored the stepping of successive glacis in piedmont
741
742 309 contexts (Figs. 8a and 8b). The relative elevation between successive glacis does not
743
744 310 systematically decrease downslope i.e. away from the residual massif (Fig. 8a) contrary to
745
746 311 the common slope evolution models (e.g., Summerfield, 1991, pp. 457-467). It may increase
747
748 312 downslope toward the main drainage axes (Grandin and Joly, 2008; Fig. 8b). The dissection
749
750 313 of rolling pediplains leads to more complex stepping patterns owing to whether erosion
751
752 314 focused on residual hills or valleys from one glacis landscape stage to the next (Figs. 8c to 8e).
753
754 315 Inselbergs are locally preserved on granitoid terrains. They seem to have formed by a
755
756 316 combination of geological factors among which rock structural control, the original relief of
757
758 317 an old and thick weathering profile and the polycyclic denudation history are the most
759
760 318 important (Thomas, 1978, 1994).
761

762
763 319 In case where a glacis is not strictly stepped into an older glacis, mostly as a
764
765 320 consequence of limited base-level fall (i.e., river down-cutting) during its development, a
766
767 321 composite (i.e., polygenic) landsurface forms. Slight oblique leveling of the early glacis up to
768
769 322 a certain elevation by the younger glacis may lead to a more or less expressed change of
770
771 323 slope in that landsurface (Fig. 6). Polygenic development is also mostly expressed in the
772
773 324 downslope parts of two successive glacis that merge into a single graded (and often
774
775
776
777
778
779
780

781
782
783 325 functional) surface, whereas they are stepped higher up in the landscape (e.g., Fig. 6a).
784
785 326 Polygenic High/Middle glacis are observed but the most common cases of polygenic
786
787 327 developments are between the Middle and Low glacis, particularly in dry regions (Boulet,
788
789 328 1970; Eschenbrenner and Grandin, 1970). In the Sahelian zone (Fig. 2) where base-level fall
790
791 329 has been limited between the Intermediate Surface and the High glacis approaching the
792
793 330 Niger River (e.g. Grimaud et al., 2014), polygenic glacis development is common between
794
795 331 these two landscape systems (see also Fig. 5).
796
797

798 332 Relief dissection and denudation did not allow a good preservation of High glacis
799
800 333 stage rolling pediplains of significant regional extent with the exception of specific areas of
801
802 334 flat sandstones. Those rolling pediplains generally have longer (>10 km) wavelength than
803
804 335 those of the Middle glacis. Low glacis pedimentation did not produce rolling pediplains.
805
806 336 From the Soudanian zone southward (Fig. 2), Low glacis systems mostly contributed to re-
807
808 337 cut or straighten downslope portions of Middle glacis landscapes (often producing a
809
810 338 polygenic surface). Further north, the Low glacis system largely developed and is still
811
812 339 functional (see below).
813
814

815 340

817 341 *4. 3. Sequential landscape development*

819 342 The High glacis pedimentation period has produced a multi-concave pediplain over
820
821 343 granite-greenstone terrains or dolerite sills provinces. The pediplain was studded with
822
823 344 relictual reliefs inherited from the bauxitic and/or the Intermediate landscape stages
824
825 345 (Grimaud et al., 2015; Figs. 7 and 9). In other geological provinces, the High glacis landscape
826
827 346 consisted in a rolling pediplain of long (>10 km) wavelength (e.g., Fig. 8c). Middle and Low
828
829 347 glacis pedimentation cycles generally formed narrower valleys than those of the High glacis
830
831 348 landscape (e.g., Figs. 8d and 8e), especially within and south of the Soudanian zone (Fig. 2).
832
833 349 Figure 10 summarizes the sequential development of a type West African landscape. Each of
834
835
836
837
838
839
840

841
842
843 350 the successive landscape stages incorporates relict landforms of various earlier generations.
844
845 351 It is a composite landsurface comprising inselbergs (not shown on the Figure), relicts of the
846
847 352 bauxitic and/or Intermediate landscapes and former glacis (Fig. 10). The Middle and Low
848
849 353 glacis landscape stages therefore integrate increasing complexity compared to earlier
850
851 354 landscapes. This is explained by a decreasing pedimentation efficiency manifested by
852
853 355 generally narrower glacis widths and would be consistent with the decreasing duration of
854
855 356 pedimentation periods through time i.e., 6, 4 and 1 My for the High, Middle and Low glacis,
856
857 357 respectively (Beauvais and Chardon, 2013). Relics of the entire West African paleolandscape
858
859 358 sequence are not always preserved on a 10-100 km scale (Fig. 10). Besides an evolving
860
861 359 drainage density, landscape stages succession implies slope direction changes or reversals
862
863 360 (Fig. 10), with implication for material transit patterns on glacis slopes through time (section
864
865 361 7.2).

866
867
868 362 Multi-concave pediplains are mostly restricted to granite-greenstone terrains or
869
870 363 areas of mafic substrate owing to iron-rich lithologies, which are more alterable than felsic
871
872 364 rocks. They tend therefore to produce thick and massive duricrusts, which have a protective
873
874 365 effect once the landscape they cap is submitted to dissection. The development of piedmont
875
876 366 glacis is favored below scarp-bounded relict paleolandscapes, the scarp being armored by
877
878 367 the ferricrete. In such contexts, glacis are also prone to dissection because their capping
879
880 368 ferricretes are mostly cemented debris of Al-Fe crusts inherited from the older, inverted
881
882 369 landsurfaces and are therefore iron-rich and resistant even though they are not underlain by
883
884 370 mafic rocks (see section 5). Over iron-poor lithologies and away from mafic sources, both the
885
886 371 lower iron content and thickness of the duricrusts reduce their strength. Pedimentation is
887
888 372 therefore more efficient at leveling interfluves to produce rolling pediplains and no strict
889
890 373 relief inversion takes place.

891
892
893
894 374
895
896
897
898
899
900

901
902
903 375 4. 4. *Summary*
904

905 376 Notwithstanding the regional spatial variability of the glacis stepping patterns
906
907 377 described above, each glacis system has type-geomorphic characteristics that may be
908
909 378 summarized as follows (Grandin and Joly, 2008). Relics of the High glacis are abandoned as
910
911 379 plateaus or residual hills that rarely occupy more than 20 % of the current landsurface over
912
913 380 100 x 100 km areas. They can attain heights of more than 100 m above the local base level for
914
915 381 the upslope portion of very large relics and not more than 30 m for their lowermost portions
916
917 382 along the main drainage axes. Middle glacis are generally eroded downslope and are still
918
919 383 connected to their upslope reliefs. They are preserved as low plateaus or relictual hills in dry
920
921 384 regions (Fig. 2), where the Low glacis developed at their expense. Large Middle glacis
922
923 385 remnants may still be functional i.e., currently subjected to runoff and sediment transport.
924
925 386 Low glacis occupy a large part of the landsurface and are still functional in dry climatic zones,
926
927 387 where they are connected to the local base level. Elsewhere, river alluviums usually mask the
928
929 388 incision of Low glacis of a few meters.
930

931
932
933 389 Excavation of the Bauxitic African Surface varies from ca. 500 m in central Côte
934
935 390 d'Ivoire to less than 30 m near the Niger River in Central Mali, with a mean value around 300
936
937 391 m (Beauvais and Chardon, 2013; Grimaud et al., 2014; Fig. 2). Incision of the High glacis is
938
939 392 typically of 50-80 m, whereas the High glacis pedimentation period contributed to 40-130 m
940
941 393 of incision of the Intermediate landscape (Grimaud et al., 2018). The three pedimentation
942
943 394 cycles therefore contributed as much excavation of the African bauxitic Surface (90-210 m)
944
945 395 as the Intermediate period of erosion (75-200 m; Grimaud et al., 2018) over comparable time
946
947 396 spans of 22-24 My (Fig. 2), leading to a long-term denudation rate of 3-9 m/My.
948
949 397 Pedimentation efficiency decreased over the Neogene in West Africa. Given the glacis widths
950
951 398 and ages in the Guinean and Soudanian zones (Grimaud et al., 2015; Fig. 2), lateral growth
952
953 399 rate ranges of glacis would typically be of 0.75-3 km/My and 0.15-1 km/My for the High and
954
955
956
957
958
959
960

961
962
963 400 Middle glacis system, respectively. Given its restricted development in the same climatic
964
965 401 zones (e.g., Fig. 7), the Low glacis system grew at lower rates (0.03-0.75 km/My), which are
966
967 402 those of the Plio-Quaternary Southwestern United States' pediments (0.03-0.36 km/My;
968
969 403 Dohrenwend and Parsons, 2009).
970
971
972 404

973 974 405 **5. Glacis regolith and weathering patterns**

975
976 406 Similarly to pedimentation efficiency, the intensity of weathering and duricrusting of
977
978 407 the glacis decreases generally from the High to the Low glacis (Boulangé et al., 1973; Grandin,
979
980 408 1976; Tardy and Roquin, 1998). This decrease is consistent with long-term Neogene climate
981
982 409 cooling and the progressively shorter duration of humid periods required for the weathering
983
984 410 of the glacis material (Beauvais et al., 2008; Beauvais and Chardon, 2013; Fig. 4). The spatial
985
986 411 and temporal variability in the nature of glacis surfaces and regolith (Fig. 11) is further
987
988 412 controlled by the interplay of three main factors, which are (i) the nature of the substrate cut
989
990 413 by pedimentation, (ii) the nature, transport dynamics and degree of preservation of clastic
991
992 414 sedimentary material that has been transiting on the glacis and (iii) the nature and intensity
993
994 415 of weathering and duricrusting undergone by the glacis after their formation. Figures 12 to
995
996 416 14 illustrate field examples of the main types of glacis regolith / ferricretes and Figure 15
997
998 417 represents various types of regolith associations on glacis. A synthetic model of the relations
999
1000 418 between pedimentation and weathering is provided in Figure 16.
1001
1002
1003
1004 419

1005 1006 420 *5. 1. Conglomeratic regolith, ferricrete and slope processes*

1007
1008 421 Remarkable and common glacis ferricretes derive from cementation of
1009
1010 422 conglomeratic material transiting on the glacis surface. The most spectacular ones are
1011
1012 423 matrix- or block supported debris flows. Depending on the landscape having been stripped
1013
1014 424 off and the pedimentation regime, conglomerates' elements range from gravel to boulder
1015
1016
1017
1018
1019
1020

1021
1022
1023 425 and consist of bauxite, Intermediate ferricrete, earlier glacia ferricrete, iron oxy-hydroxide
1024
1025 426 nodules and/or quartz debris (Figs. 12b to 12e). Conglomerates' matrixes comprise reworked
1026
1027 427 weathering profile materials ranging from clays to sands (former saprolite) and gravels made
1028
1029 428 of ferruginous nodules and quartz debris. Apart from quartz, the occurrence of fresh bedrock
1030
1031 429 clasts in debris flows is extremely rare, indicating that mostly regolith was stripped-off
1032
1033
1034 430 and/or submitted to landsliding to produce debris flows. When present in glacia transported
1035
1036 431 regolith, bedrock clasts are almost always highly ferruginized to the point of being a massive
1037
1038 432 ferricrete preserving bedrock structures such as schistosity. Such ferricretes are typical of
1039
1040 433 the Intermediate weathering profile (Fig. 12d).

1041
1042 434 Lower-slope alluvial sedimentary facies are also common, especially in the
1043
1044 435 downslope parts of glacia, even though ferruginization contributed to alter sedimentary
1045
1046 436 structures in glacia alluviums such as parallel and oblique stratifications and cross beds. The
1047
1048 437 occurrence of rounded quartz pebbles in the most distal parts of glacia near river drains
1049
1050 438 indicates that glacia pass downslope to alluvial terraces (the "glacia-terrace" concept of
1051
1052 439 Michel (1959, 1973) and Vogt (1959a)). Erosional unconformities and disconformities at the
1053
1054 440 base or within the glacia sedimentary cover are consistent features of truncation and
1055
1056 441 deposition by channelized to sheet flow down the glacia slopes. The most obvious (and best
1057
1058 442 preserved) alluvial features are channels identifiable along the basal erosional surface of the
1059
1060 443 glacia sedimentary layer (Fig. 12f). Beddings are also observed as separating successive
1061
1062 444 debris flows or within sedimentary units.

1063
1064 445 Sedimentary patterns vary spatially from coarse flows to braided channels at the
1065
1066 446 scale of single large glacia relics. This indicates space-time interplay of debris flows and
1067
1068 447 sheet floods comparable to those observed on Quaternary or functional alluvial fans and
1069
1070 448 pediments of arid or semi-arid regions of the world (Bull, 1977; Oberlander, 1997;
1071
1072 449 Dohrenwend and Parsons, 2009). Besides, functional glacia in the Soudanian and Sahelian
1073
1074
1075
1076
1077
1078
1079
1080

1081
1082
1083 450 zones (Fig. 2) provide an actualistic perspective onto the sedimentary patterns and
1084
1085 451 alluvial/colluvial processes having operated on the past West African glacis before
1086
1087 452 duricrusting (Grandin and Joly, 2008). Water and sediment transport modes on glacis
1088
1089 453 precluded the maintenance of ramified river networks but instead favored dense and
1090
1091 454 unstable channel networks that were active only during rainy episodes. Rivers maintained
1092
1093 455 their courses only at the downslope junctions of converging glacis, where alluvial
1094
1095 456 sedimentary facies can be found (e.g., Figs. 8, 9 and 10).

1098 457 Glacis conglomeratic ferricretes are usually underlain by a carapace and/or a
1099
1100 458 mottled clays horizon (Fig. 15a), implying that duricrusting is confined to the conglomeratic
1101
1102 459 layer. In other cases, thick conglomeratic covers are duricrusted only superficially, meaning
1103
1104 460 that part of their thickness became a carapace. Glacis conglomeratic overburdens are not
1105
1106 461 necessarily cemented (Fig. 12a), allowing to access original sedimentary textures that have
1107
1108 462 not been obscured by iron segregation and cementation. The conglomerates and their
1109
1110 463 matrixes consist almost exclusively of reworked Al-Fe duricrusts, carapace, mottled clays
1111
1112 464 and saprolite, which are all rich in iron oxy-hydroxides. Large quantities of iron are therefore
1113
1114 465 available in the conglomerates. Remobilization of that iron should favor cementation of the
1115
1116 466 glacis sedimentary overburden by oxy-hydroxides to form ferricretes. Such cementation
1117
1118 467 scenarios are attested to by the common examples of glacis ferricretes directly overlying
1119
1120 468 fresh bedrock. This shows that ferricretes do not result from the sole relative accumulation
1121
1122 469 of iron in a horizon of the weathering profile having successively gone through bedrock,
1123
1124 470 saprolite, mottled clays and carapace stages. In other words, lateritic weathering is not a
1125
1126 471 necessary condition for duricrusting (Grandin, 2008).

1130 472

1132 473 *5. 2. Non-conglomeratic ferricretes, relationships with the underlying regolith*

1141
1142
1143 474 Some glacia ferricretes are composite, comprising an upper conglomeratic layer and
1144
1145 475 a lower layer that results from iron aggradation/segregation and induration of the
1146
1147 476 underlying carapace (Figs. 13 and 15b). In this case, duricrusting appears to have taken place
1148
1149 477 beyond the base of the sedimentary overburden and the relative contributions of in-situ iron
1150
1151 478 accumulation (from segregation within the carapace) and absolute iron input from the
1152
1153 479 clastic sediments would be difficult to assess. Conglomeratic ferricretes are also seen to rest
1154
1155 480 directly atop a saprolite or a saprock (i.e., basal core stone-bearing saprolite; e.g., Figs. 12b,
1156
1157 481 12f and 15c) or even the bedrock. This indicates that pedimentation truncated a weathering
1158
1159 482 profile by removing its mottled clays, carapace or part or the entire thickness of its saprolite.
1160
1161 483 Those truncations are currently seen in the field and have been also imaged by geophysics
1162
1163 484 (e.g., Beauvais et al., 2003). The formation of iron nodules and/or iron segregation may be
1164
1165 485 observed immediately under the conglomerate in the truncated weathering profile,
1166
1167 486 indicating that ferruginization was not restrained to the transported sedimentary layer and
1168
1169 487 that iron originated from the conglomeratic cover. Whether the weathering horizons
1170
1171 488 underlying a conglomeratic ferricrete developed onto a preexisting saprolite or from pristine
1172
1173 489 weathering of bedrock exhumed by pedimentation would be difficult to assess in the field.

1174
1175 490 Glacia ferricretes developed from fine-grained material (clay, silt, sand or a mix of
1176
1177 491 those) have vermicular to nodular structures (Fig. 14) typically resulting from the maturation
1178
1179 492 of mottled clays by iron concretion/segregation (Tardy, 1997; Fig. 15d). Those ferricretes are
1180
1181 493 preferentially found on the distal parts of wide glacia and are ubiquitous in rolling pediplain
1182
1183 494 contexts i.e., on lower-gradient slopes than the debris flows, which are mostly restricted to
1184
1185 495 piedmont contexts. In conglomeratic ferricretes, matrixes are vermicular, as is the
1186
1187 496 duricrusted material underlying conglomeratic layers of composite ferricretes (e.g., Fig. 13).
1188
1189 497 If a comprehensive succession of weathering horizons exists under the vermiform/nodular
1190
1191 498 ferricrete down to the bedrock, the glacia surface could be considered as erosional, and the
1192
1193
1194
1195
1196
1197
1198
1199
1200

1201
1202
1203 499 ferricrete as genetically linked to the underlying bedrock (e.g., Fig. 15d). But weathering of a
1204
1205 500 composite section made of bedrock and/or saprolite topped by a fine-grained glacis
1206
1207 501 overburden would end up producing a comparable profile (Fig. 15e). Fine-grained
1208
1209 502 overburdens being mostly reworked saprolite, it would be difficult to locate the boundary
1210
1211
1212 503 between the in-situ and transported portions of the section, which would have been further
1213
1214 504 obscured by weathering after pedimentation, unless a major break in lithology or
1215
1216 505 granulometry be identified (Fig. 15e). The very large areas of functional glacis exposing
1217
1218 506 alluviums composed of clays, silts and sands suggest analog fine-grained overburdens for
1219
1220 507 past glacis systems. Weathering/duricrusting of such overburdens should end up forming a
1221
1222 508 typical vermicular / nodular ferricrete that may top weathering horizons mimicking those
1223
1224 509 produced on bedrock (e.g., Fig. 13). Most weathering profiles of West African ferricrete-
1225
1226 510 capped glacis weathering profiles may therefore be composed of fine-grained transported
1227
1228 511 material instead of resulting from weathering of bedrock even though the ferricrete is not
1229
1230 512 conglomeratic.

1233 513 There is commonly a spatial variability in the nature of the surface at the scale of a
1234
1235 514 single glacis that comprises ferricrete-free surface areas and (erosional or detrital) ferricrete-
1236
1237 515 capped surface areas (Fig. 11). In other words, the detrital layer does not systematically
1238
1239 516 cover an entire glacis and duricrusting does not necessarily affect an entire glacis surface.
1240
1241 517 Ferricrete-free glacis surfaces may be erosional and expose exhumed regolith developed
1242
1243 518 from bedrock (Fig. 15f). However, the possibility that they actually expose transported (fine-
1244
1245 519 grained) saprolite that escaped duricrusting is not precluded (Fig. 15g). In this case, only a
1246
1247 520 detailed petro-geochemical investigation would allow distinguishing an in-situ saprolite
1248
1249 521 from an overlying transported layer.

1252 522 Contrary to the inselbergs and residual massifs they contributed to exhume, West
1253
1254 523 African glacis do not expose bedrock but regolith. This could suggest that weathering has

1261
1262
1263 524 turned bedrock leveled by pedimentation into regolith. But observations along river cuts
1264
1265 525 and in trenches indicate that glacis are essentially cut into a saprolite previously formed
1266
1267 526 during an earlier weathering period (e.g., Figs. 11, 12b and 15). Observations of the steep
1268
1269 527 stripped flanks of bauxite plateaus of dry regions show that the relief carved into the bauxitic
1270
1271 528 surface by the glacis is entirely made of saprolite more than 40 m thick (e.g., Fig. 6a). With
1272
1273 529 the exception of inselbergs, the lower flanks of residual massifs and low-lying outcrops
1274
1275 530 exhumed after abandonment of the Low glacis, bedrock is mostly exposed in riverbeds.
1276
1277 531 The ubiquity of glacis systems throughout West Africa is explained by the fact that they were
1278
1279 532 easily cut through regolith instead of bedrock, as also shown for the pediments of Central
1280
1281 533 Australia by Mabbutt (1966). Most of the regolith thickness available for stripping by
1282
1283 534 pedimentation was likely produced by the Bauxitic (and Intermediate) periods(s) of intense
1284
1285 535 lateritic weathering (Grimaud et al., 2015). The thin (< 20 m) weathering profiles genetically
1286
1287 536 linked to each glacis would suggest that weathering phases following pedimentation periods
1288
1289 537 produced a regolith layer available for stripping during the next pedimentation period (e.g.,
1290
1291 538 Millot, 1980). This hypothesis would apply to the lowermost parts of glacis cut into bedrock
1292
1293 539 (e.g., cross-section, Fig. 15) and would be supported by the comparable heights of the
1294
1295 540 weathering profile and the vertical separation between successive glacis.
1296
1297
1298

1299 541 Notwithstanding the spatial variability in the nature of individual glacis surfaces and
1300
1301 542 associated regolith, main type-characteristics of ferricretes and weathering patterns of each
1302
1303 543 glacis system may be synthesized as follows (Grandin, 2008). The High glacis ferricrete can
1304
1305 544 reach 10 m in thickness in piedmont contexts and the underlying weathering profile rarely
1306
1307 545 exceeds 20 m. Middle glacis ferricretes do not exceed 5 m and are generally limited to 1 to 2
1308
1309 546 m. Their underlying weathering profile is reduced to a few meters and is not as kaolinite rich
1310
1311 547 as that of the High glacis. Ferricretes of functional Middle glacis often show evidence for
1312
1313 548 dissolution and end up acquiring vacuolar to cavernous textures (Leprun, 1979). The Low
1314
1315
1316
1317
1318
1319
1320

1321
1322
1323 549 glacis bear a thin (< 1 m) ferricrete or, more generally, at best a carapace. Carbonate
1324
1325 550 concretions may develop under its erosional surface or in its sedimentary overburden and
1326
1327 551 neo-formed clays are mostly smectites.
1328

1329 552

1330
1331
1332 553 *5. 3. Recently remobilized regolith and alluviums*
1333

1334 554 Low glacis are commonly overlain by unconsolidated alluvial and aeolian sediments
1335
1336 555 (Fig. 15h), which are actively reworked by pedimentation during each rainy season
1337
1338 556 (especially in the Soudanian and Sahelian zones; Fig. 2). It is also the case for large functional
1339
1340 557 Middle glacis. Active alluvial fans also occupy upslope sections of functional glacis in
1341
1342 558 piedmont contexts, at least in the dry zones (e.g., Fig. 5). Streams that have incised the glacis
1343
1344 559 sedimentary overburden generally flow atop the ferricrete or the carapace and expose
1345
1346 560 sections that commonly exceed 2 m in thickness. Overburdens occupy huge areas and
1347
1348 561 develop soils that are exploited for agriculture. But those soils almost never derive from
1349
1350 562 weathering profiles connected to the underlying bedrock because they are transported and
1351
1352 563 almost always overly conglomeratic ferricretes (Fig. 15h).
1353

1354
1355 564 Post-Low glacis (i.e., Quaternary) river alluviums are preserved along the drainage
1356
1357 565 network and often correlate with the unconsolidated glacis cover (Fig. 11; Fig. 15, upper
1358
1359 566 cross-section). The oldest and most remarkable alluvial terrace of regional extent has been
1360
1361 567 reported and correlated from the main rivers of Northern Guinea, Senegal, Southwestern
1362
1363 568 Mali, Ivory Coast and Burkina Faso (Vogt, 1959a, 1959b; Michel, 1969, 1973; Eschenbrenner
1364
1365 569 and Grandin, 1970; Grandin, 1976). This terrace is floored by a cemented conglomerate (the
1366
1367 570 “graviers sous-berge”) that occupies the riverbeds and has been incised of less than a few
1368
1369 571 meters (Fig. 15). Aggradation/incision cycles younger than the conglomerate have been
1370
1371 572 recognized but no systematic regional patterns have been deciphered yet (Thomas and
1372
1373
1374
1375
1376
1377
1378
1379
1380

1381
1382
1383 573 Thorpe, 1985; Hall et al., 1985; Thomas et al., 1985; Teeuw et al., 1991; Ouangrawa et al.,
1384 574 2000).

1387 575

1389 576 **6. Extent and variability of the glacis record in West Africa**

1392 577 *6.1. Geomorphic provinces and areal extent of glacis*

1394 578 The compilation of a regional landform-regolith map (Fig. 17) shows that the relics of
1395
1396 579 the three glacis systems occupy an overwhelming areal proportion of the landsurface, with
1397
1398 580 the exception of a few regions of specific geological substrate, topography or active
1399
1400 581 sedimentation. Laterally continuous bauxite-capped landforms of the African Surface form
1401
1402 582 mappable units restrained to some highly-elevated (> 500 m) areas of Pre-Cenozoic
1403
1404 583 sandstones and/or high concentration of dolerite sills (Fig. 17). Paleolandscapes capped by
1405
1406 584 the Intermediate ferricrete are well preserved on Cenozoic sedimentary basins and their
1407
1408 585 margins, as well as on Pre-Cenozoic tabular sandstones flanked by rock escarpments (Fig.
1409
1410 586 17).

1413 587 The Archean and Paleoproterozoic granite-greenstone terrains, their adjoining
1414
1415 588 mobile belts and the remaining tabular sediments of the sub-Saharan area are characterized
1416
1417 589 by glacis composite landscapes (Fig. 17) such as those illustrated on Figures 5- 8, 10 and 15.
1418
1419 590 In those landscapes, the High glacis system always occurs as relict plateaus or hills. Distant
1420
1421 591 relict massifs of the Bauxitic and/or Intermediate landscape and inselbergs remain (e.g., Fig.
1422
1423 592 6a). A large part of the composite glacis landscape geomorphic province is a Middle-Low
1424
1425 593 glacis rolling pediplain locally preserving High glacis remnants as interfluves (e.g., Figs. 6b).
1426
1427 594 The relative extent of the Low glacis system tends to grow northward going across the
1428
1429 595 Soudanian zone to become maximal in the Sahelian zone where a Low glacis province is
1430
1431 596 defined (Figs. 1 and 17b) as a vast and very flat pediplain with tens of kilometers-wide glacis
1432
1433 597 that are functional. The efficiency of pedimentation is favored by both the Sahelian climate
1434
1435
1436
1437
1438
1439
1440

1441
1442
1443 598 and the limited (< 40 m) local relief left since the abandonment of the bauxitic African
1444
1445 599 surface along the considered portion of the Niger River Valley (Grimaud et al., 2014; Chardon
1446
1447 600 et al., 2016).

1449 601 In the Saharan zone (Figs. 1 and 17b), low lands consist of active regs, dune fields
1450
1451 602 (ergs) and fluvio-aeolian sandplains that mostly blanket the subdued Intermediate or Low
1452
1453 603 glacis landscapes, whilst crystalline substrate generally crops out. South of the Sahelian
1454
1455 604 zone, bedrock is exposed mostly on the steep dissected slopes of regional topographic
1456
1457 605 massifs upon basement substrate (Figs. 1 and 17).

1459 606 The bauxitic African Surface was an etchplain i.e., a low-relief continental scale
1460
1461 607 landsurface underlain by a thick regolith resulting from a protracted period of intense
1462
1463 608 weathering and correlatively subdued mechanical erosion. As a result of stepwise dissection
1464
1465 609 of that landsurface by pedimentation, most of its regolith mantle has been removed so that
1466
1467 610 sub Saharan West Africa has become a stripped etchplain, whose remnants are preserved
1468
1469 611 only in a few patches of relict bauxitic landscapes (Fig. 17) and individual occurrences
1470
1471 612 scattered over the sub region (Beauvais and Chardon, 2013; Chardon et al., 2016). The glacis
1472
1473 613 composite landscape province (Fig. 17) constitutes the stripped African etchplain.
1474
1475 614

1476
1477
1478
1479 615

1480 615 *6. 2. Climatic zonation of paleo-glacis systems and glacis degradation processes*

1481 616 The preservation of each glacis system depends on (i) the efficiency of planation (i.e.,
1482
1483 617 the capacity of pedimentation to form wide glacis), (ii) the intensity of duricrusting and (iii)
1484
1485 618 the magnitude of glacis dismantling (Grandin, 1976). Those three factors are chiefly
1486
1487 619 dependent on latitude (Fig. 18). Their spatial variations from one glacis system to the next
1488
1489 620 could suggest an evolving latitudinal climatic zonation of West Africa over the last ca. 25 Ma
1490
1491 621 notwithstanding the duration of each glacis cycle (Fig. 18).
1492
1493
1494
1495
1496
1497
1498
1499
1500

1501
1502
1503 622 Under dry climate, glacis tend to be preserved in such a way that duricrusting
1504
1505 623 molded their pristine shape and pedimentation-driven landscape dissection leads to
1506
1507 624 plateaus with sharp edges. On-going pedimentation can eventually turn the plateau into a
1508
1509 625 residual hill (Fig. 19a) flanked by concave glacis slopes. Weathering is subdued during this
1510
1511 626 process and mechanical dismantling of the ferricrete takes place while pedimentation
1512
1513 627 disperses its erosional products downslope. Such a morphogenesis typically produces
1514
1515 628 rolling pediplains (Fig. 6b). In zones of intense pedimentation, residual hills are ultimately
1516
1517 629 erased to produce very low amplitude pediplains made of wide glacis. Under humid climates,
1518
1519 630 and typically in the forest, weathering assists degradation of the plateau-flanking slopes that
1520
1521 631 evolve by a combination of compaction of the residuum, creep and colluvial processes to
1522
1523 632 acquire convex profiles, while the ferricrete is being dissolved and dismantled and collapses
1524
1525 633 onto its underlying weathering profile that is reactivated (Fig. 19b). The combination of
1526
1527 634 those processes produces a common type of stone line i.e., a layer of angular or sub-
1528
1529 635 rounded quartz gravels and pebbles, which result from the dislocation of quartz veins by
1530
1531 636 compaction. The resulting residual hills are “demi-oranges” (Thomas, 1994) that form
1532
1533 637 multiconvex plains typical of today’s shields’ tropical rain forest (e.g., Rohdenburg, 1982;
1534
1535 638 Lecomte, 1988; Bitom et al., 2004).

1539 639 Recent morphogenesis (i.e., having taken place after duricrusting of the Low glacis
1540
1541 640 around 3 Ma ago) tends to degrade relict High and Middle glacis. Semi-arid climates of the
1542
1543 641 Sahelian and southern Saharan zones favor the development of very flat pediplains, whereas
1544
1545 642 the sub-equatorial humid climate of the Forest zone drives degradation of glacis to form
1546
1547 643 multi-convex plains. A latitudinal gradient must exist between these two modes of modern
1548
1549 644 morphogenesis across the Soudanian and especially the Guinean zones (Grandin, 1976; Figs.
1550
1551 645 1 and 17). A somewhat comparable latitudinal morphoclimatic gradient applied to each
1552
1553 646 paleo-glacis system, although with potentially contrasted climatic zone widths (Fig. 18).
1554
1555
1556
1557
1558
1559
1560

1561
1562
1563 647 Such a gradient explains systematic limited planation and duricrusting in the South (Fig. 18),
1564
1565 648 further enabling past and recent “humid” morphogenesis in today’s Forest zone.
1566
1567 649 Forest, savanna and semi-arid tropical environments have long been considered as
1568
1569 650 contrasted morphoclimatic contexts (e.g., Büdel, 1982). The latitudinal climatic zonation of
1570
1571 651 both past pediment systems and today’s landform evolution processes over West Africa
1572
1573 652 argues for a continuous spatial pattern of pedimentation - considered as the combination of
1574
1575 653 all slope shaping processes – between an arid end-member and a humid Equatorial end-
1576
1577 654 member across the inter-tropical zone (e.g., Holmes, 1955; Millot, 1980, 1983; Rohdenburg,
1578
1579 655 1969, 1982).
1580
1581 656

1582
1583
1584 657 *6. 3. Morphoclimatic specificity of West Africa, comparison with neighboring regions*
1585

1586
1587 658 The remarkable preservation of the West African glacis systems is related to the sub
1588
1589 659 region having remained for more than 100 Ma in the zone of optimal weathering conditions
1590
1591 660 for the production of Fe and Al crusts (Tardy and Roquin, 1992, 1998; Fig. 2). Such a
1592
1593 661 latitudinal stability is due to the pinning down of the African plate’s rotation pole near the
1594
1595 662 Coast of Guinea (Tardy and Roquin, 1998). Optimal duricrusting worked in two ways for the
1596
1597 663 preservation of glacis. First, weathering/duricrusting produced a major original stock of iron
1598
1599 664 during the bauxitic weathering period i.e., from the Late Cretaceous to the mid Eocene (with
1600
1601 665 a peak between 55 and 45 Ma). This original iron stock was then recycled in the Intermediate
1602
1603 666 landscape and by each glacis system (Grandin, 1976). Second, optimal conditions favored
1604
1605 667 duricrusting of Al-Fe crust dispersed on glacis to form protective duricrusts that favored
1606
1607 668 landscape dissection and paleo-glacis preservation.

1608
1609 669 Regions located further to the East and encompassing the same current latitudinal
1610
1611 670 band as sub Saharan West Africa have undergone a greater northward shift across the inter
1612
1613 671 tropical zone (and beyond) since the Late Cretaceous that likely resulted in a contrasted
1614
1615
1616
1617
1618
1619
1620

1621
1622
1623 672 morphoclimatic record. Nevertheless, those regions preserve a record of stepped pediment
1624
1625 673 systems that may correlate with those of West Africa (e.g., Fölster, 1964). A “High” glacia
1626
1627 674 system has been reported regionally under what appears as the remnants of the
1628
1629 675 Intermediate ferricrete-capped paleolandscape (De Swardt, 1964; McFarlane, 1976, and
1630
1631 676 references therein) but no systematic correlation scheme has emerged yet. Further South in
1632
1633 677 Central Africa, pediment systems occupy large regions around and within the Congo Basin
1634
1635 678 (Ruhe , 1956; Guillocheau et al., 2015). The latter authors proposed a tentative correlation
1636
1637 679 between their 9-planation surfaces model (among which the 5 latest are pediment systems)
1638
1639 680 and the West African morphoclimatic sequence as synthesized by Beauvais and Chardon
1640
1641 681 (2013). Degradation of glacia systems in Equatorial Africa under perhumid climates would be
1642
1643 682 a challenge for regional morphoclimatic correlation across the intertropical belt.
1644
1645
1646
1647 683

1648 684 **7. Implications for mineral exploration**

1650
1651 685 The great extent and spatial variability of the West African glacia landform-regolith
1652
1653 686 associations (Fig. 17) prompt caution when targeting suitable spots for surface sampling that
1654
1655 687 would reflect bedrock geochemistry as accurately as possible. Glacia regolith profiles are
1656
1657 688 indeed composite and polycyclic, resulting from uneven weathering and duricrusting of
1658
1659 689 slopes cut into a pre-existing regolith and/or the bedrock and overlain by discontinuous
1660
1661 690 detrital sedimentary layers.
1662

1663 691

1664 692 *7.1. Accessibility to the geological substrate*

1665
1666 693 Glacia ferricretes all represent an obstacle to access bedrock geochemistry. There
1667
1668 694 are three main reasons for this. First, they often represent sedimentary covers that are
1669
1670 695 allochthonous (Figs. 15a-15c, 15e) and do not derive from their underlying regolith by
1671
1672 696 weathering. Second, even if formed exclusively in-situ, and as the most evolved product of
1673
1674
1675
1676
1677
1678
1679
1680

1681
1682
1683 697 weathering, ferricretes would have lost most of the geochemical characteristics of the
1684
1685 698 bedrock (e.g., Tardy et al., 1988; Boeglin and Mazaltarim, 1989; Roquin et al., 1990). Third,
1686
1687 699 solute elemental transfers through the regolith and sedimentary cover down the glacis slope
1688
1689 700 can contribute to absolute elemental accumulation in the ferricrete, especially in iron
1690
1691 701 (Maignien, 1958, 1966; Ollier and Galloway, 1990, Beauvais, 1999; Brown et al., 2003).
1692
1693 702 Therefore, vertical geochemical mass balances through ferricrete-capped glacis weathering
1694
1695 703 profiles are often misleading indicators of weathering-controlled dispersion of bedrock
1696
1697 704 elemental concentrations. Ferricrete-free glacis surfaces pose another sizable exploration
1698
1699 705 issue. Only erosional portions of such surfaces would provide direct access to a saprolite
1700
1701 706 preserved on its parental bedrock (Fig. 15f), providing they are identified as such and not
1702
1703 707 mistaken for transported saprolite (Fig. 15g). Loose sedimentary glacis overburdens (Fig.
1704
1705 708 15h) mask their substrate. They are commonly thick (> 2m), overly a detrital ferricrete and
1706
1707 709 may be mistaken for soils. It is why even sampling at 50 cm depth - as often undertaken in
1708
1709 710 such material - is not appropriate to attain the saprolite preserved on its parental bedrock.
1710
1711

1712
1713 711 Only sampling of the bedrock or the in-situ preserved saprolite is reliable for
1714
1715 712 characterizing the geological substrate's geochemistry (propitious locations would be edges
1716
1717 713 of glacis plateaus that expose weathering horizons under the ferricrete). In all other
1718
1719 714 situations, a surface geochemical anomaly on a glacis can have several meanings. In the best
1720
1721 715 case, the surface is erosional and ferricrete-free, the anomaly signing an underlying bedrock
1722
1723 716 concentration (e.g., Au, Pt, Zn, Cu). The present work however suggests that such
1724
1725 717 configuration is rarely demonstrated. In all other - most common - cases, the anomaly would
1726
1727 718 be ambiguous. It may have been "transported" with the sedimentary cover on the glacis by
1728
1729 719 pedimentation (e.g., Sanfo et al., 1992) or may be the expression of a potentially complex
1730
1731 720 and very wide dispersion halo having been elongated downslope. Such a halo could also at
1732
1733 721 least partly result from geochemical dispersion of a bedrock anomaly through a transported
1734
1735
1736
1737
1738
1739
1740

1741
1742
1743 722 overburden by biological, gaseous or capillarity processes (Anand et al., 2014). Conversely,
1744
1745 723 the absence of a surface anomaly would not preclude the occurrence of an anomaly in the
1746
1747 724 underlying bedrock. In any case, landform-regolith mapping and establishment of a glacia
1748
1749 725 landscape chronology are required around the sampling sites in order to (i) constrain the
1750
1751 726 geomorphological context of the anomaly for locating its potential distant source or (ii)
1752
1753 727 identify glacia covers that mask potential bedrock resource(s) (Bamba, 2009).
1754
1755
1756 728
1757
1758 729 *7. 2. Geomorphological exploration guides*
1759
1760 730 Gold anomalies in detrital glacia ferricretes overlying barren bedrock are common.
1761
1762 731 Studies combining detailed landform-regolith mapping, trench studies, geochemistry and
1763
1764 732 gold particles characterization allowed documenting km-scale downslope displacement of
1765
1766 733 gold particles from their bedrock sources (Sanfo et al., 1992, 1993; Parisot et al., 1995;
1767
1768 734 Ouangrawa et al., 1996; Bamba et al., 2002). For such investigations cannot be undertaken
1769
1770 735 systematically, the geomorphological approach may prove rewarding in constraining the
1771
1772 736 potential bedrock source area of a transported anomaly based on the assumption that it has
1773
1774 737 been displaced down the slopes of a considered glacia.
1775
1776
1777 738 In rolling pediplain contexts, tracing the potential upslope source of a transported
1778
1779 739 anomaly should be straightforward, providing the glacia landscape has not been
1780
1781 740 significantly dissected and preserved its original interfluvium (e.g., Figs. 6b and 6c-6e). In such a
1782
1783 741 case, the source of the transported particles cannot be located beyond the preserved glacia
1784
1785 742 interfluvium. In dissected rolling pediplains and particularly piedmont contexts, upslope
1786
1787 743 portions of glacia are rarely preserved (e.g., Figs. 6a; 7; 10). Paleolandscape reconstruction at
1788
1789 744 the time the sampled glacia was functional is necessary to evaluate the potential path
1790
1791 745 followed by the glacia sedimentary cover during pedimentation. Instead of a cross-sectional
1792
1793 746 approach, a three-dimensional landscape reconstruction (e.g., Fig. 7) is suitable to take into
1794
1795
1796
1797
1798
1799
1800

1801
1802
1803 747 account the entire upslope drainage area that could have supplied mineralized debris to the
1804
1805 748 anomaly on a glacia. For instance, an anomaly documented in the lowermost portion of a
1806
1807 749 relictual glacia i.e., close to or along a river active at the time of pedimentation, can be
1808
1809 750 sourced from the erosion of all the glacia that were connected downslope to that drain
1810
1811 751 upstream. For functional glacia, delimitation of the upslope area that contributed to a
1812
1813 752 sampling site would be straightforward because this area is constrained by the present-day
1814
1815 753 topography.

1818 754 Maximal transportation distance on a glacia corresponds to the upslope distance
1819
1820 755 between the considered sampling site and the drainage divide at the end of the activity of
1821
1822 756 the glacia (i.e., before its abandonment and dissection). Reconstruction of the High glacia
1823
1824 757 landscape suggests that paleo-glacia widths have exceeded 20 km (Grimaud et al., 2015; Fig.
1825
1826 758 10), prompting to undertake landform-regolith mapping and paleolandscape reconstruction
1827
1828 759 on a larger scale than that of the immediate surrounding of the anomaly-bearing glacia relic.
1829
1830 760 South of the Sahelian zone (Fig. 2), dissection of the High glacia pediplain has generally
1831
1832 761 created narrower (1-10 km) Middle and Low glacia flanking subsequent valleys that are often
1833
1834 762 perpendicular to the earlier main river drain delimitating High glacia (Fig. 7). Potential
1835
1836 763 maximal transportation distances on those pediments are therefore reduced compared to
1837
1838 764 those of the High glacia and the transport direction at a high angle to that of the preexisting
1839
1840 765 glacia. The same reasoning as that exposed above applies to the tracking of the source of
1841
1842 766 transported regolith upslope on the Middle and Low glacia, bearing in mind that the cover of
1843
1844 767 these glacia can carry elements that may have previously been transported on an earlier
1845
1846 768 glacia. Potential divide migration from one glacia landscape stage to the next should also be
1847
1848 769 taken into account (e.g., Fig. 8). A given bedrock mineral concentration could indeed have
1849
1850 770 been subjected to pedimentation by successive glacia of contrasting slope directions and
1851
1852 771 therefore may not have always belonged to the same drainage sub-basin (Fig. 20).
1853
1854
1855
1856
1857
1858
1859
1860

1861
1862
1863 772 Stream sediment surveys going up river would still be valid in glacis environments,
1864
1865 773 providing that once propitious channel sections are selected, the upslope source tracing
1866
1867 774 protocol described above for glacis environment is applied. The geomorphological
1868
1869 775 exploration guides considered here do not only apply to resources transported as particles
1870
1871 776 such as gold, platinum or diamond, but also to ore deposits such as copper or manganese,
1872
1873 777 which can accumulate by downslope solute transfers through glacis cover (e.g., Sillitoe,
1874
1875 778 2005; Riquelme et al., 2018).
1876
1877 779
1878
1879
1880 780 *7. 3. Targeting concealed resource*
1881
1882 781 Glacis being mostly screens over the bedrock and given their extension, the biggest
1883
1884 782 West African exploration challenge is to detect the resources they potentially mask. A way to
1885
1886 783 contribute to targeting such resources is to identify glacis units potentially masking
1887
1888 784 mineralized bedrock lithologies, structures or dikes that were first identified and mapped
1889
1890 785 independently from scattered outcrops or boreholes. By combining the geological map and
1891
1892 786 a landform-regolith map, one obtains by a GIS overlay operation the intersection between
1893
1894 787 polygons representing glacis ferricrete units, on the one hand, and polylines or polygons
1895
1896 788 representing mineralized faults, dykes or rock units, on the other hand. As an illustration of
1897
1898 789 such a GIS request, Figure 21 shows gold, copper and manganese indices over Southwestern
1899
1900 790 Burkina Faso as well as the High glacis ferricrete relics overlying (i.e., intersecting) bedrock
1901
1902 791 lithological units bearing those indices. This representation allows (i) targeting High glacis
1903
1904 792 ferricrete relics potentially masking deposits and (ii) adapting a sampling or drilling strategy
1905
1906 793 accordingly. Those targeted glacis ferricrete units should then be studied in details and
1907
1908 794 eventually be drilled across to attain the projected trace of the mineralized structure under
1909
1910 795 the glacis cover. Such a protocol would typically reveal lateral extensions of ore bodies and
1911
1912
1913
1914
1915
1916
1917
1918
1919
1920

1921
1922
1923
1924
1925
1926
1927
1928
1929
1930
1931
1932
1933
1934
1935
1936
1937
1938
1939
1940
1941
1942
1943
1944
1945
1946
1947
1948
1949
1950
1951
1952
1953
1954
1955
1956
1957
1958
1959
1960
1961
1962
1963
1964
1965
1966
1967
1968
1969
1970
1971
1972
1973
1974
1975
1976
1977
1978
1979
1980

796 may be applied from a regional (10-100 km) (Fig. 21) to a prospect scale (0.1-1 km) if
797 landform-regolith maps of appropriate resolution are produced.
798
799 *7. 4. Other geomorphic exploration pitfalls and overlooked resources*
800 The pervasive occurrence and preservation of convexo-concave rolling pediplains
801 south of the Sahelian zone and the degradation of glacis into concave residual hills under
802 equatorial environments explain why glacis may have been overlooked, especially by
803 workers who did not investigate landforms outside the Forest zone, contrary to Grandin
804 (1976), who worked across an entire regional latitudinal corridor. Exploration geologists
805 have indeed implicitly interpreted residual hills as “demi-oranges” (e.g., Freyssinet, 1993;
806 Freyssinet et al., 2005) although they may result from pedimentation in the case of rolling
807 pediplains or from the degradation of older glacis into convex hills. A consequence of such
808 restrictive interpretation is that ferricretes / lateritic residua are considered as formed and
809 preserved essentially in-situ, whereas they could host material transported prior to
810 weathering/duricrusting. A residual hill can result from the dismantling of a wide glacis on
811 which material has been transported over several kilometers if not tens of kilometers i.e., on
812 a much larger scale than the size of the residual hill. However, detailed exploration
813 geochemical investigations or models are restricted to the slope of a single residual hill (e.g.,
814 Zeegers and Lecomte, 1992; Freyssinet, 1993; Butt, 2016). In glacis landscapes such as those
815 of West Africa, landform-regolith mapping and the establishment of a landscape chronology
816 should therefore be undertaken on a larger scale (1-20 km) than that of the considered
817 anomaly-bearing relief (0,1-1 km).
818 Given the alluvial nature of glacis overburdens, placers must be common on
819 pediments. Detailed work by Thomas and Thorp (1985) or Teuuw (1987, 2002) suggests that
820 alluvial diamonds are hosted by paleo-glacis systems’ residual hills. Recent unconsolidated

1981
1982
1983 821 glacis overburden is commonly mined for gold placers. Those artisanal mines are valuable
1984
1985 822 proxies of upslope bedrock mineralizations by using the geomorphological guides provided
1986
1987 823 above. Downslope parts of Low glacis and alluvial terraces host gold and diamond placers
1988
1989 824 (e.g., Hall et al., 1985; Teeuw et al., 1991; Ouangrawa et al., 1996). But older glacis ferricretes
1990
1991 825 should also bear numerous unsuspected alluvial placers. Although weathering of the High
1992
1993 826 glacis has contributed locally to alluvial gold concentrations, it is mostly the thick and
1994
1995 827 mature weathering profiles of the Bauxitic and Intermediate paleolandscapes that have a
1996
1997 828 high - and still largely overlooked - potential of hosting supergene ore concentrations others
1998
1999 829 that those that are known and actively mined for (Al, Mn and Au).
2000
2001 830
2002
2003
2004 831 **8. Pediments, pediplains and the topographic evolution of shields**
2005
2006 832 *8. 1. Implications for pedimentation in lateritic landscapes*
2007
2008 833 Thanks to the protective effect of the ferricretes and limited regional denudation,
2009
2010 834 there is a significant spatial and temporal variability in the glacis record from the scale of a
2011
2012 835 single pediment to that of the African sub region. As composite landform-regolith
2013
2014 836 associations, pediments erode, collect, transport, sort, transform and store regolith through
2015
2016 837 space and time. An overwhelming part the of the West African pediments are cut exclusively
2017
2018 838 in a thick (>20 m) preexisting regolith mantle and a single pediment may be both cut through
2019
2020 839 preexisting regolith upslope and through bedrock downslope. The very common occurrence
2021
2022 840 of rolling pediplains also shows that pediments encompass the entire regional relief and
2023
2024 841 therefore cap interfluvies. The West African case study therefore suggests that lateritic
2025
2026 842 pediments may not be appropriately distinguished by morphogenic classifications based on
2027
2028 843 (i) the shape or position of pediments in the landscape (Cook and Mason, 1973), (ii) the
2029
2030 844 relations between regolith and the bedrock as criteria of the pedimentation process
2031
2032 845 (Twidale, 1983), (iii) the nature of the material being cut (Dresch, 1957; Tricart, 1972;
2033
2034
2035
2036
2037
2038
2039
2040

2041
2042
2043 846 Oberlander, 1989) or (iv) the thickness of the transported overburden (Applegarth, 2004) (see
2044
2045 847 Dohrenwend and Parsons, 2009 for review). Likewise, a comprehensive definition of the
2046
2047 848 physical and chemical processes involved in pedimentation would be therefore, to our view,
2048
2049 849 vain. Pre-Neogene weathering was instrumental at preparing the thick regolith mantle made
2050
2051 850 available to stepwise pedimentation. But evaluation of the role of weathering during the
2052
2053 851 formation of glacis would not be straightforward given the imprint of the post
2054
2055 852 pedimentation weathering and duricrusting of the pediments. At best, an increasing
2056
2057 853 activation / influence of the pedogenetic processes is expected in pedimentation across the
2058
2059 854 latitudinal gradient towards the Equator (e.g., Millot, 1980, 1983; Rohdenburg, 1969, 1982).
2060
2061
2062
2063
2064

2065 856 *8. 2. Relations to epeirogeny*

2066
2067 857 Pediment systems carved the African surface while it was being submitted to long
2068
2069 858 wavelength (10^3 km) deformation that contributed to the growth of the basin-and-swell
2070
2071 859 topography of the continent after 40 Ma (Burke and Gunnell, 2008; Chardon et al., 2016). The
2072
2073 860 most prominent element of that physiography in West Africa is the Hoggar swell; but more
2074
2075 861 subtle uplift is also suggested along the marginal upward that constituted the eastern
2076
2077 862 extension of the Guinean rise up to the Jos Plateau (Grimaud et al., 2014, 2018; Chardon et
2078
2079 863 al., 2016; Fig. 2). The stepping patterns of pediment systems may not be used as a proxy of
2080
2081 864 that deformation because glacis have a roughly spatially consistent and reduced (< 80 m)
2082
2083 865 elevation range above local base level, which itself varies with river networks from sea level
2084
2085 866 to above 1300 m for the highest regional topographic massifs excluding the Hoggar
2086
2087 867 (Grimaud et al., 2014; Fig. 2). In details, the stepping pattern of successive glacis has been
2088
2089 868 compartmentalized amongst sub drainage areas due to spatially variable incision of river
2090
2091 869 segments bounded by stationary knickzones, which were already part of the West African
2092
2093 870 landscape before settlement of the High glacis pediplain for most of them (Grimaud et al.,
2094
2095
2096
2097
2098
2099
2100

2101
2102
2103 871 2014). Furthermore, glacis systems did not level out regional rock escarpments, which were
2104
2105 872 already imprinted in the Paleogene Bauxitic and (mostly) Intermediate landscapes and
2106
2107 873 remained almost stationary since then (De Swardt, 1964; Grandin and Delvigne, 1969; Burke
2108
2109 874 and Gunnell, 2008; Grandin and Joly, 2008; Grimaud et al., 2014, 2015; Fig. 17). Glacis
2110
2111 875 systems therefore adapted their slopes to differentiated and uneven river levels and
2112
2113 876 contributed in this way to distributed landscape dissection and dismantling down to the
2114
2115 877 scale of lowermost-order drains a few kilometers long (e.g., Figs. 8, 9, 10). In other words,
2116
2117 878 outside the provinces of relict African and Intermediate landscapes (Fig. 17), virtually no 20 x
2118
2119 879 20 km area of the West African topography escaped settlement of new glacis during the main
2120
2121 880 pedimentation periods, with the exception of Low glacis pedimentation at lowermost
2122
2123 881 latitudes (Fig. 18).

2126
2127 882 Thorough documentation of stepwise Cenozoic dissection of the West African sub
2128
2129 883 region therefore precludes the stepping of successively younger pediplains bounded
2130
2131 884 upstream by escarpments, which would produce continental-scale staircase patterns of
2132
2133 885 pediplains from the crest of swells down to sea level or the base level of intracratonic basins.
2134
2135 886 Such a model is suggested by Burke and Gunnell (2008, their Figure 16A) on the crest and
2136
2137 887 slopes of the Guinean Rise (Fig. 2). Staircase pediplains models derive from that of King
2138
2139 888 (1948, 1967) in which continent-wide and flat pediplains graded to sea level form by
2140
2141 889 escarpment/knickzone retreat far inland. For King, a pediplain is abandoned as a
2142
2143 890 consequence of uplift by the formation of a subsequent pediplain below a new retreating
2144
2145 891 escarpment, which will ultimately bound and protect the relic of the early pediplain in the
2146
2147 892 continental interior. King's paradigm is also explicit in the procedure that would allow
2148
2149 893 retrieving long-term continental uplift histories from the inversion of current river
2150
2151 894 longitudinal profiles (Paul et al., 2014). This procedure is indeed based on a quantitative
2152
2153 895 model that explicitly requires inlandward retreat of river knickzones in response to uplift and
2154
2155
2156
2157
2158
2159
2160

2161
2162
2163 896 is therefore invalidated by the well-documented West African case study (Grimaud et al.,
2164
2165 897 2014). A staircase model of pediplains has also been proposed by Guillocheau et al. (2015,
2166
2167 898 2017) for the Congo basin and its surrounding swells and by Dauteuil et al. (2015) for
2168
2169 899 Namibia. The definition of a pediment system by these authors as a flat pediplain connected
2170
2171 900 upslope to pediments (pediment valleys) and higher up to rivers incising the older
2172
2173 901 upstanding landsurface across escarpments (e.g., Guillocheau et al., 2015) therefore
2174
2175 902 contrasts with that implied by the West African case study. The difference between the two
2176
2177 903 models is not only conceptual. Regional correlations of West African glacia systems are
2178
2179 904 based on well-preserved regolith-landform associations and geomorphic criteria, whereas
2180
2181 905 those of Central and Southwestern Africa have to rely mostly on topographic correlations
2182
2183 906 and escarpment identification in contexts of advanced degradation of the regolith-landform
2184
2185 907 associations or in absence of type-regolith-landform associations in arid Southwestern
2186
2187 908 Africa. The topographic approach would intrinsically favor a Kingian model and vice-versa.
2188
2189 909 The West African case study indicates that pediments achieved local planation and
2190
2191 910 formed from the development of the drainage network instead of by dominant range retreat.
2192
2193 911 The difficulty to relate the regional stepping patterns of pediment systems to an inferred
2194
2195 912 pattern of uplift over West Africa suggests that shield landscape dissection schemes would
2196
2197 913 primarily be driven by long-term climatic oscillations driving pedimentation / weathering
2198
2199 914 periods along low-abrasion capacity river networks (e.g., Tricart 1959; Beauvais and Chardon,
2200
2201 915 2013).

2202 916 2203 2204 917 *8. 3. Pediment landscape evolution processes and the sediment routing system*

2205 918 Surface process models suggest that non-orogenic continental surfaces such as that
2206
2207 919 of Africa develop non-steady state (transient) landscapes with a Davisian behavior of long-
2208
2209 920 term decreasing slope angle (Davis, 1899; Bishop, 2007). African landscapes saw their relief

2221
2222
2223 921 increasing throughout the Cenozoic and should then be considered as transient over the
2224
2225 922 very long term. But the punctuated pedimentation scheme they developed does not match
2226
2227 923 that of the Davisian cycle of erosion. The main specificity of the West African landscape
2228
2229 924 dissection patterns by pedimentation is a progressively reduced area submitted to abrasion
2230
2231 925 through time, leaving increasingly wider relict surfaces of limited or no denudation as a
2232
2233 926 result of landscape dissection (Fig. 10). The stepping patterns of pediment systems have no
2234
2235 927 clear dependency on sea level variations and/or epeirogeny and contribute to limited (3-9
2236
2237 928 m/My) and distributed denudation. In contexts of enhanced uplift and correlatively higher
2238
2239 929 denudation such as the upper slope of the Hoggar swell (surface uplift and denudation > 30
2240
2241 930 m/My since ca. 35 Ma; Chardon et al., 2016; Grimaud et al., 2018), pediplains could not form
2242
2243 931 or be preserved on geological time scales.

2244
2245 932 Once duricrusted and/or abandoned as a result of dissection, pediments preserve
2246
2247 933 the underlying regolith from erosion. Regional-scale pediment systems (pediplains) form
2248
2249 934 and maintain over geological timescales in environments submitted to low river incision or
2250
2251 935 erosion rates (<10 m/Ma) and limited epeirogenic uplift. Under that condition, the
2252
2253 936 maintenance of very slowly evolving pediment landscapes poses the chicken-and-egg issue
2254
2255 937 of knowing whether the low erosional efficiency of pedimentation dictates the limited
2256
2257 938 transport and incision capacity of the river network or vice-versa. In any case, pediments are
2258
2259 939 buffer landsurfaces between the regolith mantles they contribute to exhume and the rivers
2260
2261 940 they feed with reworked regolith (Grimaud et al., 2015). Pedimentation is transport-limited
2262
2263 941 given the large amount of (old) regolith still being stored in West African landscapes, which
2264
2265 942 generates subdued and nearly constant erosion fluxes over the long-term (< 0.01
2266
2267 943 km³/km²/My). Above a 10 m/My incision/erosion rate threshold, rupture of the
2268
2269 944 pedimentation regime is expected, paleo-landforms being erased. It is only above several
2270
2271 945 tens of meters per million years of long-term erosion that denudation would potentially
2272
2273
2274
2275
2276
2277
2278
2279
2280

2281
2282
2283
2284
2285
2286
2287
2288
2289
2290
2291
2292
2293
2294
2295
2296
2297
2298
2299
2300
2301
2302
2303
2304
2305
2306
2307
2308
2309
2310
2311
2312
2313
2314
2315
2316
2317
2318
2319
2320
2321
2322
2323
2324
2325
2326
2327
2328
2329
2330
2331
2332
2333
2334
2335
2336
2337
2338
2339
2340

946 become measurable by low-temperature thermochronology (Beauvais et al., 2016). The
947 regional preservation of pediments / pediplains indicative of very slow denudation should
948 then prevent retrieval of denudation scenarios from low-temperature thermochronology for
949 periods encompassing pediments timespan of formation and over periods following their
950 abandonment. Dated relict pediments should be used instead as strict constraints on the
951 late temperature-time exhumation path provided by low-temperature thermochronology.

952

953 **8. Conclusions**

954 Throughout its surface, Sub Saharan West Africa preserves three Neogene (24-3 Ma)
955 lateritic pediment systems as well as functional pediments along the southern fringe of the
956 Sahara. A review of the landform-regolith associations, landscape chronologies, ages and
957 stepping patterns of the pediments as well as their spatial distribution and active
958 degradation modes bears implications for the long-term landscape evolution processes of
959 shields and mineral exploration strategies in the tropical belt. Those implications may be
960 summarized as follows.

961 1 – Pediments occupy an overwhelming surface of the sub region and contributed to
962 removal of a thick lateritic regolith mantle resulting from intense pre-Neogene weathering.
963 Each pediment system formed by the process of relief dissection and incorporated
964 landforms inherited from earlier landscapes. Depending on the nature of the geological
965 substrate, pediment paleolandscape stages comprised regions of multiconcave pediplains
966 and regions of multi-convexo-concave pediplains (called rolling pediplains).

967 2 - A great spatial diversity exists in the pediments regolith associations owing to the nature
968 of the substrate pediments have leveled, the origin, transport dynamics and preservation of
969 the materials that have been transiting on their surface and the intensity of weathering and
970 duricrusting their have undergone. However, detrital ferricretes and loose clastic sediments

2341
2342
2343 971 constitute by far the most common type of pediment surface. Fe-duricrusting and ferricretes
2344
2345 972 constitute a necessary condition for glaxis dissection and preservation of relictual
2346
2347 973 landscapes.
2348
2349 974 3 – Lateritic pediment surfaces are not suitable for geochemical sampling aiming at
2350
2351 975 obtaining reliable information about the composition of the bedrock or an elemental
2352
2353 976 concentration anomaly. The two main reasons for this are (i) the transported nature of the
2354
2355 977 material exposed at the surface and (ii) the lost of the geochemical characteristics of the
2356
2357 978 bedrock through the weathering processes.
2358
2359 979 4 - Landform-regolith mapping beyond the scale of modern interfluves followed by
2360
2361 980 reconstitution of past pediment landscape stages provides geomorphological exploration
2362
2363 981 guides for interpreting surface geochemical anomalies on pediments and tracing their
2364
2365 982 potential sources in case they have been “transported” on pediments. Mapping of landform-
2366
2367 983 regolith associations may also be used to target pediments masking suspected
2368
2369 984 mineralizations.
2370
2371 985 5 - Past and present latitudinal climatic zonation of pedimentation and weathering at the
2372
2373 986 scale of the sub region suggests a gradient of pedimentation processes from an arid to a
2374
2375 987 perhumid end-member across the intertropical zone. They also explain why pediments may
2376
2377 988 have been overlooked in humid equatorial environments, with important implications for
2378
2379 989 mineral exploration.
2380
2381 990 6 – Successive pediment systems have affected progressively reduced area over time,
2382
2383 991 preserving increasingly wider relictual landsurfaces. Climatic oscillations dictated
2384
2385 992 pedimentation-driven, local planation that adapted slopes to very large, spatially
2386
2387 993 differentiated, knickzone bearing river networks. The spatially consistent and limited (< 80
2388
2389 994 m) stepping pattern of pediments is independent from elevation or distance to base level.
2390
2391 995 Hence, pediments and pediplains may not be used as gauges of uplift except near coastlines.
2392
2393
2394
2395
2396
2397
2398
2399
2400

2401
2402
2403 996 Pediments form and are preserved regionally over geological timescales only for < 10 m/My
2404
2405 997 erosion regimes and are therefore indicators of very slow shield denudation.
2406
2407 998 7 – Lateritic pediments have been overlooked in the tropical belt because lateritic
2408
2409 999 duricrusted landscapes refer exclusively to in-situ weathering of bedrock for most geologists
2410
2411
2412 1000 and geochemists. Further investigations will hopefully help deciphering pediment landform-
2413
2414 1001 regolith associations for a better access to the geological substrate of tropical shields and its
2415
2416 1002 resources that may still be underestimated. Investigating pediments as markers of past
2417
2418 1003 morphogenesis is a powerful tool for understanding surface dynamics of shields and their
2419
2420 1004 sediment routing system, which contribute to a significant proportion of the Earth
2421
2422 1005 sedimentary budget and global biogeochemical cycles.
2423
2424
2425 1006
2426
2427 1007 **Acknowledgments**
2428
2429 1008 This work is published with the support of IRD (JEAi FasoLith). It has been mostly funded by
2430
2431 1009 the TopoAfrica project (ANR-08-BLAN-572 0247-02), the West African eXploration Initiative
2432
2433 1010 (WAXI) and the CNRS. Further support from TS2P (the Transform Source-to-Sink Project)
2434
2435 1011 funded by Total Exploration and Production is acknowledged. The paper benefited from the
2436
2437 1012 comments and suggestions of three anonymous reviewers. We acknowledge AMIRA
2438
2439 1013 International, the industry sponsors and the Geological Surveys / Departments of Mines in
2440
2441 1014 West Africa for their support of the WAXI project (P934A).
2442
2443
2444 1015
2445
2446
2447
2448
2449
2450
2451
2452
2453
2454
2455
2456
2457
2458
2459
2460

2461
2462
2463 **1016 References**
2464
2465 **1017** Anand, R., Lintern, M., Noble, R., Aspandiar, M., Macfarlane, C., Hough, R., Stewart, A.,
2466
2467 **1018** Wakelin, S., Townley, B., Reid, N., 2014. Geochemical dispersion through transported
2468
2469 **1019** cover in regolith-dominated terrains - toward an understanding of process. Soc. Econ.
2470
2471 **1020** Geol. Spec. Publ. 18, 97-125.
2472
2473 **1021** Applegarth, M.T., 2004. Assessing the influence of mountain slope morphology on pediment
2474
2475 **1022** form, South-Central Arizona. Phys. Geogr. 25, 225-236.
2476
2477 **1023** Aubréville, A., 1949. Climats, forêts et désertification de l'Afrique tropicale. Société d'Editions
2478
2479 **1024** géographiques maritimes et coloniales, Paris.
2480
2481 **1025** Bamba, O., 1996. L'or disséminé dans les Albitites de Larafella (Burkina Faso), évolution dans
2482
2483 **1026** les altérites et les cuirasses ferrugineuses : Métallogénie - Pétrologie – Géomorphologie.
2484
2485 **1027** Ph D Thesis, Aix-Marseille III University, Marseille, 261p.
2486
2487 **1028** Bamba, O., 2009. Morphopédologie et anomalie géochimique. Can. J. Earth Sci. 46, 939-948.
2488
2489 **1029** Bamba, O., Parisot, J.-C., Grandin, G., Beauvais, A., 2002. Ferricrete genesis and supergene
2490
2491 **1030** gold behaviour in Burkina Faso, West Africa. Geochem. Explor. Environ. Anal. 2, 3-13.
2492
2493 **1031** Baratoux, L., Metelka, V., Naba, S., Jessell, M.W., Gregoire, M., Ganne, J., 2011. Juvenile
2494
2495 **1032** Paleoproterozoic crust evolution during the Eburnean orogeny (similar to 2.2-2.0 Ga),
2496
2497 **1033** western Burkina Faso. Precambrian Res. 191, 18-45.
2498
2499 **1034** Beaudet, G., Coque, R., 1994. Reliefs et modelés des régions tropicales humides : mythes,
2500
2501 **1035** faits et hypothèses. Ann. Géogr. 577, 227-254.
2502
2503 **1036** Beauvais, A., 1999. Geochemical balance of lateritization processes and climatic signatures
2504
2505 **1037** in weathering profiles overlain by ferricretes in Central Africa. Geochim. Cosmochim. Acta
2506
2507 **1038** 63, 3939-3957.
2508
2509
2510
2511
2512
2513
2514
2515
2516
2517
2518
2519
2520

2521
2522
2523 1039 Beauvais, A., Ritz, M., Parisot, J.C., Dukhan, M., Bantsimba, C., 1999. Analysis of poorly
2524
2525 1040 stratified lateritic terrains overlying a granitic bedrock in West Africa, using 2-D electrical
2526
2527 1041 resistivity tomography. *Earth Planet. Sci. Lett.* 173, 413-424.
2528
2529 1042 Beauvais, A., Ritz, M., Parisot, J.C., Bantsimba, C., 2003. Testing etching hypothesis for the
2530
2531 1043 shaping of granite dome structures beneath lateritic weathering landsurfaces using ERT
2532
2533 1044 method. *Earth Surf. Process. Landf.* 28, 1491-1491.
2534
2535 1045 Beauvais, A., Ritz, M., Parisot, J.C., Bantsimba, C., Dukhan, M., 2004. Combined ERT and GPR
2536
2537 1046 methods for investigating two-stepped lateritic weathering systems. *Geoderma* 119, 121-
2538
2539 1047 132.
2540
2541 1048 Beauvais, A., Chardon, D., 2013. Modes, tempo, and spatial variability of Cenozoic cratonic
2542
2543 1049 denudation: The West African example. *Geochem. Geophys. Geosyst.* 14, 1590-1608.
2544
2545 1050 Beauvais, A., Ruffet, G., Henocque, O., Colin, F., 2008. Chemical and physical erosion rhythms
2546
2547 1051 of the West African Cenozoic morphogenesis: The ³⁹Ar-⁴⁰Ar dating of supergene K-Mn
2548
2549 1052 oxides. *J. Geophys. Res.-Earth Surf.* 113, F4007.
2550
2551 1053 Beauvais, A., Bonnet, N.J., Chardon, D., Arnaud, N., Jayananda, M., 2016. Very long-term
2552
2553 1054 stability of passive margin escarpment constrained by Ar-40/Ar-39 dating of K-Mn oxides.
2554
2555 1055 *Geology* 44, 299-302.
2556
2557 1056 Bishop, P., 2007. Long-term landscape evolution: linking tectonics and surface processes.
2558
2559 1057 *Earth Surf. Process. Land.* 32, 329-365.
2560
2561 1058 Bitom, D., Volkoff, B., Beauvais, A., Seyler, F., Ndjigui, P.D., 2004. Rôle des héritages
2562
2563 1059 latéritiques et du niveau des nappes dans l'évolution des modelés et des sols en zone
2564
2565 1060 intertropicale forestière humide. *C.R. Géoscience* 336, 1161-1170.
2566
2567 1061 Boeglin, J.L., Mazaltarim, D., 1989. Géochimie, degrés d'évolution et lithodépendance des
2568
2569 1062 cuirasses ferrugineuses de la région de Gaoua au Burkina Faso. *Sci. Géol. Bull.* 42, 27-44.
2570
2571
2572
2573
2574
2575
2576
2577
2578
2579
2580

2581
2582
2583 1063 Bolster, S.J.S., 1999. Regolith mapping: Is it really necessary? Aus. Inst. Geoscient. Bull. 30,
2584
2585 1064 125-135.
2586
2587 1065 Bonvallot, J., Boulangé, B., 1970. Note sur le relief et son évolution dans la région de
2588
2589 1066 Bongouanou (Côte d'Ivoire). Cah. ORSTOM Sér. Géol. 2, 171-183.
2590
2591 1067 Boulangé, B., 1984. Les formations bauxitiques latéritiques de Côte d'Ivoire. Trav. Doc.
2592
2593 1068 ORSTOM 175, 1-342.
2594
2595 1069 Boulangé, B., 1986. Relation between lateritic bauxitization and evolution of landscape. Trav.
2596
2597 1070 Int. Com. Stud. Bauxite, Alumina & Aliminum (ISCOBA) 16-17, 27-44.
2598
2599 1071 Boulangé, B., Millot, G., 1988. La distribution des bauxites sur le craton ouest-africain. Sci.
2600
2601 1072 Géol. Bull. 41, 113-123.
2602
2603 1073 Boulangé, B., Sigolo, J.B., Delvigne, J., 1973. Descriptions morphoscopiques, géochimiques
2604
2605 1074 et minéralogiques des faciès cuirassés des principaux niveaux géomorphologiques de
2606
2607 1075 Côte d'Ivoire. Cah. ORSTOM Sér. Géol. 5, 59-81.
2608
2609 1076 Boulet, R., 1970. La géomorphologie et les principaux types de sols en Haute-Volta
2610
2611 1077 septentrionale. Cah. ORSTOM Sér. Pédol. 8, 245-271.
2612
2613 1078 Bowden, D.J., 1987. On the composition and fabric of the footslop laterites (duricrusts) of
2614
2615 1079 the Sierra Leone, West Africa, and their geomorphological significance. Z. Geomor. N.F. 64,
2616
2617 1080 39-53.
2618
2619 1081 Bowden, D.J., 1997. The geochemistry and development of lateritized footslope benches:
2620
2621 1082 The Kasewe Hills, Sierra Leone. Spec. Publ. Geol. Soc. 120, 295-305.
2622
2623 1083 Bowell, R.J., Afreh, E.O., Laffoley, N.d.A., Hanssen, E., Abe, S., Yao, R.K., Pohl, D., 1996.
2624
2625 1084 Geochemical exploration for gold in tropical soils - four contrasting case studies from
2626
2627 1085 West Africa. Trans. Inst. Min. Metall. 105, B12-B33.
2628
2629 1086 Brammer, H., 1955. Visit to Haute Volta, 30th January-3rd March 1955. Gold Coast Dept. Soil
2630
2631 1087 Land-Use Surv. Techn. Rep. 9, 1-48.
2632
2633
2634
2635
2636
2637
2638
2639
2640

2641
2642
2643 1088 Brammer, H., 1956. A note on former pediment remnants in Haute Volta. *Geogr. J.* 122, 526-
2644
2645 1089 527.
2646
2647 1090 Brown, D.J., Helmke, P.H., Clayton, M.K., 2003. Robust geochemical indices for redox and
2648
2649 1091 weathering on a granitic laterite landscape in Central Uganda. *Geochim. Cosmochim.*
2650
2651 1092 *Acta* 67, 2711-2723.
2652
2653 1093 Brückner, W.D., 1955. The mantle rock (laterite) of the Gold Coast and its origin. *Geol.*
2654
2655 1094 *Rundsch.* 43, 307-327.
2656
2657 1095 Büdel, J., 1982. *Climatic geomorphology*. Princeton University Press, Princeton.
2658
2659 1096 Bull, W.B., 1977. The alluvial-fan environment. *Progr. Phys. Geogr.* 1, 222-270.
2660
2661 1097 Burke, K., Durotoye, B., 1971. Geomorphology and superficial deposits related to Late
2662
2663 1098 Quaternary climatic variation in South-Western Nigeria. *Z. Geomor. N.F.* 15, 430-444.
2664
2665 1099 Burke, K., Gunnell, Y., 2008. The African erosion surface: A continental scale synthesis of
2666
2667 1100 geomorphology, tectonics, and environmental change over the past 180 million years.
2668
2669 1101 *Geol. Soc. Am. Mem.* 201, 1-66.
2670
2671 1102 Butt, C.R.M., 2016. The development of regolith exploration geochemistry in the tropics and
2672
2673 1103 sub-tropics. *Ore Geol. Rev.* 73, 380-393.
2674
2675 1104 Butt, C.R.M., Bristow, A.P.J., 2013. Relief inversion in the geomorphological evolution of sub-
2676
2677 1105 Saharan West Africa. *Geomorphology* 185, 16-26.
2678
2679 1106 Butt, C.R.M., Lintern, M.J., Anand, R.R., 2000. Evolution of regoliths and landscapes in deeply
2680
2681 1107 weathered terrain - implications for geochemical exploration. *Ore Geol. Rev.* 16, 167-183.
2682
2683 1108 Butt, C.R.M., Zeegers, H., 1989. Classification of geochemical exploration models for
2684
2685 1109 tropically weathered terrains. *J. Geochem. Explor.* 32, 65-74.
2686
2687 1110 Castaing, C., Le Metour, J., Billa, M., Donzeau, M., Chevremont, P., Egal, E., Zida, B.,
2688
2689 1111 Ouedraogo, I., Koté, S., Kaboré, B.E., Ouedraogo, C., Thieblemont, D., Guerrot, C.,
2690
2691
2692
2693
2694
2695
2696
2697
2698
2699
2700

2701
2702
2703 1112 Cocherie, A., Tegye, M., Itard, Y., Milesi, J.P., 2003. Carte géologique et minière du
2704
2705 1113 Burkina Faso à 1/1 000 000. BRGM/BUMIGEB.
2706
2707 1114 Chardon, D., Chevillotte, V., Beauvais, A., Grandin, G., Boulangé, B., 2006. Planation, bauxites
2708
2709 1115 and epeirogeny: One or two paleosurfaces on the West African margin? *Geomorphology*
2710
2711 1116 82, 273-282.
2712
2713 1117 Chardon, D., Grimaud, J.L., Rouby, D., Beauvais, A., Christophoul, F., 2016. Stabilization of
2714
2715 1118 large drainage basins over geological time scales: Cenozoic West Africa, hot spot swell
2716
2717 1119 growth, and the Niger River. *Geochem. Geophys. Geosyst.* 17, 1164-1181.
2718
2719 1120 Colin, F., Vieillard, P., 1991. Behavior of gold in the lateritic equatorial environment -
2720
2721 1121 Weathering and surface dispersion of residual gold particles at Dondo Mubi, Gabon. *Appl.*
2722
2723 1122 *Geochem.* 6, 279-290.
2724
2725 1123 Colin, F., Beauvais, A., Ruffet, G., Henocque, O., 2005. First Ar-40/Ar-39 geochronology of
2726
2727 1124 lateritic mangiferous pisolites: Implications for the Palaeogene history of a West
2728
2729 1125 African landscape. *Earth Planet. Sci. Lett.* 238, 172-188.
2730
2731 1126 Cook, R.U., Mason, P.F., 1973. Desert Knolls Pediment and associated landforms in the
2732
2733 1127 Mojave Desert, California. *Rev. Géomorph. Dyn.* 22, 49-60.
2734
2735 1128 Dautheil, O., Bessin, P., Guillocheau, F., 2015. Topographic growth around the Orange River
2736
2737 1129 valley, southern Africa: A Cenozoic record of crustal deformation and climatic change.
2738
2739 1130 *Geomorphology* 233, 5-19.
2740
2741 1131 Daveau, S., Lamotte, M., Rougerie, G., 1962. Cuirasses et chaines birrimiennes en Haute-Volta.
2742
2743 1132 *Ann. Géogr. Franç.* 387, 260-282.
2744
2745 1133 Davis, W. M., 1899. The geographical cycle. *Geogr. J.* 14, 481-504.
2746
2747 1134 De Swardt, A.M.J., 1964. Lateritisation and landscape development in parts of Equatorial
2748
2749 1135 Africa. *Z. Geomor. N.F.* 8, 313-333.
2750
2751
2752
2753
2754
2755
2756
2757
2758
2759
2760

2761
2762
2763 1136 Dohrenwend, J.C., Parsons, A.J., 2009. Pediments in arid environments, in: Parsons, A.,
2764
2765 1137 Abrahams, A. (Eds.), *Geomorphology of desert environments*, 2 ed. Springer Netherlands,
2766
2767 1138 The Netherlands, pp. 377-411.
2768
2769 1139 Dresch, J., 1952a. Dépôts de couverture et relief en Afrique occidentale française. Proc. XVIIth
2770
2771 1140 Int. Geogr. Congr., Washington, 323-326.
2772
2773 1141 Dresch, J., 1952b. Dépôts superficiels et relief du sol au Dahomey septentrional. C. R. Acad.
2774
2775 1142 Sci. Paris 234, 1566-1568.
2776
2777 1143 Dresch, J., 1957. Pédiments et glacis d'érosion, pédiplaines et inselbergs. Inf. Géogr. 21, 183-
2778
2779 1144 196.
2780
2781 1145 Eschenbrenner, V., Grandin, G., 1970. La séquence de cuirasses et ses différenciations entre
2782
2783 1146 Agnibiléfrou et Diébougou (Haute-Volta). Cah. ORSTOM Sér. Géol. 2, 205-246.
2784
2785 1147 Fölster, H., 1964. Morphogenese der Südsudanesischen Pediplane. Z. Geomor. N. F. 8, 393-
2786
2787 1148 423.
2788
2789 1149 Fölster, H., 1969a. Late Quaternary erosion in SW-Nigeria. Bull. Ass. Sén. Et. Quat. Ouest Afr.
2790
2791 1150 21, 29-35.
2792
2793 1151 Fölster, H., 1969b. Slope development in SW-Nigeria during late Peistocene and Holocene.
2794
2795 1152 Göttinger Bodenkdl. Ber. 10, 3-56.
2796
2797 1153 Fölster, H., Moshrefi, N., Ojenuga, A.G., 1971. Ferralitic pedogenesis on metamorphic rocks,
2798
2799 1154 SW-Nigeria. Pédologie 21, 95-124.
2800
2801 1155 Freyssinet, P., 1993. Gold dispersion related to ferricrete pedogenesis in South Mali:
2802
2803 1156 application to geochemical exploration. Chron. Rech. Min. 510, 25-40.
2804
2805 1157 Freyssinet, P., Butt, C.R.M., Morris, R.C., Piantone, P., 2005. Ore-forming processes related to
2806
2807 1158 lateritic weathering. Econ. Geol. 100th Anniversary volume, 681-722.
2808
2809 1159 Gavaud, M., 1977. Les grands traits de la pédogenèse au Niger méridional. Trav. Doc.
2810
2811 1160 ORSTOM 76, 1-102.
2812
2813
2814
2815
2816
2817
2818
2819
2820

- 2821
2822
2823 1161 Goldfarb, R.J., André-Mayer, A.S., Jowitt, S.M., Mudd, G.M., 2017. West Africa: The World's
2824
2825 1162 premier Paleoproterozoic gold province. *Econ. Geol.* 112, 123-143.
2826
2827 1163 Grandin, G., 1976. Aplanissements cuirassés et enrichissement des gisements de manganèse
2828
2829 1164 dans quelques régions d'Afrique de l'Ouest. *Mém. ORSTOM* 82, 1-276.
2830
2831 1165 Grandin, G., 2008. Les cuirasses latéritiques - aluminisation et ferruginisation, in: Dewolf, Y.,
2832
2833 1166 Bourrié, G. (Eds.), *Les formations surperficielles. Genèse - typologie - classification -*
2834
2835 1167 *paysages et environnements - ressources et risques.* Ellipses, Paris, pp. 362-372.
2836
2837 1168 Grandin, G., Delvigne, J., 1969. Traits généraux de l'évolution du réseau hydrographique
2838
2839 1169 dans la région du confluent Bandama - N'Zi (Côte d'Ivoire). *Bull. Ass. Sén. Et. Quat. Ouest*
2840
2841 1170 *Afr.* 23, 7-14.
2842
2843 1171 Grandin, G., Hayward, D.F., 1975. Aplanissements cuirassés de la péninsule de Freetown
2844
2845 1172 (Sierra Leone). *Cah. ORSTOM Sér. Géol.* 7, 11-16.
2846
2847 1173 Grandin, G., Joly, F., 2008. Glacis - Genèse, dynamique et formations corrélatives, in: Dewolf,
2848
2849 1174 Y., Bourrié, G. (Eds.), *Les formations surperficielles. Genèse - typologie - classification -*
2850
2851 1175 *paysages et environnements - ressources et risques.* Ellipses, Paris, pp. 201-216.
2852
2853 1176 Grimaud, J.L., Chardon, D., Beauvais, A., 2014. Very long-term incision dynamics of big rivers.
2854
2855 1177 *Earth Planet. Sci. Lett.* 405, 74-84.
2856
2857 1178 Grimaud, J.L., Chardon, D., Metelka, V., Beauvais, A., Bamba, O., 2015. Neogene cratonic
2858
2859 1179 erosion fluxes and landform evolution processes from regional regolith mapping (Burkina
2860
2861 1180 Faso, West Africa). *Geomorphology* 241, 315-330.
2862
2863 1181 Grimaud, J.L., Rouby, D., Chardon, D., Beauvais, A., 2018. Cenozoic sediment budget of West
2864
2865 1182 Africa and the Niger delta. *Basin Res.*, doi:10.1111/bre.12248.
2866
2867 1183 Guillocheau, F., Chelalou, R., Linol, B., Dauteuil, O., Robin, C., Mvondo, F., Callec, Y., Colin, J.-
2868
2869 1184 P., 2015. Cenozoic landscape evolution in and around the Congo Basin: Constraints from
2870
2871
2872
2873
2874
2875
2876
2877
2878
2879
2880

2881
2882
2883 1185 sediments and planation surfaces, in: De Wit, M.J. et al. (Eds.), Geology and resource
2884
2885 1186 potential of the Congo Basin. Springer-Verlag, Berlin Heidelberg, pp. 271-313.
2886
2887 1187 Guillocheau, F., Simon, B., Baby, G., Bessin, P., Robin, C., Dauteuil, O., 2017. Planation
2888
2889 1188 surfaces as a record of mantle dynamics: the case example of Africa. Gondwana Res., doi:
2890
2891 1189 10.1016/j.gr.2017.1005.1015.
2892
2893 1190 Gunnell, Y., 2003. Radiometric ages of laterites and constraints on long-term denudation
2894
2895 1191 rates in West Africa. Geology 31, 131-134.
2896
2897 1192 Hall, A.M., Thomas, M.F., Thorp, M.B., 1985. Late Quaternary alluvial placer development in
2898
2899 1193 the humid tropics. The case of the Birim diamond placer, Ghana. J. Geol. Soc. 142, 777-
2900
2901 1194 787.
2902
2903 1195 Hilton, T.E., 1963. The geomorphology of North-Eastern Ghana. Z. Geomor. N.F. 7, 308-325.
2904
2905 1196 Holmes, C.D., 1955. Geomorphic development in humid and arid regions: a synthesis. Am. J.
2906
2907 1197 Sci. 253, 377-390.
2908
2909 1198 King, L.C., 1948. On the Age of the African land-surfaces. Q. J. Geol. Soc. Lond. 104, 439-459.
2910
2911 1199 King, L.C., 1967. The morphology of the Earth, second ed. Oliver and Boyd, Edinburgh.
2912
2913 1200 Lamotte, M., Rougerie, G., 1953. Les cuirasses ferrugineuses allochtones. Signification
2914
2915 1201 paléoclimatique et rapports avec la végétation. IV Réunion. African. de l'Ouest, Abidjan, 89-
2916
2917 1202 90.
2918
2919 1203 Lamotte, M., Rougerie, G., 1962. Les apports allochtones dans la formation des cuirasses
2920
2921 1204 ferrugineuses. Rev. Géomor. Dyn. 13, 145-160.
2922
2923 1205 Le Cocq, A., 1986. Carte pédologique et carte des capacités agronomiques des sols à 1/100
2924
2925 1206 000, Région de Bassar (Togo). ORSTOM, Notice explicative 102, 1-103.
2926
2927 1207 Lecomte, P., 1988. Stone line profiles - Importance in geochemical exploration. J. Geochem.
2928
2929 1208 Explor. 30, 35-61.
2930
2931
2932
2933
2934
2935
2936
2937
2938
2939
2940

- 2941
2942
2943 1209 Lecomte, P., Zeegers, H., 1992. Humid tropical terrains (rainforests), in: Butt, C.R.M., Zeegers,
2944
2945 1210 H. (Eds.), Regolith exploration geochemistry in tropical and subtropical terrains. Elsevier,
2946
2947 1211 Amsterdam, pp. 241-294.
2948
2949 1212 Leprun, J.C., 1979. Les cuirasses ferrugineuses des pays cristallins de l'Afrique occidentale
2950
2951 1213 sèche - g n se, transformation, d gradation. Sci. G ol. M m. 58, 1-224.
2952
2953 1214 Mabbutt, J.A., 1966. Mantle-controlled planation of pediments. Am. J. Sci. 264, 78-91.
2954
2955 1215 Maignien, R., 1958. Le cuirassement des sols en Guin e, Afrique Occidentale. M m. Serv.
2956
2957 1216 Carte G ol. Alsace Lorraine 16, 1-239.
2958
2959 1217 Maignien, R., 1966. Compte rendu de recherches sur les lat rites. UNESCO, Paris.
2960
2961 1218 Markwitz, V., Hein, K.A.A., Jessell, M.W., Miller, J., 2016. Metallogenic portfolio of the West
2962
2963 1219 African craton. Ore. Geol. Rev. 78, 558-563.
2964
2965 1220 McFarlane, M.J., 1976. Laterite and landscape. Academic Press, London.
2966
2967 1221 Mensching, H., 1966. Fl chenbildung in der Sudan-und Sahel-Zone (Ober-Volta und Niger). Z.
2968
2969 1222 Geomor. N.F. 10, 1-29.
2970
2971 1223 Metelka, V., Baratoux, L., Naba, S., Jessell, M.W., 2011. A geophysically constrained litho-
2972
2973 1224 structural analysis of the Eburnean greenstone belts and associated granitoid domains,
2974
2975 1225 Burkina Faso, West Africa. Precambrian Res. 190, 48-69.
2976
2977 1226 Metelka, V., Baratoux, L., Jessell, M.W., Barth, A., Jezek, J., Naba, S., 2018. Automated
2978
2979 1227 regolith landform mapping using airborne geophysics and remote sensing data, Burkina
2980
2981 1228 Faso, West Africa. Remote Sens. Environ. 204, 964-978.
2982
2983 1229 Meyer, B., 1992. A detailed soil differentiation of slopes with slight inclination in the
2984
2985 1230 Niamtougou plain in North-Togo. Z. Geomor. N.F. 91, 124-134.
2986
2987 1231 Michel, P., 1959. L' volution g omorphologique des bassins du S n gal et de la Haute-
2988
2989 1232 Gambie, ses rapports avec la prospection mini re. Rev. G omorph. Dyn. 10, 117-143.
2990
2991
2992
2993
2994
2995
2996
2997
2998
2999
3000

- 3001
3002
3003 1233 Michel, P., 1969. Les grandes étapes de la morphogenèse dans les bassins des fleuves
3004
3005 1234 Sénégal et Gambie pendant le Quaternaire. Bull. IFAN 31, 293-324.
3006
3007 1235 Michel, P., 1973. Les bassins des fleuves Sénégal et Gambie, étude géomorphologique. Mém.
3008
3009 1236 ORSTOM 63, 1-752.
3010
3011 1237 Michel, P., 1974. Les glacis cuirassés d'Afrique occidentale et centrale. Géomorphologie des
3012
3013 1238 glacis : Colloques scientifiques de l'Université de Tours, Tours, France, pp. 70-80.
3014
3015 1239 Milesi, J.P., Ledru, P., Feybesse, J.L., Dommanget, A., Marcoux, E., 1992. Early Proterozoic
3016
3017 1240 Ore-Deposits and Tectonics of the Birimian Orogenic Belt, West Africa. Precambrian Res.
3018
3019 1241 58, 305-344.
3020
3021 1242 Millot, G., 1980. Les grands aplanissements des socles continentaux dans les pays
3022
3023 1243 subtropicaux, tropicaux et désertiques. Mém. H. Sér. Soc. Géol. France 10, 295-305.
3024
3025 1244 Millot, G., 1970. The geology of clays. Springer-Verlag, Berlin.
3026
3027 1245 Millot, G., 1983. Planation of continents by intertropical weathering and pedogenetic
3028
3029 1246 processes. IInd International Seminar on lateritisation processes, Sao Paulo, Brazil, July 4-
3030
3031 1247 12 1982, 53-63.
3032
3033 1248 Nahon, D.B., Boulangé, B., Colin, F., 1992. Metallogeny of weathering : an introduction. in:
3034
3035 1249 Martini, I.P., Chesworth, W. (Eds.), Weathering, soils and paleosols. Elsevier, Amsterdam,
3036
3037 1250 pp 445-467.
3038
3039 1251 Nahon, D., Millot, G. , Paquet, H., Ruellan, A., Tardy, Y., 1977. VII. Digestion et effacement des
3040
3041 1252 cuirasses ferrugineuses par les encroûtements calcaires en pays aride, Sahara et
3042
3043 1253 Mauritanie. Sci. Géol., Bull. 30, 289-296.
3044
3045 1254 Oberlander, T.M., 1989. Slope and pediment systems, in: Thomas, D.S.G. (Ed.), Arid zone
3046
3047 1255 geomorphology. Belhaven, London, pp. 56-84.
3048
3049 1256 Oberlander, T.M., 1997. Slope and pediment systems, in: Thomas, D.S.G. (Ed.), Arid zone
3050
3051 1257 geomorphology. Wiley, Chichester, pp. 135-163.
3052
3053
3054
3055
3056
3057
3058
3059
3060

3061
3062
3063 1258 Ollier, C.D., Galloway, R.W., 1990. The Laterite Profile, Ferricrete and Unconformity. *Catena*
3064
3065 1259 17, 97-109.
3066
3067 1260 Ollier, C.D., Pain, C.F., 1996. Regolith stratigraphy: principles and problems. *AGSO J. Aust.*
3068
3069 1261 *Geol. Geophys.* 16, 197-202.
3070
3071 1262 Ouangrawa, M., Grandin, G., Parisot, J.-C., Baras, E., 1996. Dispersion mécanique de l'or dans
3072
3073 les matériaux de surface : exemple du site aurifère de Piéla (Burkina-Faso). *Pangea* 25, 25-
3074 1263 40.
3075
3076 1264
3077
3078 1265 Parisot, J.-C., Ventose, V., Grandin, G., Bourges, F., Debat, P., Tollon, F., Millot, L., 1995.
3079
3080 1266 Dynamique de l'or et d'autres minéraux lourds dans un profil d'altération cuirassé du
3081
3082 1267 Burkina Faso (Afrique de l'Ouest). Intérêt pour l'interprétation de la mise en place des
3083
3084 1268 matériaux constituant les cuirasses de haut-glacis. *C.R. Acad Sci. Paris* 301, 295-302.
3085
3086 1269 Paul, J.D., Roberts, G.G., White, N., 2014. The African landscape through space and time.
3087
3088 1270 *Tectonics* 33, 898-935.
3089
3090 1271 Payne, A.L., 1969. Exploration on pediments. *Econ. Geol.* 64, 117.
3091
3092 1272 Pease, R.C., 2015. Understanding Pediments for Mineral Exploration, in: Pennell, W.M.,
3093
3094 1273 Garside, L.J. (Eds.), *Geological Society of Nevada's Symposium, Sparks, May 14-23, 2015.*
3095
3096 1274 *New Concepts and Discoveries*, pp. 1365-1372.
3097
3098 1275 Pélissier, P., Rougerie, G., 1953. Problèmes morphologiques dans le bassin de Siguiri (Haut
3099
3100 1276 Niger). *Bull. I.F.A.N.* 15, 1-47.
3101
3102 1277 Pèltre, P., 1977. Le "V Baoulé" (Côte d'Ivoire centrale). Héritage géomorphologique et
3103
3104 1278 paléoclimatique dans le tracé du contact forêt - savane. *Trav. Doc. ORSTOM* 80, 1-198.
3105
3106 1279 Porto, C.G., 2016. Geochemical exploration challenges in the regolith dominated Igarape
3107
3108 1280 Bahia gold deposit, Carajas, Brazil. *Ore Geol. Rev.* 73, 432-450.
3109
3110 1281 Riquelme, R., Tapia, M., Campos, E., Mpodozis, C., Carretier, S., González, R., Muñoz, S.,
3111
3112 1282 Fernandez-Mort, A., Sanchez, C., Marquardt, C., 2017. Supergene and exotic Cu
3113
3114
3115
3116
3117
3118
3119
3120

3121
3122
3123 1283 mineralization occurs during periods of landscape stability in the Centinela Mining
3124
3125 1284 District, Atacama Desert. Basin. Res., doi: 10.1111/bre.12258.
3126
3127 1285 Rohdenburg, H., 1969. Hangpedimentation and klimawechsel als wichtigste faktoren der
3128
3129 1286 flächen- und stufenbildung in den wechselfeuchten tropen an beispielen aus Westafrika,
3130
3131 1287 besonders aus dem schichtstufenland Südost-Nigerias. Göttinger Bodenkdl. Ber. 10, 57-
3132
3133 1288 133.
3134
3135 1289 Rohdenburg, H., 1982. Geomorphologisch-bodenstratigraphischer Vergleich zwischen dem
3136
3137 1290 Nordostbrasilianischen Trockengebiet und immerfeucht-tropischen Gebieten
3138
3139 1291 Sfidbrasilien mit Ausf'tirungen zum Problemkreis der Pediplain-Pediment-
3140
3141 1292 Terrassentreppen. Catena Suppl. 2, 74-122.
3142
3143 1293 Roquin, C., Freyssinet, P., Zeegers, H., Tardy, Y., 1990. Element distribution patterns in
3144
3145 1294 laterites of southern Mali. Consequence for geochemical prospecting and mineral
3146
3147 1295 exploration. Appl. Geochem. 5, 303-315.
3148
3149 1296 Ruhe, R.V., 1956. Landscape evolution in the High Ituri, Belgian Congo. Publ. Inst. Nat. Et.
3150
3151 1297 Agron. Congo Belge 66, 1-108.
3152
3153 1298 Sanfo, A., Colin, F., Delaune, M., Boulangé, B., Parisot, J.-C., Bradley, R., Bratt, J., 1993. Gold:
3154
3155 1299 a useful tracer in sub-Sahelian laterites. Chem. Geol. 107, 323-326.
3156
3157 1300 Sanfo, Z., Grandin, G., Parisot, J.-C., Pale, F., 1992. Aplanissements latéritisés anciens, glaciais
3158
3159 1301 récents et indices d'or dans la région d'Aribinda (Burkina Faso), in: Schmidt, J., Gall, Q.
3160
3161 1302 (Eds.), Mineralogical and geochemical records of paleoweathering. ENSPM Mém. Sci.
3162
3163 1303 Terre, Paris, pp. 1-16.
3164
3165 1304 Scott, K.M., Pain, C.F., 2008. Introduction, in: Scott, K.M., Pain, C.F. (Eds.), Regolith Science.
3166
3167 1305 Springer Science, Dordrecht, pp. 1-6.
3168
3169 1306 Sillitoe, R.H., 2005. Supergene Oxidized and Enriched Porphyry Copper and Related Deposits.
3170
3171 1307 Econ. Geol. 100th Anniversary Volume, 723-768.
3172
3173
3174
3175
3176
3177
3178
3179
3180

3181
3182
3183 1308 Summerfield, M.A., 1985. Plate tectonics and landscape development on the African
3184
3185 1309 continent, in: Morisawa, M., Hack, J.T. (Eds.), Tectonic geomorphology. Allen & Unwin,
3186
3187 1310 Boston, pp. 27-51.
3188
3189 1311 Summerfield, M.A., 1991. Global geomorphology. Longman Scientific & Technical, Harlow.
3190
3191 1312 Summerfield, M.A., 1996. Tectonics, geology, and long-term landscape development, in:
3192
3193 1313 Adams, W.M., Goudie, A.S., Orme, A.R. (Eds.), Physical geography of Africa. Oxford
3194
3195 1314 University Press, Oxford, pp. 1-17.
3196
3197 1315 Tardy, Y., 1997. Petrology of laterites and tropical soils. Balkema, Rotterdam.
3198
3199 1316 Tardy, Y., Mazaltarim, D., Boeglin, J.L., Roquin, C., Pion, J.C., Paquet, H., Millot, G., 1988.
3200
3201 1317 Lithodépendance et homogénéisation de la composition minéralogique et chimique des
3202
3203 1318 cuirasses ferrugineuses latéritiques. C. R. Acad. Sci. Paris 307, 1765-1772.
3204
3205 1319 Tardy, Y., Roquin, C., 1992. Geochemistry and evolution of lateritic landscapes, in: Martini,
3206
3207 1320 I.P., Chesworth, W. (Eds.), Weathering, soils and paleosols. Elsevier, Amsterdam, pp. 407-
3208
3209 1321 444.
3210
3211 1322 Tardy, Y., Roquin, C., 1998. Dérive des continents, paléoclimats et altérations tropicales.
3212
3213 1323 Editions BRGM, Orléans.
3214
3215 1324 Teeuw, R.M., 1987. Variations in the composition of gravel layers across the landscape.
3216
3217 1325 Examples from Sierra Leone. Geo-Eco. Trop. 11, 151-169.
3218
3219 1326 Teeuw, R.M., 2002. Regolith and diamond deposits around Tortiya, Ivory Coast, West Africa.
3220
3221 1327 Catena 49, 111-127.
3222
3223 1328 Teeuw, R.M., Thomas, M.F., Thorp, M.B., 1991. Geomorphology applied to exploration for
3224
3225 1329 tropical placer deposits, Alluvial mining. Elsevier Applied Science, London, New York, pp.
3226
3227 1330 458-480.
3228
3229 1331 Thomas, M.F., 1978. The study of inselbergs. Z. Geomor. N. F. 31, 1-41.
3230
3231
3232
3233
3234
3235
3236
3237
3238
3239
3240

- 3241
3242
3243 1332 Thomas, M.F., 1980. Timescale of landform development on tropical shields - A study from
3244
3245 1333 Sierra Leone, in: Cullingford, R.A., Davidson, D.A., Lewin, J. (Eds.), Timescales in
3246
3247 1334 Geomorphology. Wiley, Chichester, pp. 333-354.
3248
3249 1335 Thomas, M.F., 1989. The role of etch processes in landform development. 2. Etching and the
3250
3251 1336 formation of relief. Z. Geomorph. N. F. 33, 257-274.
3252
3253 1337 Thomas, M.F., 1994. Geomorphology in the tropics: A study of weathering and denudation in
3254
3255 1338 low latitudes. Wiley & Sons, New York.
3256
3257 1339 Thomas, M.F., Thorp, M.B., 1985. Environmental change and episodic etchplanation in the
3258
3259 1340 humid tropics of Sierra Leone: the Koidu etchplain, in: Douglas, J., Spencer, T. (Eds.),
3260
3261 1341 Environmental change and tropical geomorphology. George Allen & Unwin, London, pp.
3262
3263 1342 239-267.
3264
3265 1343 Thomas, M.F., Thorp, M.B., Teeuw, R.M., 1985. Paleogeomorphology and the occurrence of
3266
3267 1344 diamondiferous placer deposits in Koidu, Sierra Leone. J. Geol. Soc. 142, 789-802.
3268
3269 1345 Thomas, M.F., Summerfield, M.A., 1987. Long-term landform development: key themes and
3270
3271 1346 research problems, in: Gardiner, V. (Ed.), International Geomorphology 1986, Part II. John
3272
3273 1347 Wiley & Sons, London, pp. 935-956.
3274
3275 1348 Tricart, J., 1972. The landforms of the humid tropics, forests and savannas. Longman,
3276
3277 1349 London.
3278
3279 1350 Tricart, J., Michel, P., Vogt, J., 1957. Oscillations climatiques quaternaires en Afrique
3280
3281 1351 Occidentale. Fifth Congr. INQUA, Madrid-Barcelona, 1957, 187-188.
3282
3283 1352 Tricart, J., 1959. Observations sur le façonnement des rapides des rivières intertropicales.
3284
3285 1353 Bull. Sect. Géogr. Com. Trav. Hist. Sci. LXXI, 289-313.
3286
3287 1354 Twidale, C.R., 1983. Pediments, peneplains, and ultiplains. Rev. Géomor. Dyn. 32, 1-35.
3288
3289 1355 Twidale, C.R., 1991. A Model of Landscape Evolution Involving Increased and Increasing
3290
3291 1356 Relief Amplitude. Z Geomor. N.F. 35, 85-109.
3292
3293
3294
3295
3296
3297
3298
3299
3300

3301
3302
3303 1357 Twidale, C.R., Bourne, J.A., 2013. Do pediplains exist? Suggested criteria and examples. Z.
3304
3305 1358 Geomor. 57, 411-428.
3306
3307 1359 Valeton, I., 1991. Bauxites and Associated Terrestrial Sediments in Nigeria and Their Position
3308
3309 1360 in the Bauxite Belts of Africa. J. Afr. Earth Sci. 12, 297-310.
3310
3311 1361 Valeton, I., 1994. Element Concentration and Formation of Ore-Deposits by Weathering.
3312
3313 1362 Catena 21, 99-129.
3314
3315 1363 Vasconcelos, P.M., Brimhall, G.H., Becker, T.A., Renne, P.R., 1994. Ar-40/Ar-39 Analysis of
3316
3317 1364 Supergene Jarosite and Alunite - Implications to the Paleoweathering History of the
3318
3319 1365 Western USA and West-Africa. Geochim. Cosmochim. Acta 58, 401-420.
3320
3321 1366 Vogt, J., 1959a. Aspects de l'évolution morphologique récente de l'ouest africain. Ann. Géogr.
3322
3323 1367 Franç. 367, 193-206.
3324
3325 1368 Vogt, J., 1959b. Observations nouvelles sur les alluvions inactuelles de Côte d'Ivoire et de
3326
3327 1369 Haute-Guinée, 84^{ème} Congr. Soc. Sav., Dijon, pp. 205-210.
3328
3329 1370 Ye, J., Chardon, D., Rouby, D., Guillocheau, F., Dall'asta, M., Ferry, J.N., Broucke, O., 2017.
3330
3331 1371 Paleogeographic and structural evolution of northwestern Africa and its Atlantic margins
3332
3333 1372 since the early Mesozoic. Geosphere 13, 1254-1284.
3334
3335 1373 Zeegers, H., Lecomte, P., 1992. Seasonnally humid tropical terrains (savannas), in: Butt,
3336
3337 1374 C.R.M., Zeegers, H. (Eds.), Regolith exploration geochemistry in tropical and subtropical
3338
3339 1375 terrains. Elsevier, Amsterdam, pp. 203-240.
3340
3341 1376 Zeegers, H., Leprun, J.C., 1979. Evolution des concepts en altérologie tropicale et
3342
3343 1377 conséquences potentielles pour la prospection géochimique en Afrique occidentale
3344
3345 1378 soudano-sahélienne. Bull. Bur. Rech. Géol. Min. 2-3, 229-239.
3346
3347 1379
3348
3349
3350
3351
3352
3353
3354
3355
3356
3357
3358
3359
3360

3361
3362
3363 1380 **Figure captions**
3364
3365 1381
3366
3367 1382 **Figure 1.** Definition of the main elements of a lateritic weathering profile.
3368
3369 1383
3370
3371 1384 **Figure 2.** Topography, drainage, climatic zonation and political borders of Sub-Saharan
3372
3373 West Africa. Climatic zones are adapted from Aubréville (1949). Savannas typically
3374 1385
3375 encompass the Guinean and Soudanian zones. For convenience, the Saharan, Sahelian and
3376 1386
3377 Soudanian zones are grouped in the present work as “dry regions”. Al: Algeria; Be: Benin; BF:
3378 1387
3379 Burkina Faso; C: Cameroon; G: Gambia; GB: Guinea Bissau; Gu: Guinea; IC: Ivory Coast; L:
3380 1388
3381 Liberia; Ma: Mali; Mau: Mauritania; Mo: Morocco; Na: Nigeria; Ni: Niger; Se: Senegal; SL: Sierra
3382 1389
3383 Leone; T: Togo.
3384 1390
3385
3386 1391
3387
3388 1392 **Figure 3.** Gold dispersion model through the regolith for ferricrete-capped West African
3389
3390 landscapes (adapted from Freyssinet et al., 2005). The model is mostly based on the
3391 1393
3392 examples of the Syama mine (e.g., Fig. 2) and Banankoro prospect (Mali).
3393 1394
3394
3395 1395
3396
3397 1396 **Figure 4.** Synthetic representation (a) and Ar-Ar chronology (b) of the West African landform-
3398
3399 regolith sequence (modified after Beauvais and Chardon, 2013 and Grimaud et al., 2015). Ar-
3400 1397
3401 Ar dates (solid circles) are from Beauvais et al. (2008) for cryptomelane samples from
3402 1398
3403 Tambao locality (Fig. 2). Ar-Ar dates from Syama (Southern Mali) are from Vasconcelos et al.
3404 1399
3405 (1994) (Fig. 2). Colored vertical stripes correspond to the weathering periods of each
3406 1400
3407 generation of landform-regolith association as deduced from Ar-Ar dating in Tambao.
3408 1401
3409
3410 1402
3411
3412 1403 **Figure 5.** Remnants of the West African morphoclimatic sequence as exposed in the Goren
3413
3414 greenstone belt near Kaya, Central Burkina Faso. Above: east-looking GoogleEarth view;
3415 1404
3416
3417
3418
3419
3420

3421
3422
3423 1405 below: interpretation based on field survey and photointerpretation (vertical exaggeration:
3424
3425 1406 x3). Areas in white are steep post-High glacis incision slopes exposing saprolite. Position of
3426
3427 1407 the 501 m height spot is 13.040825°N / 1.211588°E.
3428
3429 1408
3430
3431 1409 **Figure 6.** Sketch cross-sections of the two main glacis landscapes in West Africa. (a)
3432
3433 1410 Piedmont of a bauxite-capped mesa in greenstone belt terrain (inspired from field surveys in
3434
3435 1411 the Kongoussi area, Northern Burkina Faso). Dashed lines represent the maximum original
3436
3437 1412 extent of each glacis surfaces. (b) Rolling pediplain of the Middle glacis over granitoid or
3438
3439 1413 sandstone terrains. Bedrock is shown in grey and saprolite in yellow. Note the different
3440
3441 1414 scales in (a) and (b).
3442
3443 1415
3444
3445 1416 **Figure 7.** Three successive glacis landscape stages of West African granite-greenstone
3446
3447 1417 terrains (modified after Eschenbrenner and Grandin, 1970). (a) High glacis stage. (b) Early
3448
3449 1418 settlement of the Middle glacis (yellow). (c) Installation of the Low glacis (light blue). The
3450
3451 1419 model is based on regional field surveys in Northern Ivory Coast and Southwestern Burkina
3452
3453 1420 Faso across the Guinean and Soudanian zones (Fig. 2).
3454
3455 1421
3456
3457 1422 **Figure 8.** Dissection patterns of West African glacis systems (modified after Grandin and Joly,
3458
3459 1423 2008). (a) Piedmont configuration of downslope-decreasing incision through time. (b)
3460
3461 1424 Piedmont configuration of downslope-increasing incision through time. Patterns (b) are
3462
3463 1425 favored along main river segments of enhanced/accelerated down cutting (i.e., base-level
3464
3465 1426 lowering), as opposed to patterns in (a) that are produced along main river segments of
3466
3467 1427 mitigated/reduced down cutting (see Grimaud et al., 2014). (c)-(e) dissection scenarios of a
3468
3469 1428 rolling pediplain. A High glacis rolling pediplain (c) may be degraded in two main types of
3470
3471 1429 landscapes depending on where dissection focuses. Landscape (d) results if erosion
3472
3473
3474
3475
3476
3477
3478
3479
3480

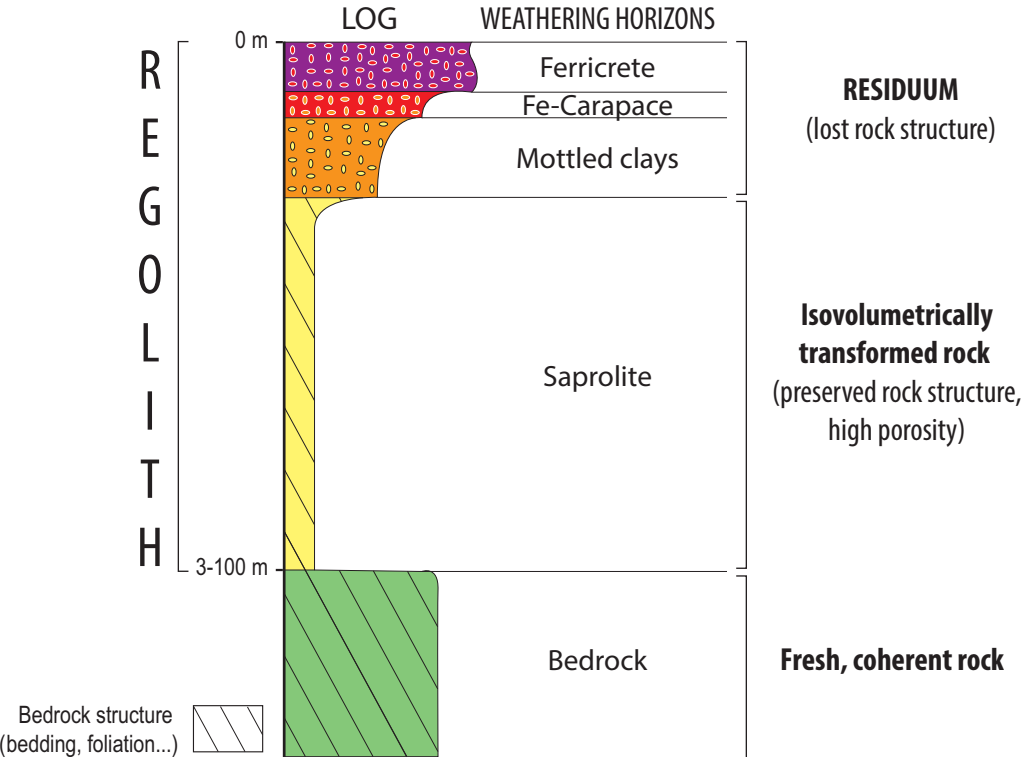
3481
3482
3483 1430 predominates along the main river drains of the initial rolling plain. Landscape (e) results if
3484
3485 1431 erosion predominates in crestal regions of the initial rolling plain (black arrows point to the
3486
3487 1432 main river drain i.e., the local base level). In (d), the main slope portions of former glacis are
3488
3489 1433 preferentially preserved. In (e), mostly valley bottoms of the former rolling pediplain are
3490
3491 1434 preserved. In this case, the relief inversion concept strictly applies, as lower parts of the
3492
3493 1435 ancient landscape become the highest parts of the new landscape.
3494
3495
3496 1436
3497
3498 1437 **Figure 9.** (a) High glacis ferricrete relicts over southwestern Burkina Faso. (b) Corresponding
3499
3500 1438 geomorphic map reconstitution of the High glacis pediplain (modified after Grimaud et al.,
3501
3502 1439 2015).
3503
3504
3505 1440
3506
3507 1441 **Figure 10.** Idealized cross-sections of the successive landscape stages in West Africa. Black
3508
3509 1442 arrows locate the main river drains and white arrows the drainage divides. Such a landscape
3510
3511 1443 evolution model would typify the Soudanian or Sahelian zones (Fig. 2), where the original
3512
3513 1444 shapes of High and Middle glacis inverted landforms are preferentially preserved as plateaus
3514
3515 1445 (see Fig. 19).
3516
3517 1446
3518
3519 1447 **Figure 11.** Detailed cross-section of a Middle glacis near Bania, ca. 100 km south of the Ivory
3520
3521 1448 Coast – Burkina Faso border (modified from Eschenbrenner and Grandin, 1970). Upslope
3522
3523 1449 part of the Middle glacis is an erosional, ferricrete-free surface exposing exhumed (old)
3524
3525 1450 saprolite that was turned into mottled clays at the surface. Downslope part of the glacis is
3526
3527 1451 erosional in the sense that it stripped-off the saprolite, but is depositional in the sense that it
3528
3529 1452 carries a detrital colluvial layer that passes downslope to river alluviums. The ferricrete
3530
3531 1453 developed by duricrusting of most of the transported material. A thin weathering layer
3532
3533 1454 developed into the bedrock under the downslope portion of the glacis.
3534
3535
3536
3537
3538
3539
3540

3541
3542
3543 1455
3544
3545 1456 **Figure 12.** Field illustrations of glacis conglomeratic overburdens. (a) Block-supported
3546
3547 1457 debris flow (High glacis near Timbou, Guinea). The cobble is a bauxite. (b) Heterogeneous
3548
3549 1458 debris-flow facies underlain by dolerite core stones (High glacis near Kokoro, Burkina Faso).
3550
3551 1459 Cobbles are made of bauxite. The fine-grained saprolite and mottled clay horizons are
3552
3553 1460 missing from this weathering profile, suggesting its truncation by the debris flow. (c) Debris-
3554
3555 1461 flow with bauxite (light colored) and Intermediate ferricrete clasts in a matrix made of iron
3556
3557 1462 oxy-hydroxide nodules and pebbles (High glacis, near Basnéré, Burkina Faso). (d)
3558
3559 1463 Conglomerate comprising exclusively Intermediate ferricrete clasts (Middle glacis, near Kaya,
3560
3561 1464 Burkina Faso). (e) Matrix-supported debris flow with Intermediate ferricrete cobbles
3562
3563 1465 (carapace of the Low glacis, near Matam, Senegal). (f) Basal alluvial channel carved in a
3564
3565 1466 sandstone saprolite (High glacis, south of Bobo Dioulasso, Burkina Faso). Channel material
3566
3567 1467 consists of quartz pebbles and iron nodules in a kaolinite-rich silty clay matrix. Cementation
3568
3569 1468 increases upward in the channel. Only cases (b) to (d) are ferricretes.
3570
3571 1469
3572
3573 1470 **Figure 13.** Photograph (left) and interpretation (right) of a composite glacis ferricrete
3574
3575 1471 composed of a conglomeratic layer overlying a vermiform facies developed from the
3576
3577 1472 underlying mottle clays (High glacis, near Tikaré, Burkina Faso). The fine-grained material is
3578
3579 1473 likely preserved on its parental bedrock from which it derived by weathering. However, a
3580
3581 1474 transported origin cannot be precluded (see text for further explanation).
3582
3583 1475
3584
3585 1476 **Figure 14.** Glacis ferricretes derived from fine-grained material. (a) and (b) are exposed
3586
3587 1477 weathered surfaces and (c) and (d) are fresh cuts. (a) Fine-grained nodular ferricrete (Middle
3588
3589 1478 glacis, near Kedougou, Eastern Senegal). (b) Nodular ferricrete (High glacis, Niokolo Koba
3590
3591 1479 national park, Eastern Senegal). (c) Vermiform ferricrete (High glacis, near Kongoussi,
3592
3593
3594
3595
3596
3597
3598
3599
3600

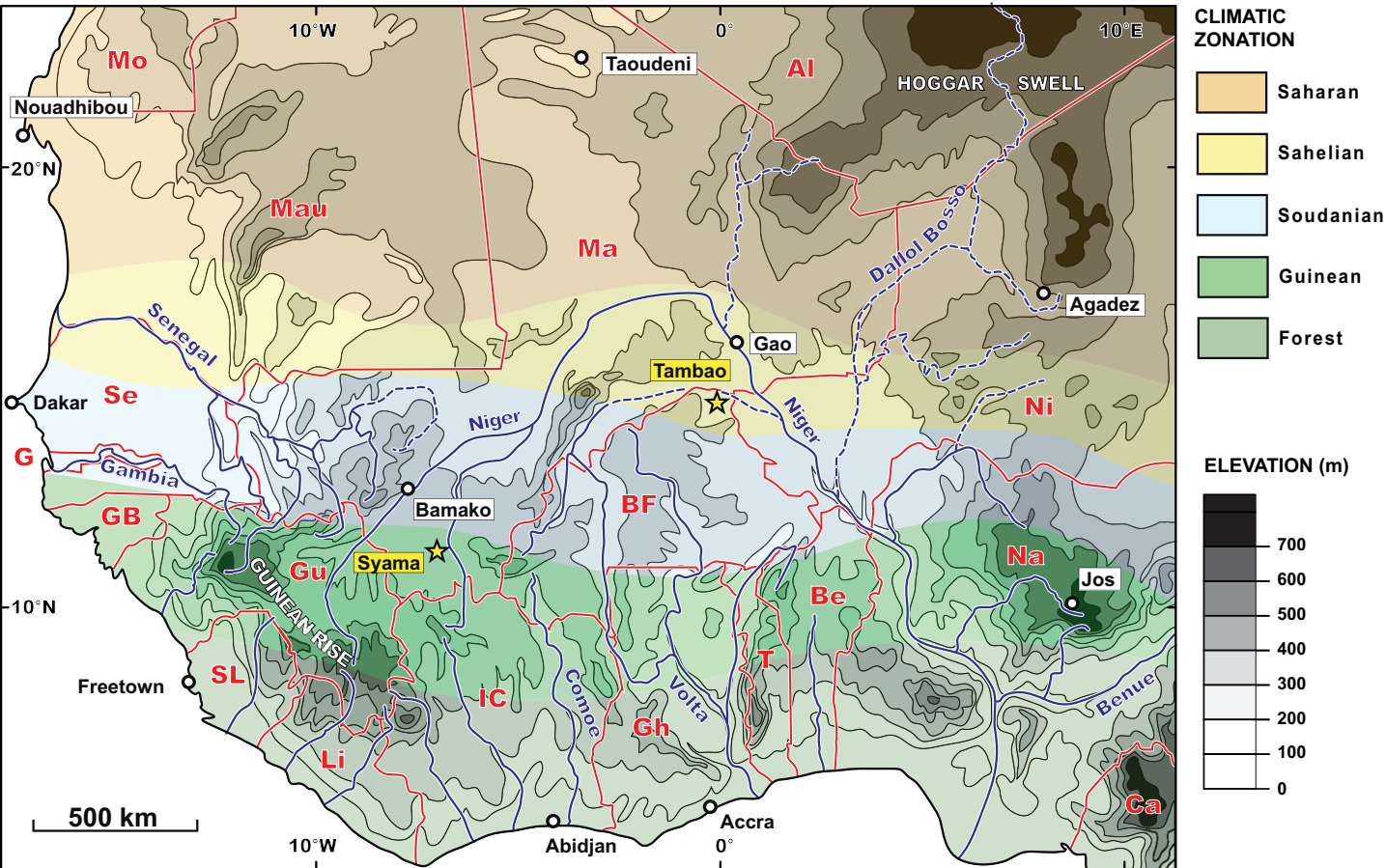
3601
3602
3603 1480 Central Burkina Faso). (d) Proto-nodular ferricrete (High glacia, near Tambakounda, Eastern
3604
3605 1481 Senegal). The iron oxy-hydroxides nodules are in dark grey / black. Nodular and vermiform
3606
3607 1482 ferricretes, and especially those exposed on weathered surfaces, should not be mistaken for
3608
3609 1483 conglomeratic ferricretes. Nodules generally have amoeboid / knucklebone shapes that
3610
3611 1484 distinguish them from gravels or cobbles.
3612
3613 1485
3614
3615 1486 **Figure 15.** Type-logs of West African glacia. Bottom cross-sections illustrate potential
3616
3617 1487 geomorphic contexts of the logs. In (a), the ferricrete is confined to the cover conglomerate
3618
3619 1488 and underlain by a weathering profile derived from bedrock. (b) Same as (a) but with the
3620
3621 1489 ferricrete extending beyond the base of the conglomerate (the conglomerate may also
3622
3623 1490 occupy part, or the entire thickness of, the carapace). (c) The ferricrete is restrained to the
3624
3625 1491 cover conglomerate that rests upon a truncated weathering profile. (d) Weathering profile
3626
3627 1492 developed from exhumed bedrock. (e) The glacia weathering profile affects both a fine-
3628
3629 1493 grained transported cover and the underlying bedrock. (f) Erosional surface exposing a
3630
3631 1494 truncated weathering profile (mottled clays formed at the surface). (g) Fine-grained cover
3632
3633 1495 overlying a truncated weathering profile. (h) Detrital sediments overlying a conglomeratic
3634
3635 1496 ferricrete. Question marks indicate contacts that may not be readily detected between
3636
3637 1497 comparable saprolites of contrasted origins (in-situ and transported). Emoticons refer to the
3638
3639 1498 suitability of the surface sampling medium for bedrock exploration geochemistry. The
3640
3641 1499 problem in (d) is that the ferricrete may not be distinguished from that in (e) (see text for
3642
3643 1500 further explanation). On the bottom cross-section, the residuum (mostly ferricrete and
3644
3645 1501 carapace) is shown by a single reddish color. Cover material and weathering horizons
3646
3647 1502 distribution patterns may be more uneven than shown on the cross-sections and further
3648
3649 1503 complexity may arise from later dissection / denudation.
3650
3651 1504
3652
3653
3654
3655
3656
3657
3658
3659
3660

3661
3662
3663 1505 **Figure 16.** Denudation / weathering scenario for the establishment of a typical West African
3664
3665 1506 lateritic glacis system. (a) Cross-section of a common landform-regolith association. The old
3666
3667 1507 surface is preserved as a mesa capped by a duricrust topping in-situ formed weathering
3668
3669 1508 profile I (i.e., for instance, the Bauxitic or Intermediate landsurface). The younger surface is
3670
3671 1509 a glacis whose development led to relief dissection of the upper/older surface. (b) Sequential
3672
3673 1510 development of the regolith profile for a given column located in (a). Stage 1 results from
3674
3675 1511 older weathering (and therefore dominant “chemical” denudation) leading to the
3676
3677 1512 establishment of landscape I and its underlying weathering profile (I). Stage 2 shows the
3678
3679 1513 configuration after shaping of the glacis by pedimentation, which has stripped off
3680
3681 1514 weathering profile I and eroded part of the underlying bedrock. Stage 3 shows the
3682
3683 1515 configuration after the weathering (II) and ultimate duricrusting of the glacis surface
3684
3685 1516 (ferricrete is restricted here to the transported overburden; e.g., case of Figs. 15a-15c) as a
3686
3687 1517 consequence of climate change. Columns in (a) and (b) are not to scale. Paleolandscape I
3688
3689 1518 could as well be a preexisting glacis. In this case, weathering profile I could already be
3690
3691 1519 composite (with an in-situ and a transported part).
3692
3693 1520
3694
3695 1521 **Figure 17.** Simplified geology (a) and regolith-landform map (b) of West Africa. Landform-
3696
3697 1522 regolith provinces are distinguished on the basis of the generation of landform-regolith
3698
3699 1523 association best preserved in the present-day landscape. (a) is adapted from Ye et al. (2017);
3700
3701 1524 (b) is from the present work. See Figure 2 for comparison with topography and climatic
3702
3703 1525 zonation. The sedimentary cover is overwhelmingly silico-clastic and mainly consists of
3704
3705 1526 sandstones and siltstones. The main rivers are shown both in (a) and in (b).
3706
3707 1527
3708
3709 1528 **Figure 18.** Paleo-zonation of the development and preservation patterns of the West African
3710
3711 1529 glacis systems (modified after Grandin, 1976).
3712
3713
3714
3715
3716
3717
3718
3719
3720

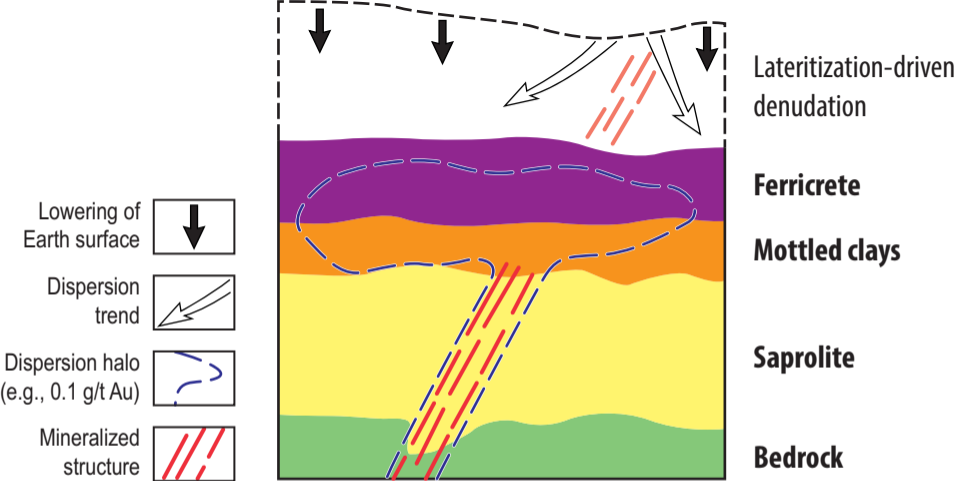
3721
3722
3723 1530
3724
3725 1531 **Figure 19.** Comparative scenarios of glacis ferricrete plateau degradation leading to a
3726
3727 1532 residual hill. (a) Under arid or semi-arid climate. (b) Under humid climate typical of rainforest
3728
3729 1533 environments (modified after Grandin, 1976).
3730
3731
3732 1534
3733
3734 1535 **Figure 20.** Cross-section illustrating transport of mineralized material on successive glacis to
3735
3736 1536 form “transported” geochemical anomalies. The black star represents a surface geochemical
3737
3738 1537 anomaly expressed through a weathering profile and the white stars represent anomalies
3739
3740 1538 mechanically transported on glacis. Large grey arrows show material transport paths on
3741
3742 1539 glacis. Mineralization B first produced a dispersion halo and a surface anomaly through the
3743
3744 1540 old weathering profile. This mineralized weathering profile was then stripped off by
3745
3746 1541 pedimentation to form glacis 1, eventually leading to a transported anomaly on the new
3747
3748 1542 glacis surface. Formation of glacis 2 later led to reworking of the same mineralization that
3749
3750 1543 was still preserved under glacis 1. But this time, because of the creation of a new drainage
3751
3752 1544 divide, mineralized elements were transported in an opposite direction down the glacis 2
3753
3754 1545 slope. Bedrock mineralization B is currently concealed under glacis 2.
3755
3756 1546
3757
3758
3759 1547 **Figure 21.** Gold and copper occurrences and High glacis ferricrete remnants overlying
3760
3761 1548 mineralized bedrock map units, Southwestern Burkina Faso (same map area as Fig. 9).
3762
3763 1549 Sources are Baratoux et al. (2011) and Metelka et al. (2012) for bedrock geology and Castaing
3764
3765 1550 et al. (2003) and the 1/200,000 scale geological maps for mineral occurrences (artisanal and
3766
3767 1551 industrial mining sites, prospects and soil geochemical anomalies). Specific mineralized
3768
3769 1552 bedrock map units such as detrital sediments and ultramafic rocks are too small to be
3770
3771 1553 represented at this scale (4 and 0.4 km² for the entire map area, respectively).
3772
3773 1554
3774
3775
3776
3777
3778
3779
3780



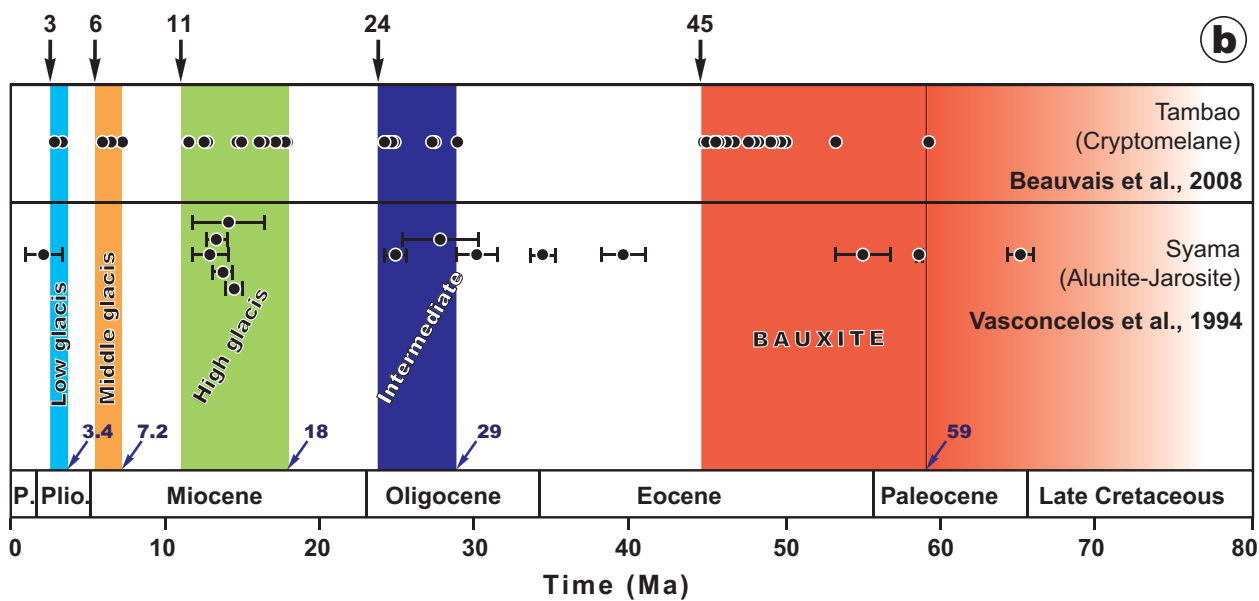
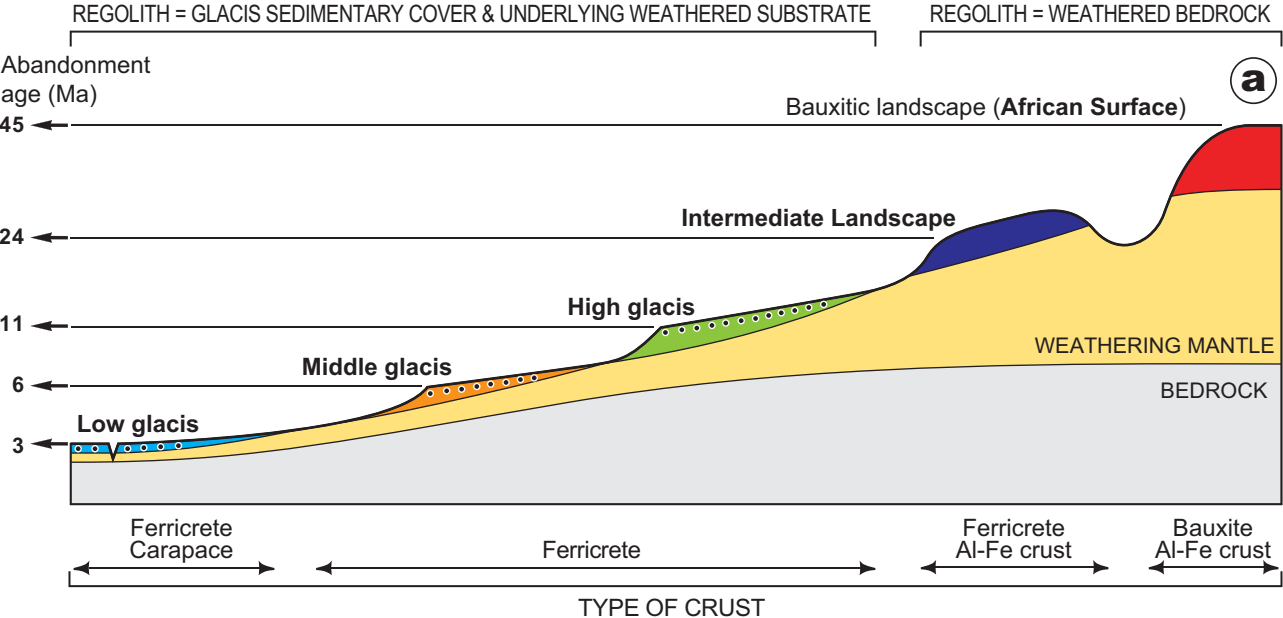
Chardon et al., Figure 1



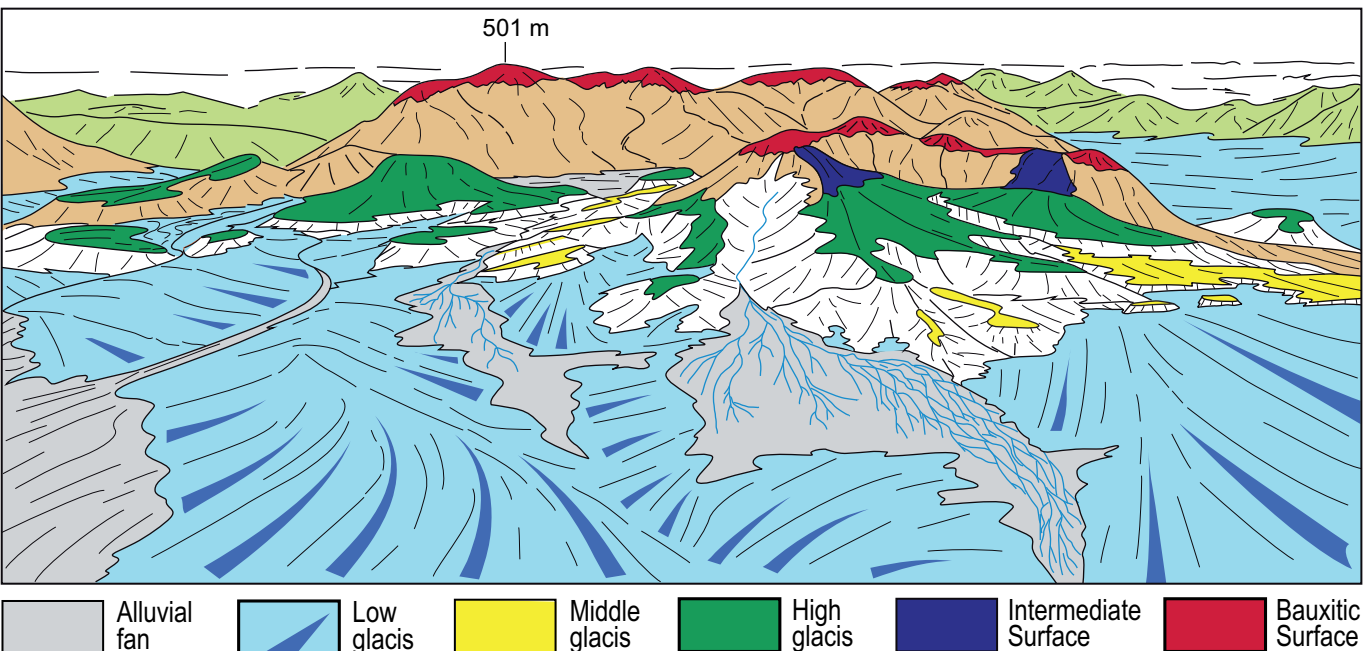
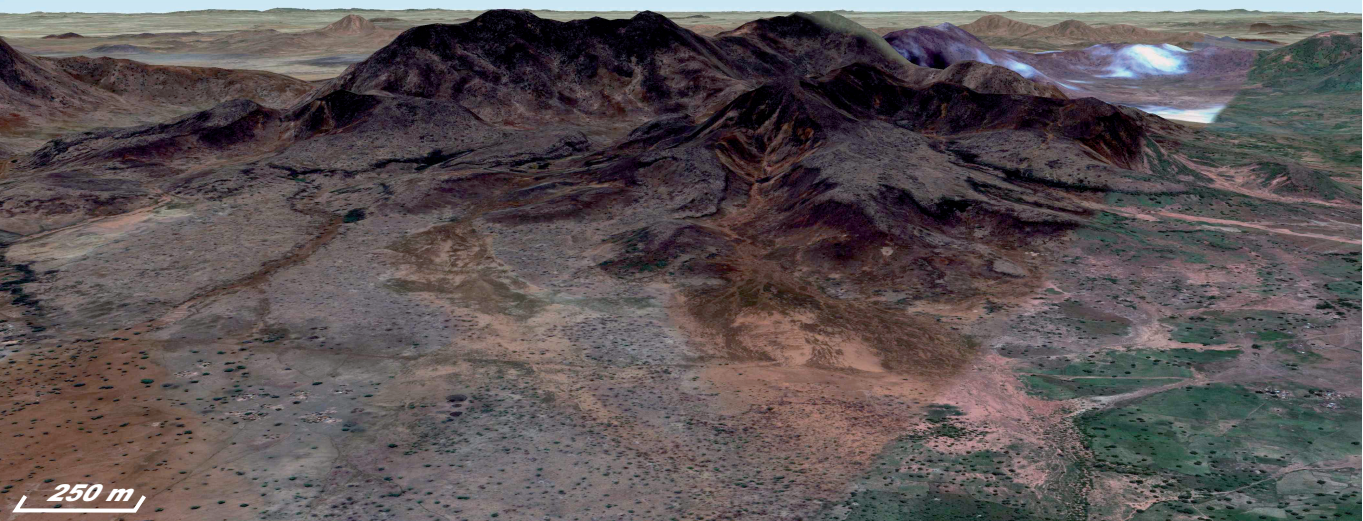
Chardon et al., Figure 2



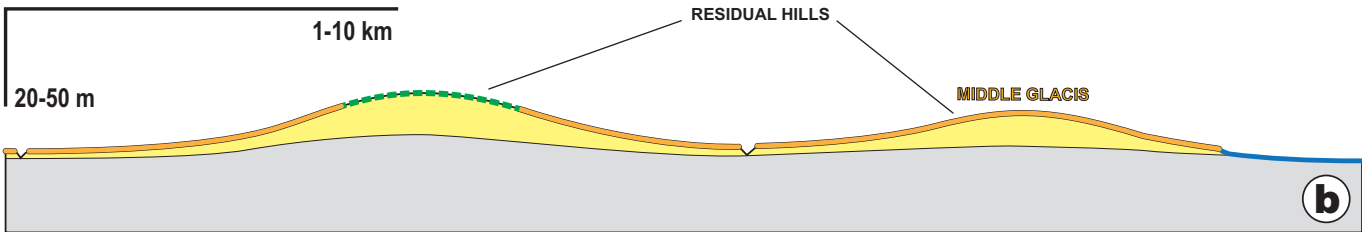
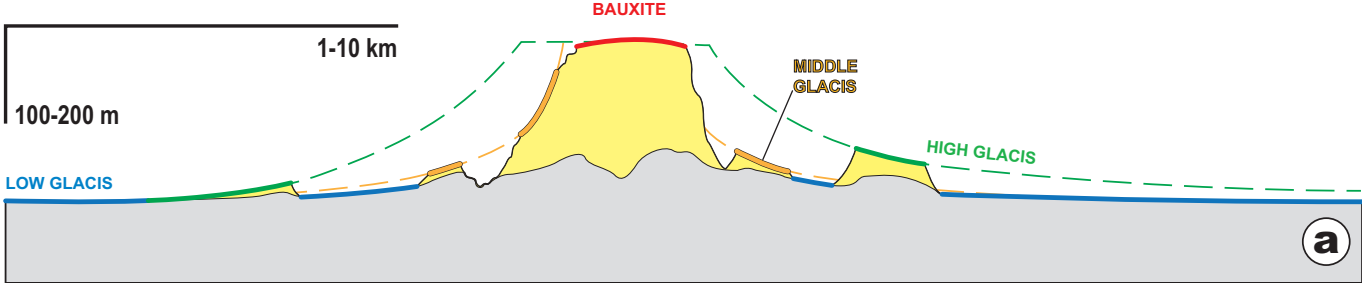
Chardon et al., Figure 3



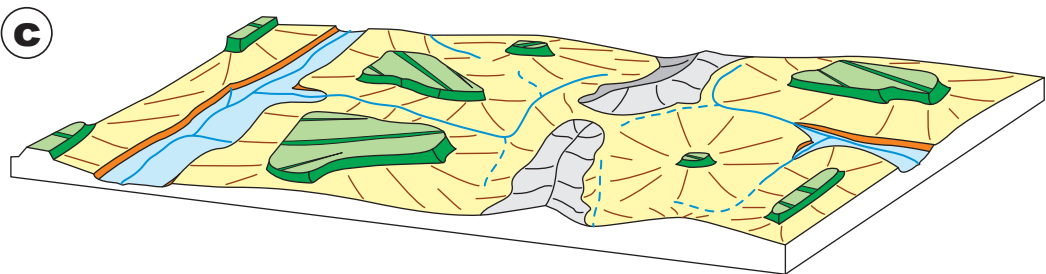
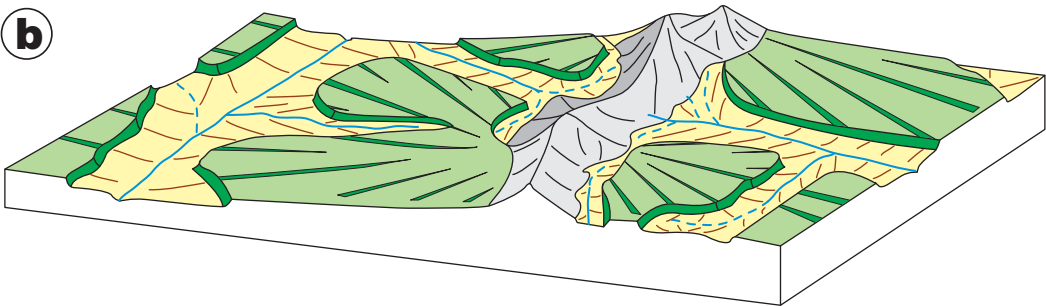
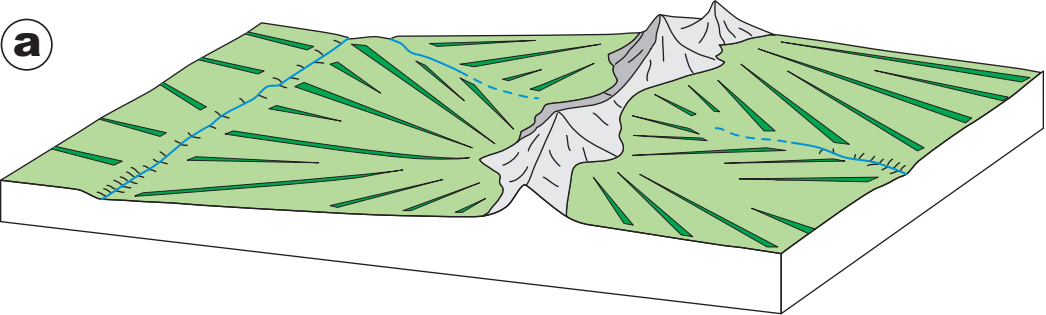
Chardon et al., Figure 4



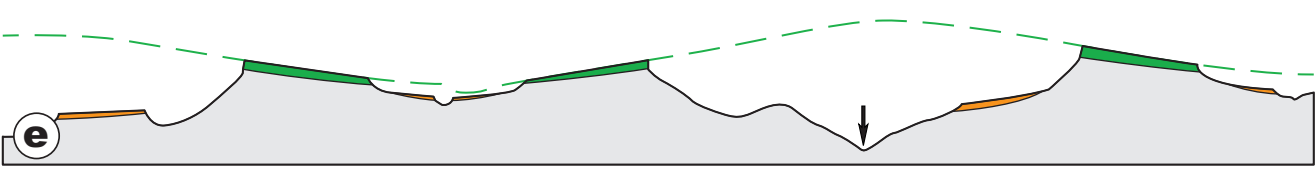
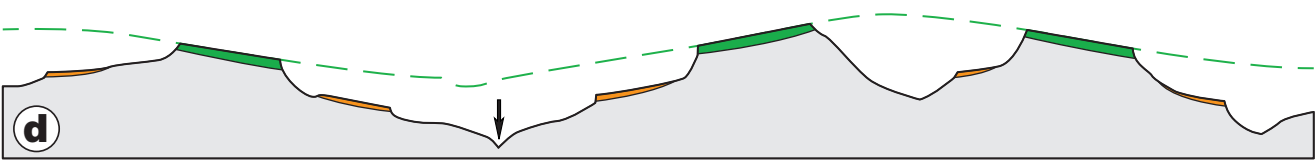
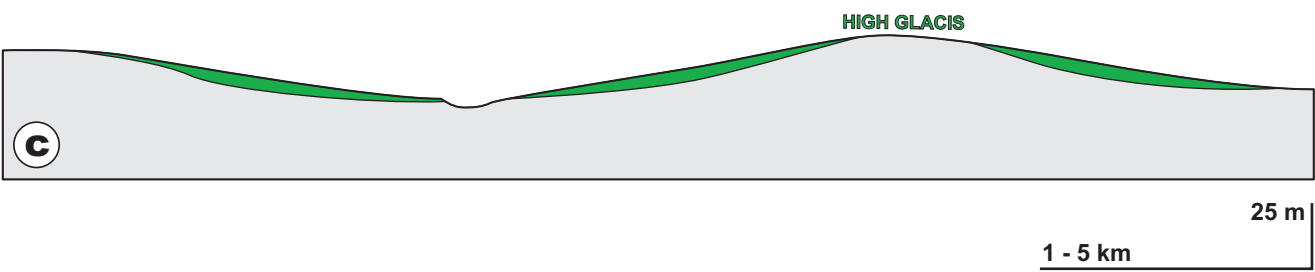
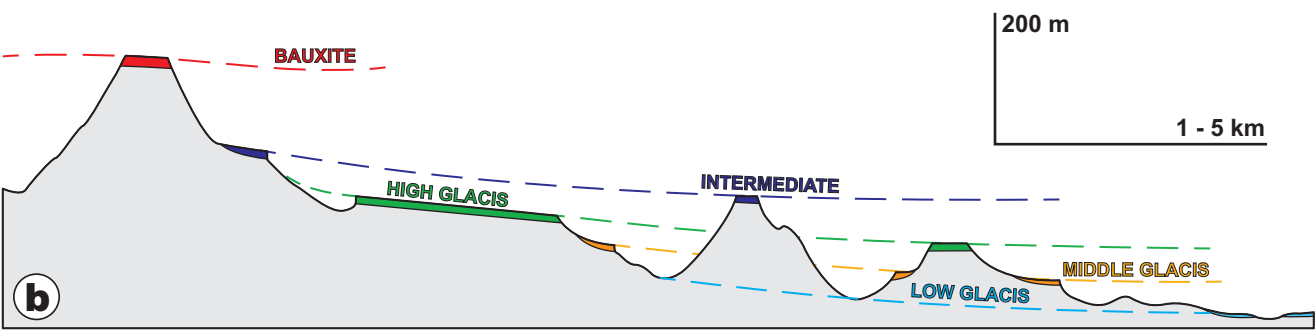
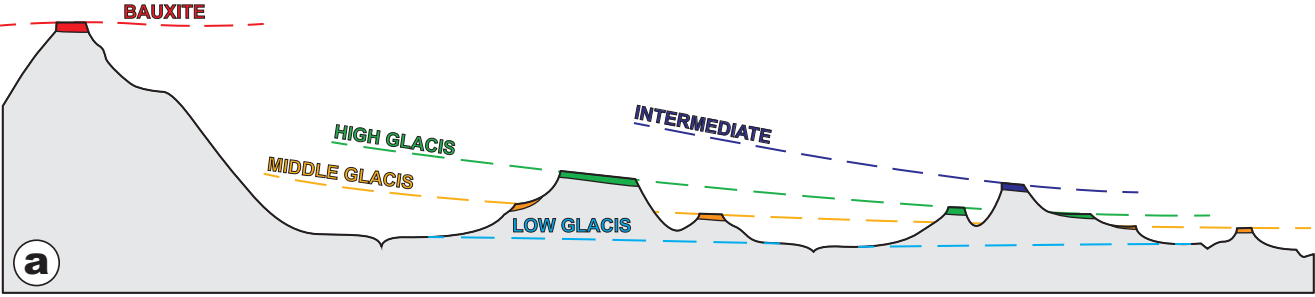
Chardon et al., Figure 5



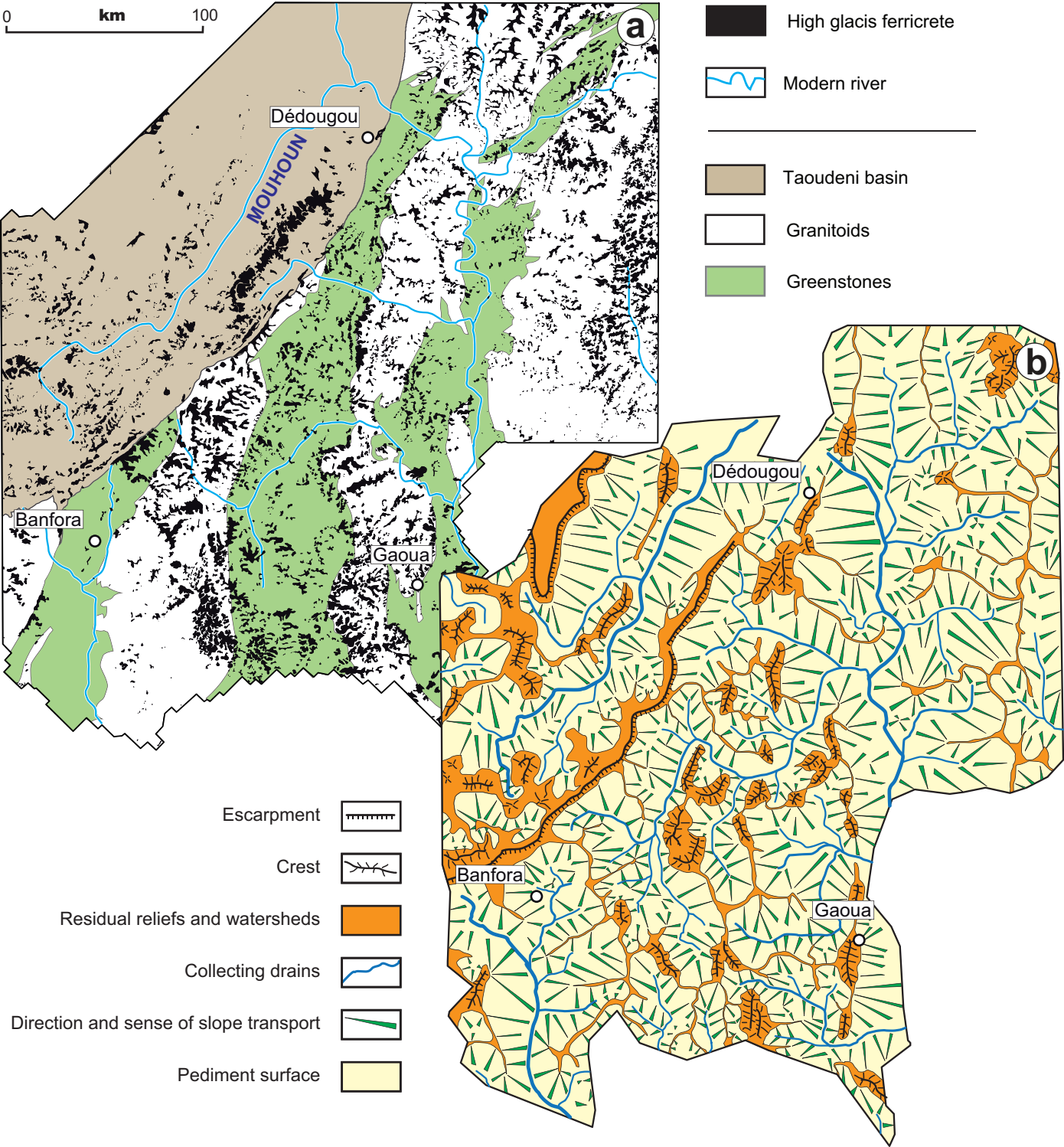
Chardon et al., Figure 6



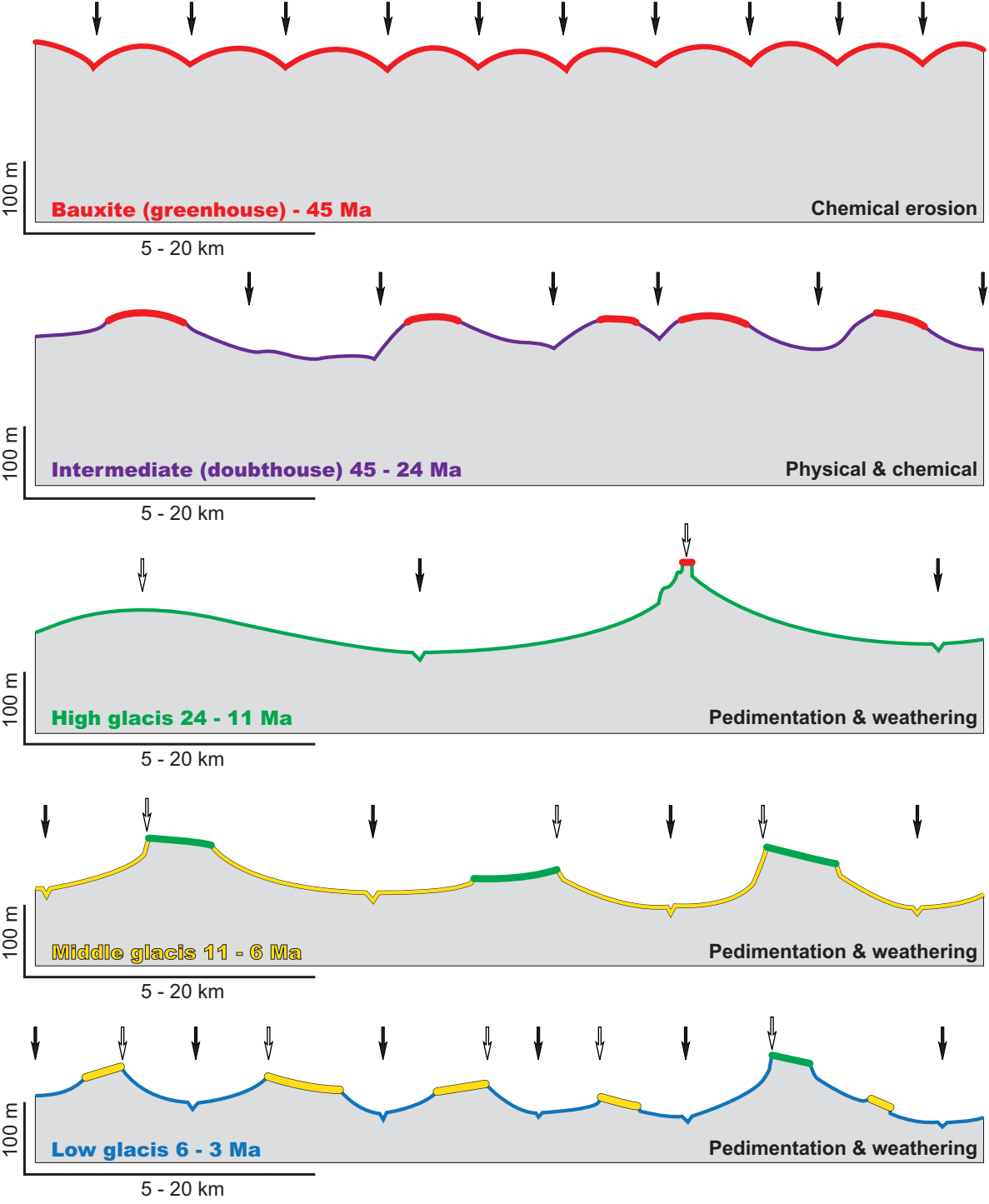
Chardon et al., Figure 7



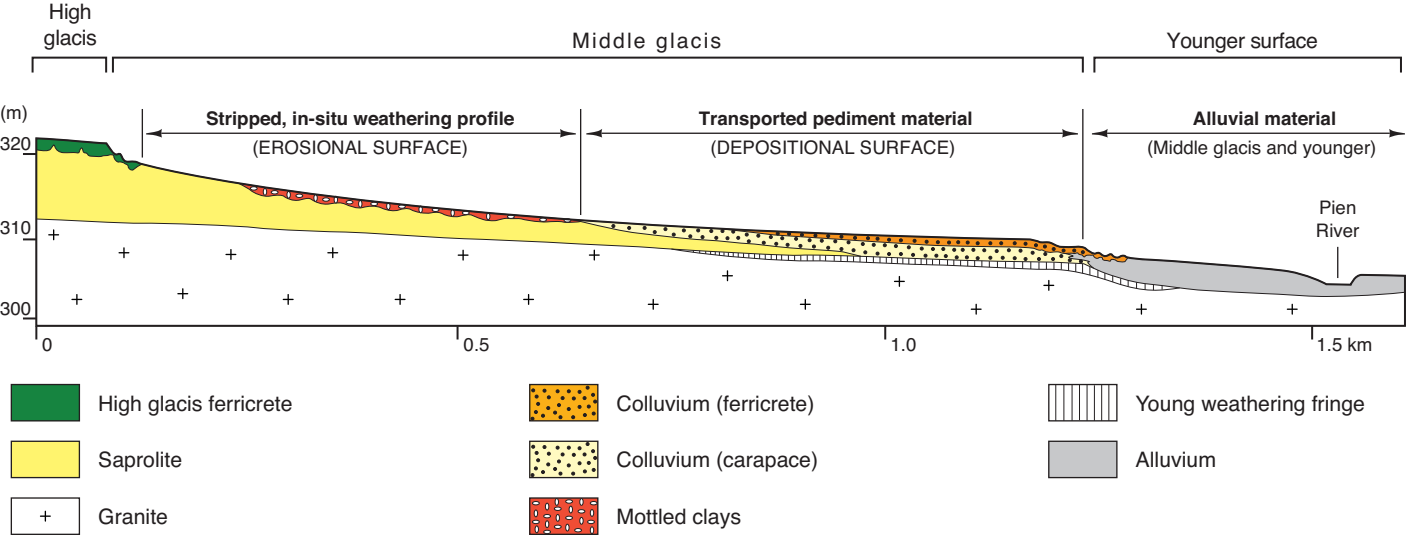
Chardon et al., Figure 8



Chardon et al., Figure 9



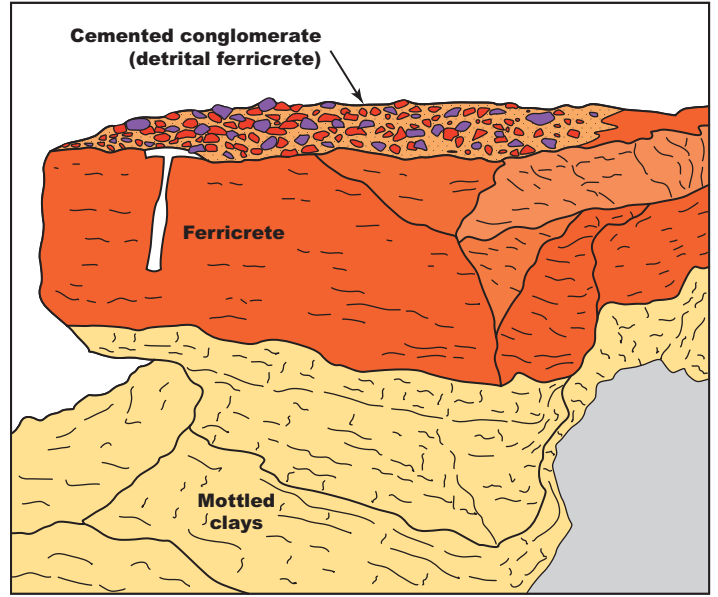
Chardon et al., Figure 10



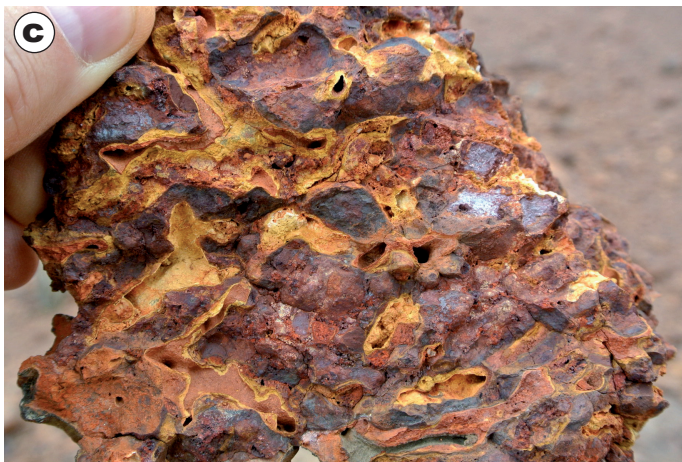
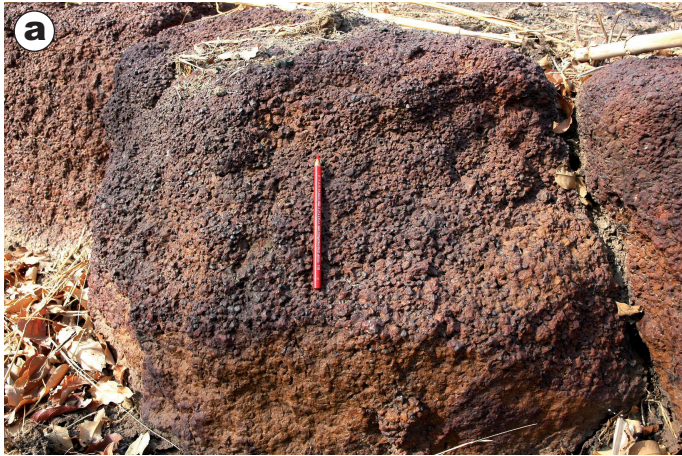
Chardon et al., Figure 11



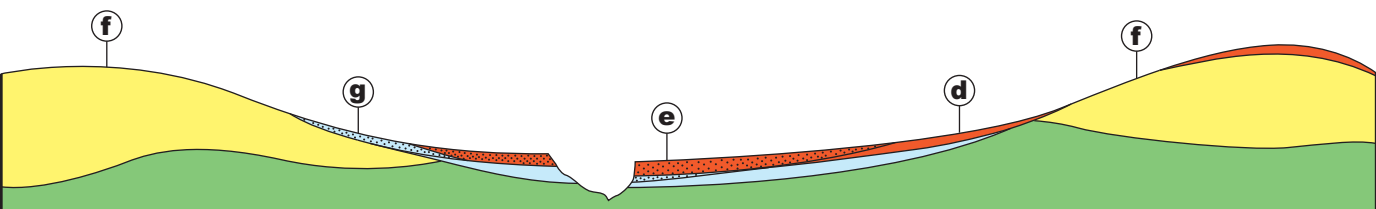
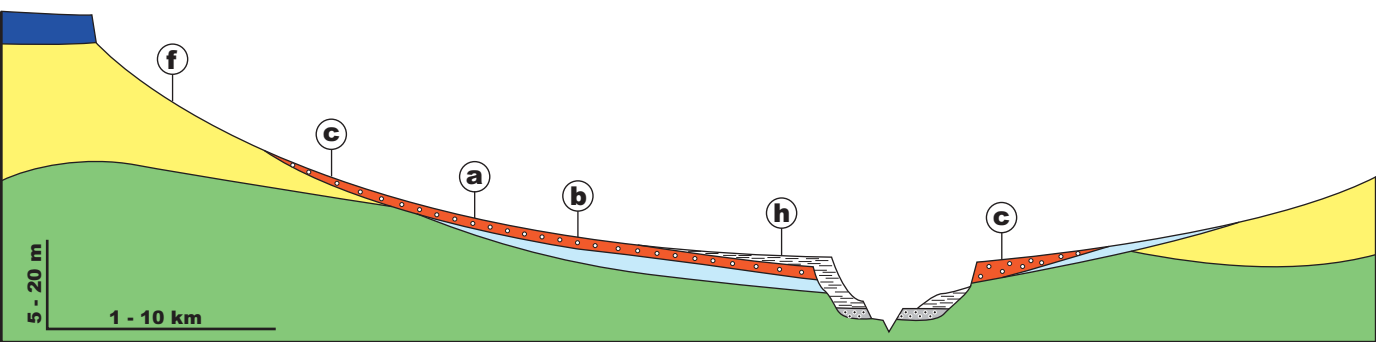
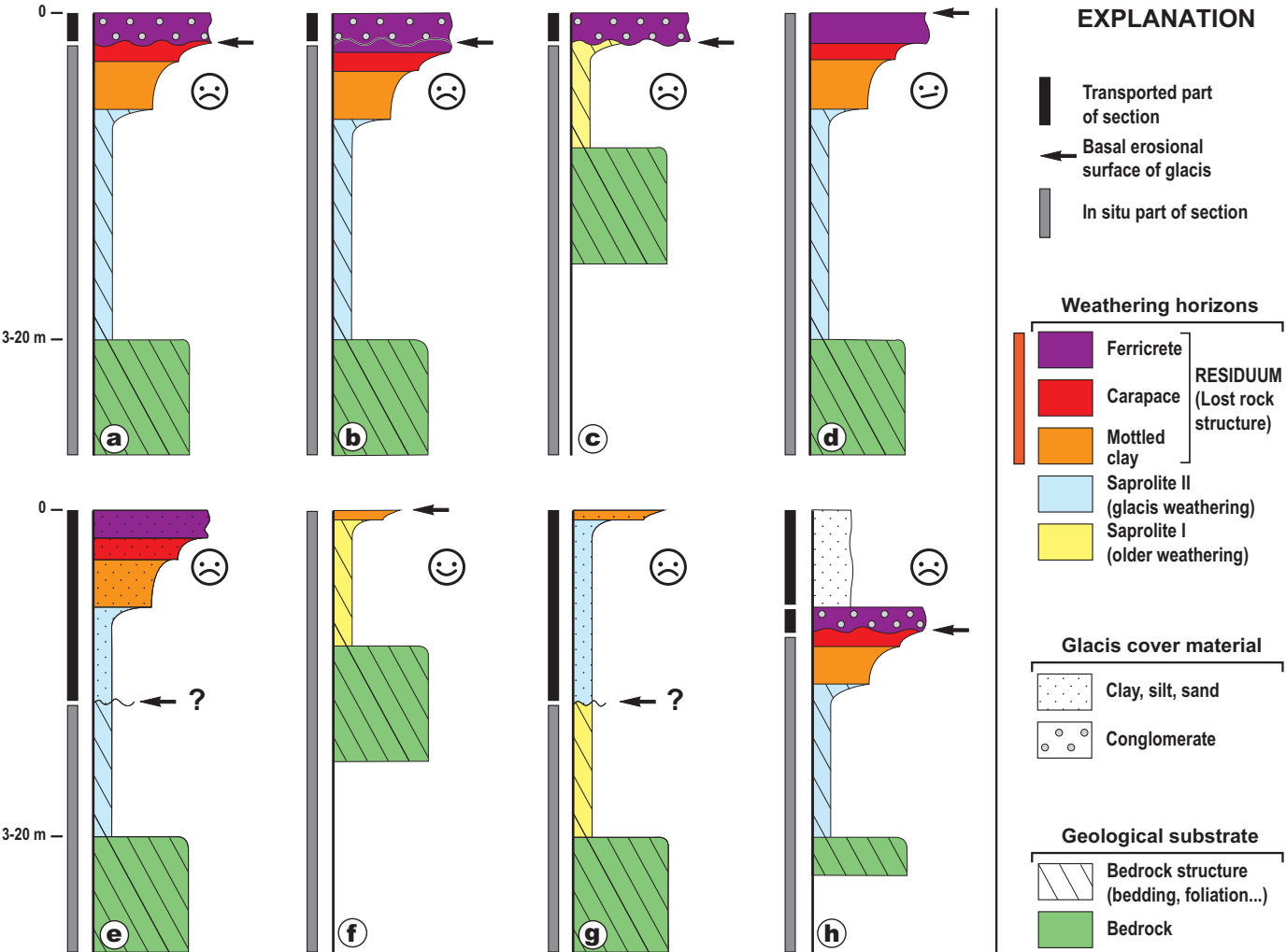
Chardon et al., Figure 12



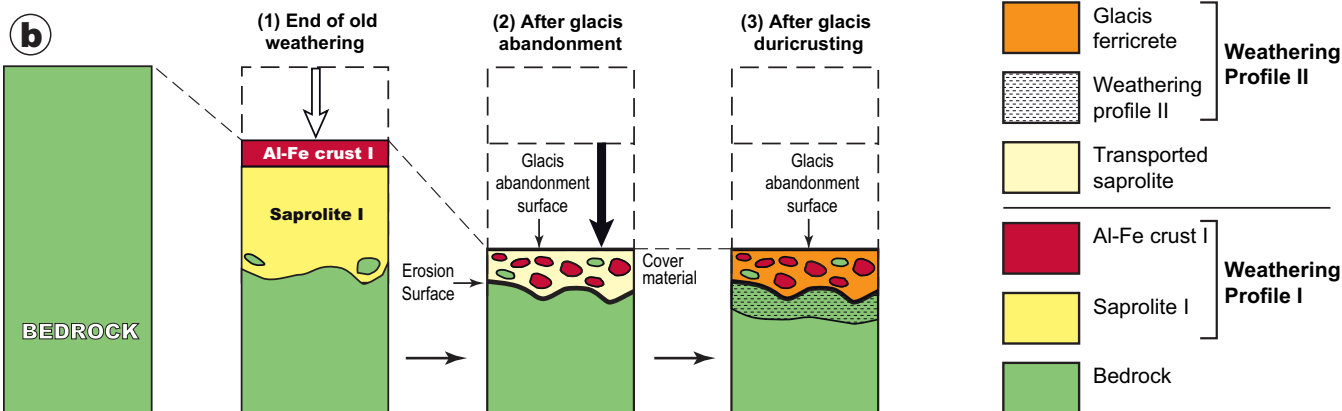
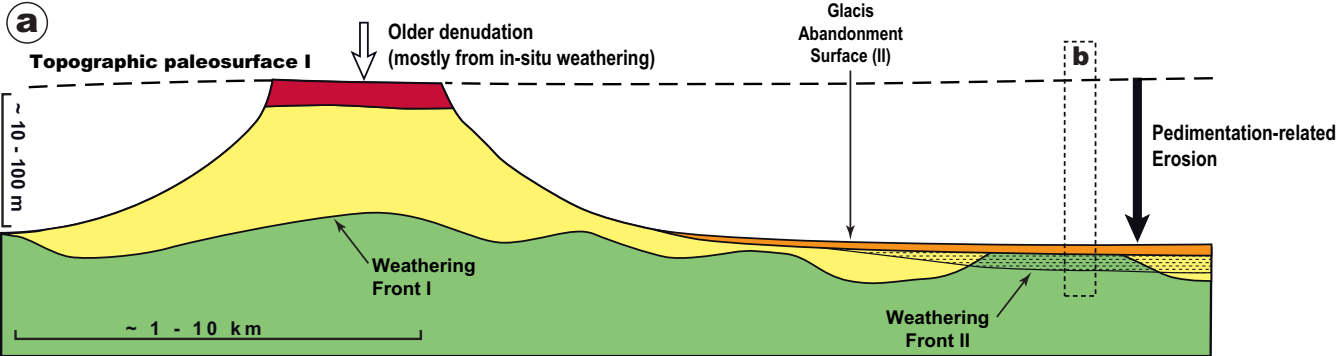
Chardon et al., Figure 13



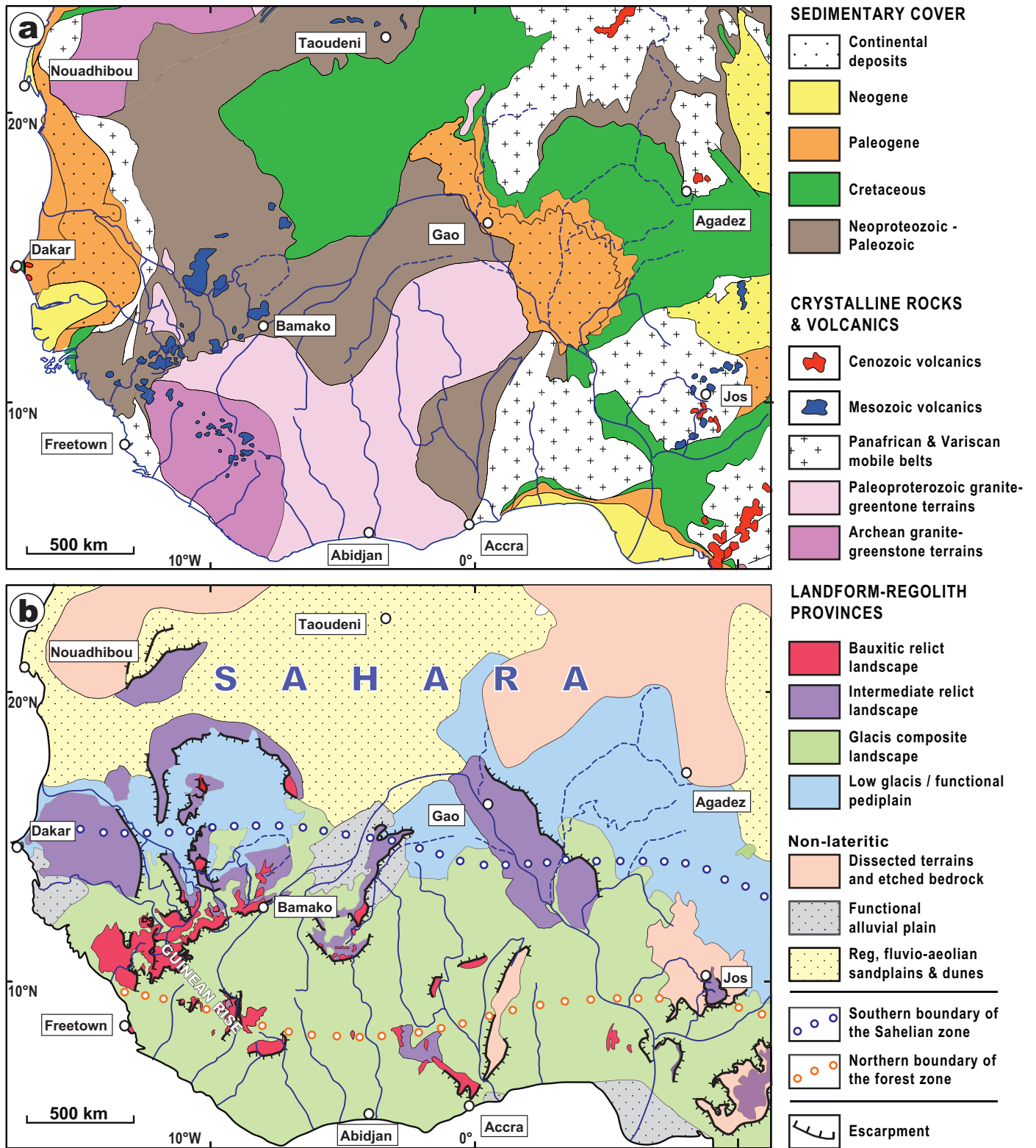
Chardon et al., Figure 14



Chardon et al., Figure 15

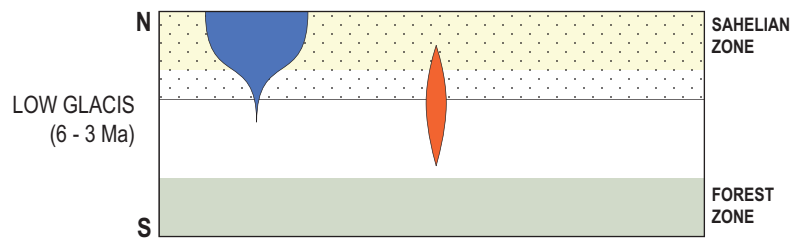
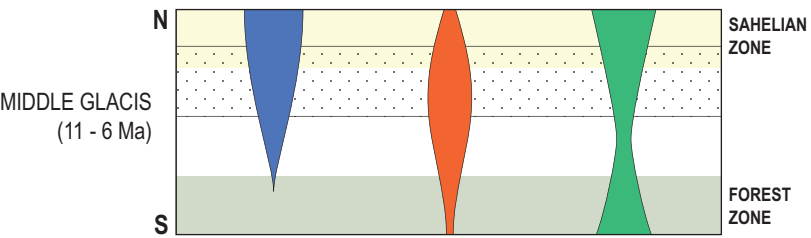
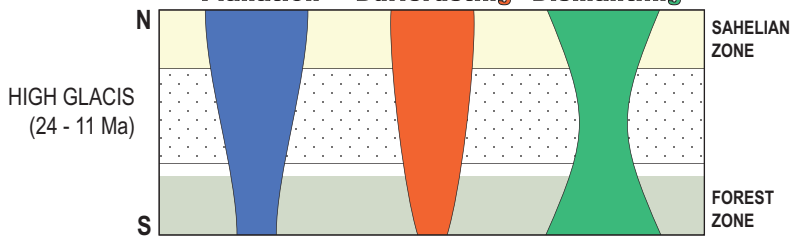



Chardon et al., Figure 16



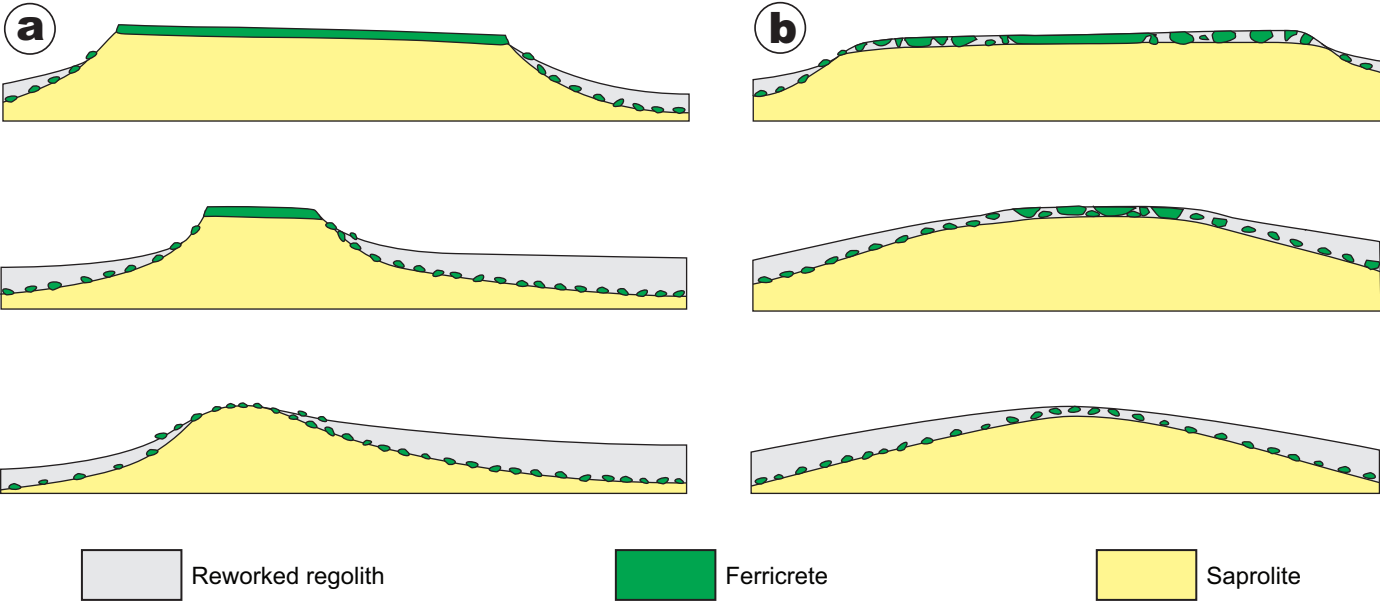
Chardon et al., Figure 17

Planation **Duricrusting** **Dismantling**

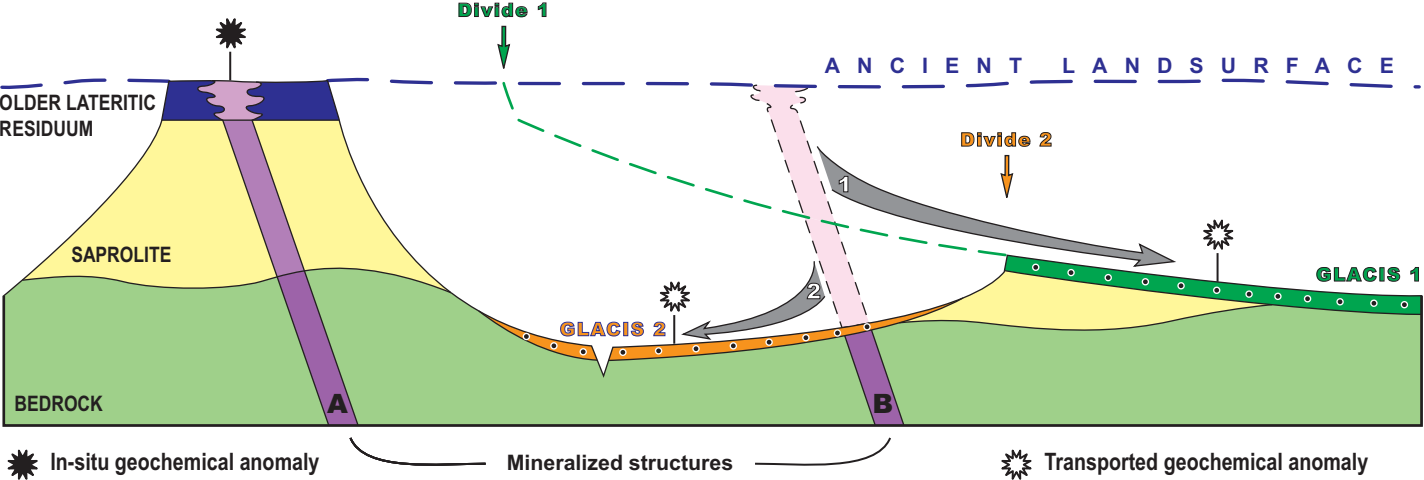


 Zone of current optimal preservation

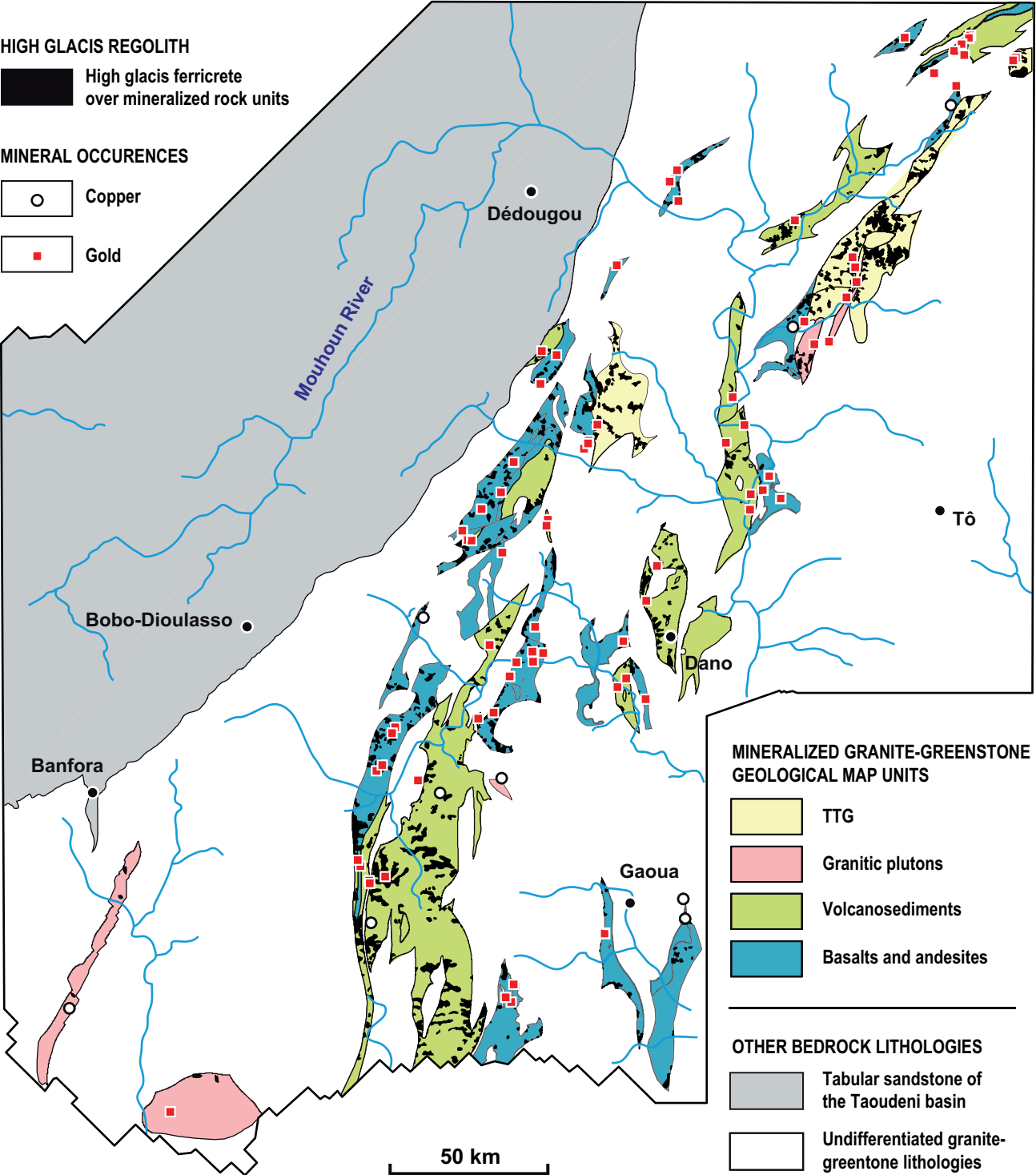
Chardon et al., Figure 18



Chardon et al., Figure 19



Chardon et al., Figure 20



Chardon et al., Figure 21